AGARD

ADVISORY GROUP FOR AEROSPACE RESEARCH & DEVELOPMENT

7 RUE ANCELLE 92200 NEUILLY SUR SEINE FRANCE

AGARD CONFERENCE PROCEEDINGS No. 316

Corrosion Fatigue

NORTH ATLANTIC TREATY ORGANIZATION

SMP

DISTRIBUTION AND AVAILABILITY
ON BACK COVER

AGARD-CP-316

NORTH ATLANTIC TREATY ORGANIZATION

ADVISORY GROUP FOR AEROSPACE RESEARCH AND DEVELOPMENT

(ORGANISATION DU TRAITE DE L'ATLANTIQUE NORD)

AGARD Conference Proceedings No. 316

CORROSION FATIGUE

Papers presented at the 52nd Meeting of the AGARD Structures and Materials Panel
held in Çeşme, Turkey, on 5–10 April 1981

THE MISSION OF AGARD

The mission of AGARD is to bring together the leading personalities of the NATO nations in the fields of science and technology relating to aerospace for the following purposes:

- Exchanging of scientific and technical information;
- Continuously stimulating advances in the aerospace sciences relevant to strengthening the common defence posture;
- Improving the co-operation among member nations in aerospace research and development;
- Providing scientific and technical advice and assistance to the North Atlantic Military Committee in the field of aerospace research and development;
- Rendering scientific and technical assistance, as requested, to other NATO bodies and to member nations in connection with research and development problems in the aerospace field;
- Providing assistance to member nations for the purpose of increasing their scientific and technical potential;
- Recommending effective ways for the member nations to use their research and development capabilities for the common benefit of the NATO community.

The highest authority within AGARD is the National Delegates Board consisting of officially appointed senior representatives from each member nation. The mission of AGARD is carried out through the Panels which are composed of experts appointed by the National Delegates, the Consultant and Exchange Programme and the Aerospace Applications Studies Programme. The results of AGARD work are reported to the member nations and the NATO Authorities through the AGARD series of publications of which this is one.

Participation in AGARD activities is by invitation only and is normally limited to citizens of the NATO nations.

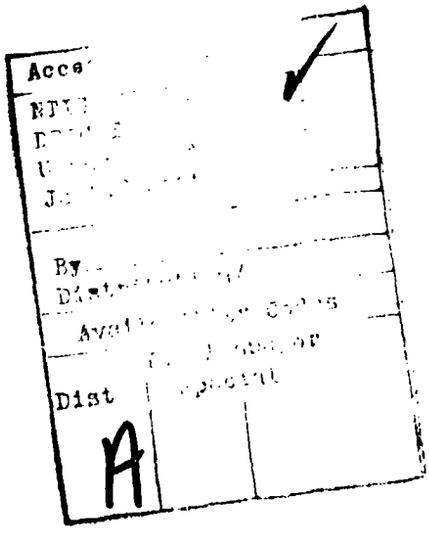

Published October 1981

ISBN 92-835-1402-5

Printed by Technical Editing and Reproduction Ltd
Harford House, 7–9 Charlotte St, London, W1P 1HD

PREFACE

Failure by fatigue and degradation by corrosion continue to be major considerations in aircraft design. Environmental effects are known to influence both the initiation and the propagation of fatigue cracks whereas dynamic loading may cause a more rapid deterioration of a corrosion protection system. Therefore the conjoint action of dynamic loading and environmental attack, i.e. corrosion fatigue, requires special attention.

In corrosion fatigue studies in the past years emphasis has been on investigations of a rather fundamental nature involving smooth specimens and constant amplitude loading in an aggressive aqueous environment. Such studies have undoubtedly contributed to the understanding of the phenomenon but have yielded few data which can be directly applied in the design and in the maintenance of an aircraft structure.

This situation was pointed out to the AGARD Structures and Materials Panel by Professor Wolfgang Bunk then a Panel Member for Germany. This had led to the establishment of a Sub-Committee under his chairmanship in the spring of 1977. Five pilot papers were presented then, four of these have been published in AGARD Report No. 659.
It was decided to start a Corrosion Fatigue Cooperative Testing Programme involving laboratories on both sides of the Atlantic. As coordinators were appointed Dr. J.J. DeLuccia (NADC-USA) and Dr. R.J.H. Wanhill (NLR-Netherlands).

In order to promote applicability of the results to aircraft structures a bolted joint in aluminium alloy sheet with a state-of-the-art protection system was selected as the common specimen.
Sheet from a single heat of bare 7075-T76 material was donated by the ALCOA Company. The Voi-Shan corporation made available several thousand Hi-Lok fasteners. The specimens of the so-called core programme were manufactured by the U.S. Air Force Materials Laboratory. The U.S. Naval Air Development Center applied the protection system.

In order to make the results readily comparable, detailed instructions as to testing procedures were developed by the two coordinators. These instructions were distributed in the so-called CFCTP-manual. For reasons of simplicity constant amplitude loading was agreed for the core programme.
The object was to see whether several laboratories on both sides of the Atlantic, working to a carefully prepared and mutually agreed set of rules, testing specimens from a single batch, could produce the same results, or whether there were hidden sources of scatter.
The core programme would be followed by a supplemental programme involving flight simulation loading, other alloys, other protection systems, and even other specimen designs.

Important aspects of the programme are that some specimens are precorroded in aqueous 5 % NaCl acidified by sulphur dioxide and fatigued in salt fog. The majority of the participants had to acquire special equipment for those purposes and have thus added to their testing facilities.

At the Specialists Meeting the results of the core programme have been presented. They may serve as a basis for the assessment of the effectiveness of sharing between different laboratories an investigation of a size prohibitive for its execution at a single laboratory.
Additional papers have been presented, stimulating thought on the fundamentals of corrosion fatigue on the one hand and of its combat for real structures on the other hand.
In the final session the scope and the content of the supplemental programme were discussed. It is proposed to give it the project title:
Aircraft Environment Simulation Fatigue Testing.

The results of the core programme are not included in the present volume. They will be published in an AGARD Report, together with the CFCTP handbook. The Conference Proceedings comprise only a brief presentation on the scope of both the core and the supplemental programme, in addition to the papers of a more general nature.

Herewith I would like to express my sincere gratitude to all those who have contributed to the CFCTP and the Specialists Meeting, to the two coordinators in particular who will undoubtedly, with the help of others, carry on to bring the supplemental programme to an equally successful ending.

H.P. van Leeuwen
Chairman of Sub-Committee
on Corrosion Fatigue

CONTENTS

AN AGARD-COORDINATED CORROSION FATIGUE COOPERATIVE TESTING PROGRAMME (CFCTP) AND ITS CONTINUATION, AIRCRAFT ENVIRONMENT SIMULATION FATIGUE TESTING(AESFT)

by
R.J.H. Wanhill, National Aerospace Laboratory NLR, Amsterdam, The Netherlands
J.J. De Luccia, Naval Air Development Center, Warminster, USA

1. BACKGROUND

Aluminium alloy aircraft structures are susceptible to corrosion and fatigue. Corrosion occurs under both static conditions and cyclic loading resulting from take-off, flight and landing. Thus the conjoint action of corrosion and cyclic loading, i.e. corrosion fatigue, must be considered. General corrosion is unlikely: attack concentrates at joints, which provide (1) stress concentrations and faying surface contacts that wear away and crack the applied protection systems, (2) crevices for moisture entrapment, (3) galvanic couples when steel or titanium fasteners are used, and (4) fatigue critical locations, e.g. fastener holes.

Many corrosion fatigue tests have been done on aluminium alloys. However, few included critical details, like joints, under realistic cyclic load histories and in service - like environments. Even fewer used practical corrosion protection systems. Consequently, in 1977 the AGARD Structures and Materials Panel appointed the present authors as coordinators for a Corrosion Fatigue Cooperative Testing Programme (CFCTP). The programme included eight laboratories in Europe and North America.

This chapter summarises the objectives, scope and technical requirements of the CFCTP, including an overview of a supplemental testing programme, Aircraft Environment Simulation Fatigue Testing (AESFT). Full results from all participants in the CFCTP and AESFT will be published in AGARD documents.

2. THE CFCTP

2.1 Objectives

The objectives of the CFCTP were:

(1) To provide a cooperative testing effort resulting in better understanding of corrosion fatigue and its prevention.

(2) To familiarise participants with fatigue tests in atmospheric corrosion environments.

2.2 Scope

The CFCTP is a programme of round-robin testing. This so-called core programme forms a basis for establishing confidence in corrosion fatigue testing before proceeding to the more complex conditions required by the AESFT. Eight laboratories participated in the core programme, which is outlined in figure 1. The specimen represents a fatigue-critical aircraft structural joint. The fatigue loading was constant amplitude.

The pre-exposure and corrosion fatigue environments were chosen to be severe and potentially able to simulate service environments without the necessity for long time exposure and testing.

2.3 Technical Requirements

The complexity of the CFCTP required a manual in which all technical requirements and test details were specified. Figure 2 summarises the contents: headings are evident except the cold box, which enables service simulation of brittle cracking of paint and primer layers on the specimen. Note that the manual also contains the technical requirements for the supplemental programme AESFT.

3. THE AESFT

As an extension of the CFCTP the supplemental programme AESFT has the following objectives besides those listed in section 2.1:

(3) Assessment of current protection systems for aircraft structures

(4) To help develop new protection systems.

The individual contributions to the supplemental programme (AESFT) are broadly defined and testing has commenced at several laboratories. An overview of the planned supplemental activities is given in figure 3. Most of these include the same specimen type and test environment as in the CFCTP, but with addition of realistic flight-by-flight fatigue loading, FALSTAFF and MINITWIST.

MATERIAL

- 3.2 mm THICK 7075-T76 ALUMINIUM ALLOY SHEET

SPECIMEN

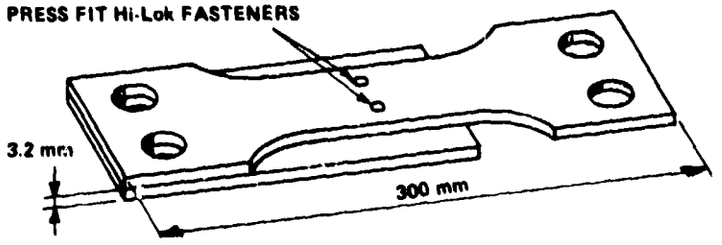

PROTECTION SYSTEM

- CHROMATE CONVERSION + INHIBITED EPOXY POLYAMIDE PRIMER (EXCEPT FASTENER HOLES) + ALIPHATIC POLYURETHANE TOPCOAT

PROTECTION SYSTEM DAMAGE

- TWO STRESS CYCLES AT LOW TEMPERATURE TO CRACK PAINT AND PRIMER AROUND THE FASTENER HEADS

FATIGUE LOADING

- CONSTANT AMPLITUDE, $S_{min}/S_{max} = 0.1$

FATIGUE ENVIRONMENTS

- LABORATORY AIR; 5 °/o AQUEOUS NaCl SALT SPRAY WITH pH 4

STATIC PRE-EXPOSURE

- 72 HOURS IN 5 °/o AQUEOUS NaCl + SO_2 AT 315 K

TEST PROGRAMME

SCHEDULES	NUMBER OF SPECIMENS		CYCLE FREQUENCY
	S_{max} = 210 MPa	S_{max} = 144 MPa	
FATIGUE IN AIR	4	4	2 Hz
PRE-EXPOSURE AND FATIGUE IN AIR	4	4	
FATIGUE IN SALT SPRAY	4	4	0.5 Hz
PRE-EXPOSURE AND FATIGUE IN SALT SPRAY	4	4	

Fig. 1 The CFCTP core programme

Fig. 2 Summary of the CFCTP manual

U.S. NAVAL AIR DEVELOPMENT CENTER	● 7075–T76 $1^1/2$ DOGBONE SPECIMENS ● INTERFERENCE AND SLIGHT PRESS FIT FASTENERS ● CORROSION PROTECTION SYSTEMS ● CONSTANT AMPLITUDE LOADING AND FALSTAFF ● ALTERNATING PERIODS OF STATIC EXPOSURE AND FATIGUE
U.S. AIR FORCE MATERIALS LABORATORY	● 7075–T76 $1^1/2$ DOGBONE SPECIMENS ● REPAIR FASTENERS (SLEEVE BOLTS) ● CORROSION PROTECTION SYSTEMS ● CONSTANT AMPLITUDE LOADING AND FALSTAFF
VOUGHT CORPORATION, USA	● 7075–T76 $1^1/2$ DOGBONE SPECIMENS ● VARIABLE ENVIRONMENTS
UNIVERSITY OF SASKATCHEWAN, CANADA	● 7075–T76 $1^1/2$ DOGBONE SPECIMENS ● CONSTANT AMPLITUDE LOADING AND FALSTAFF
NATIONAL AEROSPACE LABORATORY – DELFT TECHNOLOGICAL UNIVERSITY, THE NETHERLANDS	● 7075–T6, 7475–T761, 2024–T3, 2024–T3/ARAMIDE FIBER LAMINATE, $1^1/2$ DOGBONE SPECIMENS ● SLIGHT PRESS FIT FASTENERS ● CORROSION PROTECTION SYSTEMS ● CONSTANT AMPLITUDE LOADING, FALSTAFF AND MINITWIST ● TEST SCHEDULES SIMILAR TO CORE PROGRAMME
INDUSTRIEANLAGEN BETRIEBSGESELLSCHAFT, WEST GERMANY	● 7075–T6, 7475–T761 $1^1/2$ DOGBONE SPECIMENS ● SLIGHT PRESS FIT FASTENERS ● CORROSION PROTECTION SYSTEMS ● FALSTAFF ● TEST SCHEDULES AS PER CORE PROGRAMME
NORWEGIAN DEFENCE RESEARCH ESTABLISHMENT	● 7075–T6, 7075 RETROGRESSION AND REAGE, $1^1/2$ DOGBONE SPECIMENS ● SLIGHT PRESS FIT FASTENERS ● CORROSION PROTECTION SYSTEMS ● FALSTAFF ● TEST SCHEDULES AS PER CORE PROGRAMME
ROYAL AIRCRAFT ESTABLISHMENT, ENGLAND	● 7075–T6 $1^1/2$ DOGBONE SPECIMENS ● 7075–T6, 7010–T7651, 7010–T73651, 7010–T7351, 7050–T73651, 7475–T7351, CENTER NOTCHED SHEET SPECIMENS ● INTERFERENCE FIT FASTENERS AND CORROSION PROTECTION SYSTEMS (DOGBONE SPECIMENS) ● CONSTANT AMPLITUDE LOADING AND FALSTAFF ● DOGBONE SPECIMEN TEST SCHEDULES AS PER CORE PROGRAMME AND ADDITIONAL PRE–EXPOSURE ● CENTER NOTCHED SPECIMENS TESTED IN SALT SPRAY
SOCIETE NATIONALE INDUSTRIELLE AEROSPATIALE, FRANCE	● 2024–T3 $1^1/2$ DOGBONE SPECIMENS ● SLIGHT PRESS FIT FASTENERS ● CORROSION PROTECTION SYSTEMS ● MINITWIST

FALSTAFF = Fighter Aircraft Loading Standard For Fatigue

MINITWIST = shortened version of TWIST = Transport Wing STandard

Fig. 3 Overview of planned aircraft environment simulation fatigue testing activities

Mechanisms of Corrosion Fatigue of Aluminum Alloys

D.J. Duquette
Materials Engineering Department
Rensselaer Polytechnic Institute
Troy, New York 12181
U.S.A.

Abstract

An overview of experimental variables which are considered critical to understanding the mechanisms of corrosion fatigue of high strength aluminum alloys is presented. Based on this overview, an examination of previously proposed mechanisms is attempted. These models include anodic dissolution, surface energy reduction, and hydrogen embrittlement. It is concluded that hydrogen embrittlement of process zones at alloy surfaces (for crack initiation) and at crack tips (for crack propagation) best explains observed results. A general model of corrosion fatigue of these alloys is proposed. This model suggests that the nature of the naturally formed oxide film on aluminum alloys may be a critical factor. Chemical or mechanical damage of the film allows hydrogen ingress. The presence of second phase particles which may act as sinks for dislocation transported hydrogen, may also be a necessary prerequisite to significant amounts of reduction in fatigue resistance associated with corrosion.

Introduction

It is well known that high strength aluminum alloys are highly susceptible to environmental degradation in the presence of halide ions. In the unstressed state, this degradation may be manifested by localized corrosion such as pitting, crevice corrosion or exfoliation (grain boundary attack). However, under conditions of applied or residual stresses, these alloys may suffer from stress corrosion cracking (SCC) or, if cyclic loads are present, from corrosion fatigue. In some circumstances, these two phenomena may be additive and a form of "stress-corrosion fatigue" may be observed. In general, SCC is reported as time delayed failure of smooth or of notched specimens, often at applied stress levels below the nominal yield strength of the alloy. Alternatively if high aspect ratio flaws such as pre-cracks are present, measurable crack growth may be observed which generally increases with stress intensity (K) until a plateau value of crack growth rate ($da/dt \alpha v$) is reached. Both types of data are schematically described in figure 1. Under cyclic loading conditions, similar trends are observed, except that the data which are obtained are generally described as stress (S or σ) vs numbers of cycles to failure (N_f) on semi-log plots for smooth or notched alloys. For the case of controlled, observable crack growth the data are generally plotted as crack growth increment per cycle (da/dN) vs the range of stress intensity (ΔK)(fig. 2). While halide has been shown to significantly increase crack propagation rates (and decrease time to failure) it should be noted that distilled water, and even moist air have been shown to be very effective in inducing environmentally assisted cracking in several high strength aluminum alloys.

Aluminum Alloy Metallurgy

The aluminum alloys which are most seriously affected by environmental degradation of mechanical properties are precisely those of most interest for commercial application i.e. high strength/low density alloys. As a class, they are generally utilized in a precipitation hardened condition obtained by appropriate heat treatment. In general, the precipitates are intermetallic compounds which are formed and distributed as small particles by a solutionizing heat treatment, followed by a quench to maximize the vacancy concentration of the alloy. Aging temperatures and time determine the rate of nucleation and growth, and determine the size, distribution and morphology of the precipitates. The initial G.P. zones are considered to be coherent with the matrix and the final precipitates, η, maintain partial coherency with the matrix {111} plane.(1,2), although as many as seven other matrix/precipitate coherencies have been reported.(1,2) In the peak aged condition slip is considered to be highly planar, while in the underaged or overaged condition slip is generally considered to be more diffuse.

General Fatigue Behavior of High Strength Al Alloys

The fatigue resistance of the more commonly used Al alloys such as 2024 (Al-4Cu) and 1075 (Al-5Zn-2Mg) is considered to be poor when the alloys are tested in the peak hardened

condition. The 10^7 cycle fatigue limit in neutral environments is $\sim$ 0.3-0.35 of the UTS, and when cracks form, crack propagation rates are relatively rapid when compared with ferrous alloys. On smooth specimens in the high cycle fatigue regime, or in notched single crystals in inert atmospheres at relatively low stresses, cracks initiate in the stage I (crystallographic) mode and, as in many other alloy systems, convert to a stage II mode at some critical (but as yet undetermined) crack length (for a nominal applied stress below σ_{ys}). For pre-cracked (fracture mechanics) specimens cracks are generally considered to grow only in the stage II mode. The specific process by which cracks initiate is still somewhat open to interpretation. Several models for crack initiation processes have been proposed and include resolution of ordered precipitates sheared by the slip process (3,4) or, alternatively, disordering of these precipitates thus creating a "soft" region along slip planes where stage I cracking initiates and grows.(5) However, at low applied stresses, approaching the endurance limit, evidence of precipitate by-pass resulting in sessile dislocation loops in the matrix of high purity Al-Zn-Mg alloys has been reported.(6) According to this model the sessile loops generate dilational stresses across slip planes leading to weak planes for crack initiation. It is possible that all of the models may be valid depending on combinations of applied stresses, precipitate morphologies, slip plane orientations etc., and that no simple micro-process can explain all of the observed results.

Corrosion Fatigue Behavior of High Strength Al Alloys

A. Gaseous Environments

Corrosion fatigue of precipitation hardened Al alloys has been observed in environments as innocuous as damp laboratory air. In general, this environment has little or no effect on crack initiation processes, but reductions in the general S-N_f behavior have been reported. Additionally, crack propagation experiments indicate significant increases in da/dN for a given ΔK.(7,8)(fig.3) In order to observe a significant effect, water vapor must be present in the environment, oxygen alone having little or no effect on either fatigue lives or fatigue crack propagation rates.(9) In fact, virtually identical crack propagation rates have been observed for a 7075 type alloy in wet argon, wet oxygen and wet air.(7) While the presence of some water vapor is important, increases in water vapor concentrations in air do not increase crack propagation rates significantly when a critical concentration of water vapor has been exceeded.(8) The water vapor effect has been linked to a form of hydrogen embrittlement (9,10), although gaseous hydrogen does not appreciably affect fatigue resistance.

Water vapor has also been shown to affect crack paths in single crystals of an Al-Zn-Mg alloy. In dry air for a peak hardened alloy, conventional stage I cracking in {111} planes was observed, but exposure to moist air increased crack propagation rates and cracks grew in {100} planes.(11,12) The effect is frequency sensitive and no appreciable effect is observed at 50 Hz, although a marked effect is noted at 5 Hz.(12) Also, a test started 50 Hz but switched to 5 Hz alters the crack path out of the slip band; but a test began at 5 Hz and switched to 50 Hz does not move the crack path back to the slip band.(fig. 4) These results indicate that the effect is time dependent and that the process is a bulk alloy effect, rather than simply being strictly a surface related effect. In other experiments Wei and his co-workers have convincingly confirmed that the effect is in fact a bulk effect, but that the rate limiting step is not necessarily diffusion. Rather it appears to be related to a surface reaction of the water vapor on the aluminum alloy fracture surface which releases the damaging specie, presumed to be hydrogen.(10,13)

The specific process by which hydrogen embrittles the alloy under cyclic deformation conditions is still open to question and most of the "classical" hydrogen cracking models have been invoked. These include high internal pressures at voids or defects in the alloy (14), surface energy reduction by the embrittling specie due to adsorption (15-17), effects of slip reversibility (18) and changes in the mechanical properties of the oxide film.(19) The high internal pressure theory suggests that hydrogen preferentially diffuses to regions of high hydrostatic stress ahead of a growing crack, precipitates, and increases the local tensile forces during the crack advance. Adsorption effects are though to lower the surface energy required to create new crack surfaces, although the energy associated with crack tip plasticity is generally ignored. Hydrogen or other surface reactive species may also affect surface slip reversibility or alternatively crack tip plasticity resulting in less crack blunting as the crack surfaces are unloaded.

B. Aqueous Environments

While the previously cited results of the effects of gaseous environments are relatively recent, severe corrosion fatigue of Al alloys in aqueous, particularly saline, environments has been recognized for some time. Some of the earliest observations indicated that, for Al-Zn-Mg alloys, fracture surface appearance showed distinct differences when saline environments and dry air were compared.(20,21) Specifically "ductile" striations (type "A") were observed in dry air, while "brittle" striations (type "B") were observed to occur in the saline solutions. Examples of these two morphologies are shown in fig. 5 The type "A" striations were observed to be non-crystallographic and showed extensive shear, while type "B" striations were identified as occurring on or near {100} planes.

It has also been observed that crack propagation rates were typically 3-10X more rapid in aqueous environments when compared to dry air.(10,22) Also it has been reported that, the more aggressive is the solution toward general corrosion of the aluminum alloys, the lower is fatigue resistance when tested in those environments. Thus increasing ionic concentration, particularly of halides, and both acid and basic solutions (where corrosion rates of aluminum increase) decrease fatigue resistance.(23) Lowering the corrosive nature of the solutions by adding inhibitors, such as nitrates, conversely increases the fatigue resistance.(17) However, it has been shown that cathodic polarization of the alloy, (cathodic protection) may actually decrease fatigue resistance in nominally neutral solutions.(fig. 6) Anodic polarization, which invariably increases corrosion rates virtually always results in a degradation in fatigue resistance.(23,24) The general consensus of experiments utilizing polarization as a variable, are that small amounts of cathodic polarization slightly increase fatigue resistance but that large amounts of polarization lead to decreases in fatigue resistance. These results are by no means unequivocal, however. When significant amounts of cathodic polarization are applied, the evolution of hydrogen at the alloy surface results in a shift in the solution pH in the positive direction, and basic solutions are known to be corrosive to aluminum alloys. Additionally, the aqueous solution in growing cracks is quite different from the bulk solution and, in some cases, may be quite independent of surface polarization.(25,26)

A recent experimental program in our laboratories has been specifically addressed toward understanding the mechanism of corrosion fatigue in a 7075 alloy and its high purity Al-Zn-Mg-Cu analogue. A summary of the results of this program follows:

1) It has been shown that Cl^- ion is not a prerequisite to induce lowered fatigue resistance in either alloy, particularly under conditions of cathodic polarization. Sulfate ion, while less damaging under free corrosion conditions, is equally aggressive at equivalent cathodic potentials. In chloride solutions under freely corroding conditions, surface pits dominate the crack nucleation event, but fatigue resistance in sulfate solutions where pitting is not observed is equivalent to that observed in distilled water. (fig. 2,7)

2) In distilled water or in sulfate solutions, under free corrosion conditions, only ductile situations are observed on the fracture surfaces, versus brittle situations invariably observed in chloride solutions. Under cathodic polarization conditions brittle situations are observed on all fracture surfaces.

3) Pre-corrosion experiments in NaCl followed by tests in laboratory air result in significant decreases in fatigue resistance. However, this effect is at least partially reversible. Post exposure heat treatments prior to fatigue testing increase fatigue resistance with larger increases observed as heat treatment times are extended.(Table I)

4) In aggressive environments, the cyclic stress is the primary mechanical factor controlling the fatigue resistance. The magnitude of mean stress is only of secondary importance.(fig. 8)

5) Corrosion fatigue resistance of aluminum alloys is less sensitive to Mode III (torsional) loading than to Mode I (tensional) loading.(fig. 9)

6) Heat treatments which improve SCC resistance, (eg.T73) have little or no effect on corrosion fatigue behavior in Cl^- solutions.

Specific Mechanisms of Corrosion Fatigue of Al Alloys

As already briefly mentioned, there are at least three principal mechanisms which have been suggested to explain the reduction of fatigue lives in Al alloys exposed to aggressive environments.

A. Strain Enhanced Dissolution

Older versions of this mechanism suggested that strained atomic bonds are more likely to lead to atomic dissolution (corrosion) than are unstrained bonds. Refinements to the mechanism include the role of plastic strain associated with dislocations intersecting the free surface of a metal or alloy during fatigue, resulting in preferential attack of emerging slip bands.(27) It has also been suggested that this preferential attack accellerates further slip processes in a kind of autocatalytic process. Evidence for such a model has been shown for mild steels and for copper alloys under controlled corrosion conditions.(28-30) It has also been shown that if corrosion rates are sufficiently low, fatigue resistance is unaffected by the environment. Another version of the strain assisted dissolution model is the film rupture theory. According to this mechanism, mechanical rupture of an otherwise protective film leads to rapid localized corrosion at the film rupture site, leading to crack initiation in emerging slip bands, and subsequently to corrosion assisted crack growth due to the high stress concentrations associated with crack tips.(24,31-36)

While these mechanism can be used to explain results observed for aluminum alloys exposed to liquid phase corrosive solutions, it is difficult to relate them to the significant decreases in fatigue resistance observed in water vapor or in deaerated distilled water. Additionally, the observation that the effects of pre-corrosion are at least partially reversible through conventional heat treatments suggests that this mechanism may be untenable even for aqueous corrosion fatigue. Thus, it may be considered that strain assisted dissolution processes cannot adequately explain either crack initiation

processes or enhanced crack propagation process for these alloys.

B. Surface Energy Reductions

According to this theory, specific species which are strongly adsorbed at surfaces serve to lower the local bond energy and accordingly lead to increases in crack propagation rates. Some investigators have also suggested that reductions in surface energy may enhance plasticity and cause early crack initiation and propagation.(37) Still other investigators have suggested that surface energy reductions in growing cracks may reduce crack tip plasticity and thus induce brittleness.(17) Problems with acceptance of adsorption models have generally centered on the large amount of plastic energy associated with crack growth vs the relatively small amount of surface energy ($\sim 10^3$:1). Thus even large changes in surface energy should not appreciably affect cracking tendencies. Also, the observation that $SO_4^=$ ion is at least as damaging as Cl^- ion under cathodic changing conditions would tend to discount a specific species explanation.

C. Hydrogen Assisted Cracking

The possibility that aluminum alloys may suffer from hydrogen embrittlement was strongly suggested by experiments which showed that, for thin specimens, air borne water vapor caused totally brittle failures in Al-Zn-Mg alloys.(38,39) In fact, brittle intergranular cracks were observed by high voltage transmission electron microscopy in thin foils of these alloys with no signs of anodic dissolution or plasticity. Further experiments indicated that, after exposure of this alloy to water vapor, voids were observed to grow from interactions with a focused electron beam. Also, fracture of these specimens in a mass spectrometer was accompanied with the release of clearly identifiable amounts of hydrogen.(39) Tensile experiments in an Al-Mg alloy (5086) charged with tritium also showed discontinuous yielding associated with tritium release.(40) It appears certain then, that Al alloys which contain hydrogen are accordingly embrittled and that there appears to be a dislocation - hydrogen interactions.

Proposed Mechanism of Corrosion Fatigue of Al Alloys

On the basic of the results presented in this discussion, and on recently obtained but yet unpublished results obtained at Rensselaer, it appears that this latter mechanism, that of hydrogen embrittlement, can successfully be applied to corrosion fatigue of high strength aluminum alloys. Table II summarizes some of the relevent arguments with support or lack of support for either a hydrogen embrittlement process or an anodic dissolution process. Perhaps the most significant observations are that water vapor alone can produce increases in crack propagation rates, which are equivalent to increases in rates obtained in distilled H_2O alone or with Na_2SO_4 additions. Also, the partial reversibility of damage when tested in air after exposure to pre-corrosion is strongly indicative of a dissolved species rather than an adsorbed species which is responsible for embrittlement. Other periferal observations such as the effects of load mode (Mode I or tension being worse than Mode III or torsion) and the absence of mean stress effects permit the presentation of a qualitative model for corrosion fatigue of high strength Al alloys. According to this model hydrogen, dissolved in the alloy, in the process zone at a crack tip, embrittles this region and causes increases in crack propagation rates. The specific process by which the embrittlement occurs remains elusive, although it may be significant that those alloys which have small, semi-coherent particles are the most susceptible to failure. Consideration that the non-coherent precipitate-matrix interface at grain boundaries in statically loaded specimens is the preferred crack path, suggests that hydrogen may collect at these interfaces to cause decohesion. Under cyclic loading conditions, the mobile dislocations may act as short circuit paths for hydrogen to precipitate at interfaces in the grain interiors in preference to grain boundary regions. Thus the fracture path is shifted to transgranular, since effective diffusion rates are enhanced still more than are grain boundary diffusion rates. It may be significant to note that, for alloys with equiaxed grains, low cyclic stresses and small amounts of cathodic charging result in intergranular crack initiation and early propagation even under cyclic loading conditions. As the cracks elongate however, the local effective stress increases, dislocation densities and mobilities increase, and the cracks shift to a transgranular mode.(Table III) The crack path shift to {110} or {112} planes from the {111} slip planes (in non-aqueous environments) which has been reported may also be associated with a particular precipitate/matrix interfacial plane where hydrogen collects. Since it has also been shown that sulfate is as effective as chloride in reducing fatigue resistance if external sources of hydrogen, (cathodic charging) are applied, the specific role of chloride appears to be related to chemical damage of the otherwise protective film allowing the ingress of hydrogen to the alloy. In the absence of chemical damage to the film, mechanical damage by slip step intersection, first with the free surface for crack initiation, and subsequently with advancing fracture surfaces, allows hydrogen to enter the alloy, again presumably carried by dislocations. Thus non-chloride containing aqueous media (water vapor, distilled water, $SO_4^=$ solution, etc.) all behave in a similar manner. According

to this model, only the process zone at the crack tip need contain hydrogen to cause accellerated crack growth. Thus the normally low bulk diffusion rates generally reported for hydrogen in aluminum alloys need not be rate controlling.

A second aspect of the model is the requirement for a specific distribution and morphology of strengthening precipitates. Thus alloys such as 1100 Al (commercially pure) or 2024 (Al-Cu) would not necessarily be expected to be embrittled. Likewise, overaging or underaging heat treatments which alter precipitate/matrix relationships would be expected to alter the sensitivity of alloys to corrosion fatigue.

In summary, the key to the corrosion fatigue phenomenon in Al alloys may be related to the method by which hydrogen enters the alloy. Since the naturally formed film on the alloy appears to exhibit a low permeation to hydrogen, those mechanical or chemical events which weaken or damage the film may control the crack initiation/propagation process. This would then help to explain the effects of cyclic stress range and the lack of effect of mean stress level (mechanical factors) and the effects of such variables as chloride ion, high or low pH, applied potentials or currents, and solution chemistry in general.

Summary

To summarize, a model for corrosion fatigue of high strength Al alloys is proposed which is dependent on surface film integrity. Chemical or mechanical damage to the film, allowing exposure of hydrogen to emerging dislocations (slip planes) which effectively "pump" hydrogen into the crack process zone. It is further suggested that the hydrogen collects at precipitate matrix interfaces and, through some still unknown specific mechanism, causes separation of the interfaces. The model is an extension of previous models proposed for stress corrosion cracking of these alloys, except that the cyclic nature of the dislocation motion creates a preferentially high diffusion path into the process zone rather than into the normal high diffusity zone of grain boundaries.

References

1. J.T. Staley: Met. Eng. Quarterly, 1976, vol. 16, p. 52.
2. C.E. Lyman and J.B. VanderSande: Met. Trans., 1976, vol. 7A, p. 1211.
3. P.J.E. Forsyth, Acta Met., 1963, 11, 703.
4. C.A. Stubbington and P.J.E. Forsyth, J. Inst. Metals, 1961, 90, 374.
5. Calabrese, C. and Laird, C., The cyclic stress-strain response of metals and alloys, Proc. 3rd Int. Conf on Fracture, Munich, 1973, Vol. 6, V231; Cyclic stress-strain response of two-phase alloys, I. Microstructures containing particles penetrable by dislocations, II. Particles not penetrable by dislocations, Mater. Sci. Eng., 13, 141, 1974.
6. D.J. Duquette and P. R. Swann, Acta Met., 1976, 24, 241.
7. A. Hartman: Int. J. of Fract. Mech., 1965, vol. 1, p. 167.
8. R.P. Wei: Eng. Fract. Mech., 1970, vol. 1, p. 633.
9. T. Broom and A. Nicholson: J. Inst. of Metals, 1960, vol. 89, p. 183.
10. R.P. Wei: Int. J. of Fract. Mech., 1968, vol. 4, p. 159.
11. M. Nageswararao, G. Kralik and V. Gerold: Z. Metallik, 1975, vol. 66, p. 479.
12. M. Nageswararao and V. Gerold: Met. Trans., 1976, vol. 7A, p. 1847.
13. S.J. Hudak and R.P. Wei: Corrosion Fatigue ed. O. Devereux, A.J. McEvily and R.W. Staehle, 1971, p. 433, NACE, Houston.
14. C. Zapffe and C. Sims, Trans. Met. Soc. AIME, (1941), 145, 225.
15. R.M. Pelloux: Fracture 1969, op. cit., p. 731.
16. R.J. Selines and R.M. Pellous: Met. Trans., 1972, vol. 3, p. 2525.
17. R.E. Stoltz and R.M. Pelloux: Met. Trans., 1972, vol. 3, p. 2433.
18. R.M.N. Pelloux: ASM Trans. Quart., 1969, vol. 62, p. 281.
19. J.C. Grosskreutz: Surface Sci., 1967, vol. 8, p. 173.

20. C.A. Stubbington, Metallurgia, 1963, vol. 65, p. 109.

21. P.J.E. Forsyth: Acta Met., 1963, vol. 11, p. 703.

22. R.P. Wei and J.D. Landes: Int. J. of Fract. Mech., 1969, vol. 5, p.69.

23. R.J. Jacko, Ph.D. Thesis, Rensselaer Polytechnic Institute, (1978).

24. F.P. Ford: Ph.D. Thesis, Cambridge University, 1973.

25. B.F. Brown, C.T. Fujii and E.P. Dahberg: J. Electrochem. Soc., 1969, vol. 116, p. 218.

26. A.J. Sedricks, J.A.S. Green and D.L. Novak: Localized Corrosion, op cit., p. 569.

27. D. Whitwham and U.R. Evans: J. Iron and Steel Inst., 1950, vol. 165, p. 72.

28. D.J. Duquette and H.H. Uhlig, Trans. ASM, (1968), 61, 449.

29. D.J. Duquette and H.H. Uhlig, Trans. ASM, (1969), 62, 829.

30. H.N. Hahn and D.J. Duquette, Acta Met., (1978), 26, 279.

31. K. Laute: Oberflächentech, 1933, vol. 10, p. 281.

32. T. Pyle, V. Rollines and D. Howard: Corrosion Fatigue: Chemistry, Mechanics and Microstructure, op. cit., p. 312.

33. T. Pyle, V. Rollins and D. Howard: J. Electrochem. Soc., 1975, vol. 122, p. 1445.

34. C. Patel, T. Pyle and V. Rollins: Met. Sci., 1977, vol. 11, p. 185.

35. C. Patel, T. Pyle and V. Rollins: Nature, 1977, vol. 266, p. 517.

36. F.P. Ford and T.P. Hoar: Proc. of 3rd Int. Conf. on Strengthening of Metals and Alloys, Cambridge, 1973, paper 95.

37. S.P. Lynch: in Mechanisms of Environment Sensitive Cracking of Materials, 1977, p. 201, The Metals Society, London.

38. G.M. Scamans and C.D.S. Tuck: Second Int. Cong. on Hydrogen in Metals, Paris, 1977, paper 4A11.

39. L. Montgrain and P.R. Swann: Hydrogen in Metals, op. cit., p. 575.

40. J.A. Donovan: Met. Trans., 1976, vol. 7A, p. 1677.

Acknowledgement

The support of the U.S. Office of Naval Research and the continued encouragement of Dr. P.A. Clarkin are gratefully acknowledged.

TABLE I

The Effect of a Re-Heat Treatment Duration on Subsequent Fatigue Properties in Air

Pre-Corrosion: 24 hours in aerated 0.5 NaCl

Re-heat treat: Solutionize at 470°C for x hours
Age at 121°C for 24 hours

Fatigue in air: Mean stress 276 MPa, Cyclic Stress ± 96 MPa

Time at 470°C	N_f
0 hours	30,000 cycles
3 hours	85,000 cycles
6 hours	101,000 cycles
24 hours	> 13,000,000 cycles

TABLE II

Effect of Cyclic Load on the Fracture Morphology of Al-5.5Zn-2.5Mg-1.5Cu in 0.5M NaCl Polarized to -1.75V vs. SCE

Cyclic Stress MN/m^2 at σ_m = 207 MN/m^2	% Intergranular Failure
76	0
69	0
55	0
41	10
28	26
17	35

TABLE III

A Summary of Experimental Observations on the Mechanisms of Corrosion Fatigue of Al Alloys

Experimental Observation	Hydrogen Embrittlement	Enhanced Anodic Dissolution
Sensitivity to water in both the liquid and vapor form.	Strong support for H.E.	Water vapor should have no effect when crack is notfilled with a liquid phase.
Crack path shift reported from {111} to {100} in aggressive solutions.	Consistent with environmentally induced cleavage.	Not easily attributable.
Sensitivity to Anion Type and Concentration.	Affects the passivation rate and oxide film stability which control both mechanisms.	
Decreased fatigue resistance in both acid and basic Na_2SO_4.	Consistent if modifications in the oxide are more important than H^+ concentration of bulk solution.	Supportive because both make the oxide less stable and make dissolution easier.
Decreased fatigue resistance with cathodic polarization in NaCl.	Supportive, higher surface hydrogen concentration.	Some support, can be explained by changes in oxide film.
Decreased fatigue resistance with anodic polarization in NaCl.	Consistent with the improtective nature of oxide and higher H^+ activity.	Supportive, increasing dissolution rate increases rate of cracking.
Decreased fatigue resistance in Na_2SO_4 with cathodic polarization.	Parallel behavior as in NaCl because there is increased hydrogen in both solutions.	Some support due to less protective oxide film.
Similarity between potential dependence for fatigue and hydrogen permeation in NaCl.	Strong support.	Can be explained by modifications in oxide film behavior.
Fatigue in deaerated solutions.	Consistent with easier H entry.	Can be explained by resultant changes in the oxide film.
Pre-exposure effect and the partial reversibility upon reheat treatment.	Unambiguous support for H.E.	Cannot be explained.
Insensitivity of fatigue lives to mean stress in aggressive environments.	Consistent with idea of H transport by mobile dislocation which are produced by cyclic stress component.	Consistent with mechanism because the cyclic stress controls the slip step area exposed.
Insensitivity to aggressive environments under Mode III loading compared to Mode I loading.	Supportive, there is no hydrostatic stress component in Mode III to concentrate H in the crack tip region.	Not supportive unless effect is due to the inability of the solution to get to the crack tip region. This is considered unlikely in the dynamic fatigue testing.

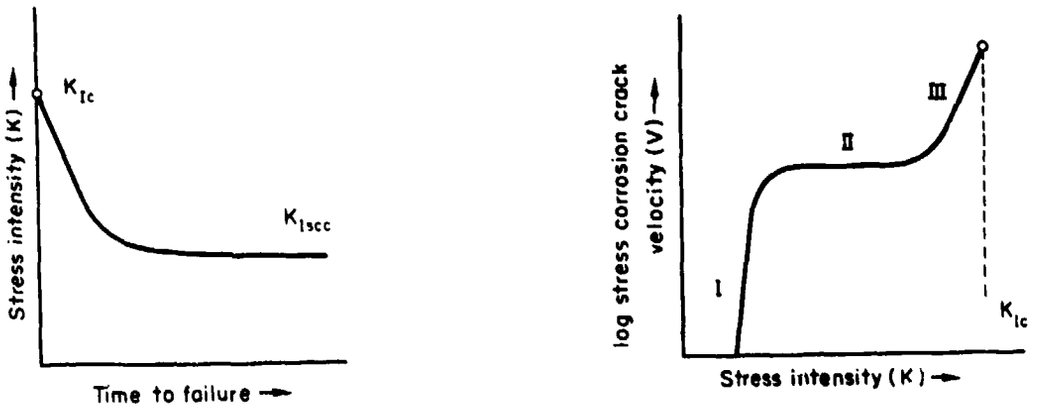

Figure 1. a) Schematic diagram of stress intensity factor (K) versus time to failure in a stress corrosion environment at K. Below K_{ISCC} failure should not be observed. This type of data is also reported as stress versus time to failure for smooth specimens, and a threshold stress level is then determined.

b) Schematic diagram of crack velocity versus stress intensity factor for an alloy susceptible to SCC. K_{ISCC} is often described by the intersection of stage I cracking with the K axis. Stage III cracking is not always observed and K_{IC} is the fracture toughness of the alloy in the absence of environment.

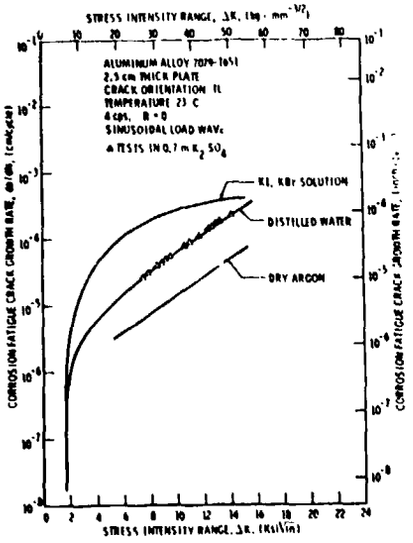

Figure 2.

Figure 2. Typical fatigue crack propagation data for a precipitation hardened aluminum alloy. It should be noted that crack propagation rates in distilled water and in 0.7 m K_2SO_4 are identical and greater than in argon but that halides considerably increase crack propagation rates at virtually all ΔK values.

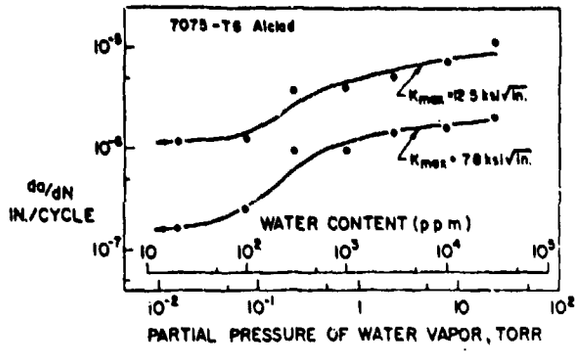

Figure 3.

Figure 3. Typical crack propagation data for a precipitation hardened aluminum alloy as a function of the partial pressure of water vapor. Note that the behavior is similar for each K_{max} value, but that there is a marked increase in crack propagation rates at $p_{H_2O} > 10^{-1}$ torr. With the exception of the transition zone between 10^{-1} and 10^{0} torr da/dN^2 is virtually constant.

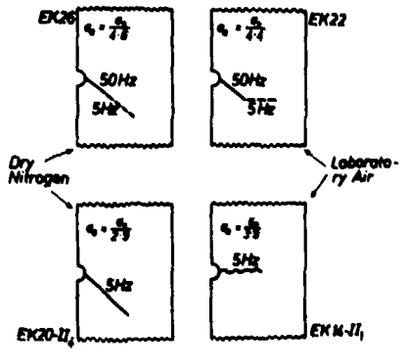

(a)

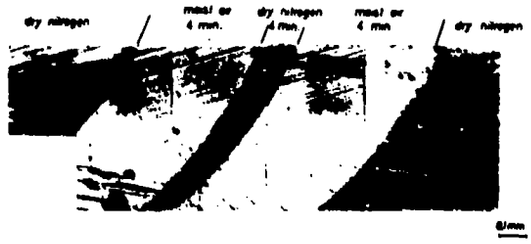

(b)

Figure 4. a) Schematic diagram of crack propagation in high purity Al Zn Mg alloy single crystals exposed to dry N_2 and to laboratory air (with some unmeassured water vapor present) as a function of frequency. In N_2 cracks grow crystallographically independent of test frequency. However, in air, decreasing test frequency either causes the crack to deviate to a stage II mode or, if the test is begun at a low frequency, the stage I mode is not observed. These data suggest a time dependent reaction in laboratory air.

b) Fracture surface of an Al Zn Mg single crystal showing that, at a constant frequency, crack propagation rates are considerably increased in moist air vs. in dry N_2.

(a) (b)

Figure 5. Fatigue fracture surfaces of 7075 T6 tested in (a) dry air showing ductile or type A striations and (b) in 0.5 NaCl showing brittle or type B striations. Tests of this alloy in distilled water or in 0.5 N Na_2SO_4 produce striations similar to type A but the application of cathodic potentials in Na_2SO_4 causes a change to type B. Arrows indicate direction of crack growth and brackets indicate crack advance per cycle.

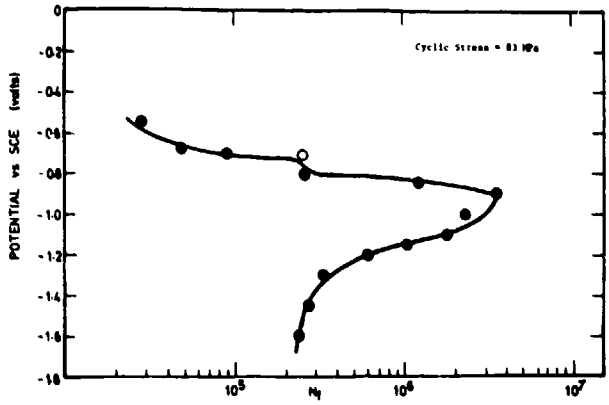

Figure 6.

Figure 6. Fatigue life versus electrochemical potential for a 7075-T6 alloy in 0.5 N NaCl. The open circle corresponds to the corrosion potential. Small cathodic potentials increase fatigue lives, but larger deviations for the corrosion potential cause a decrease in fatigue resistance. Anodic polarization always decreases fatigue resistance.

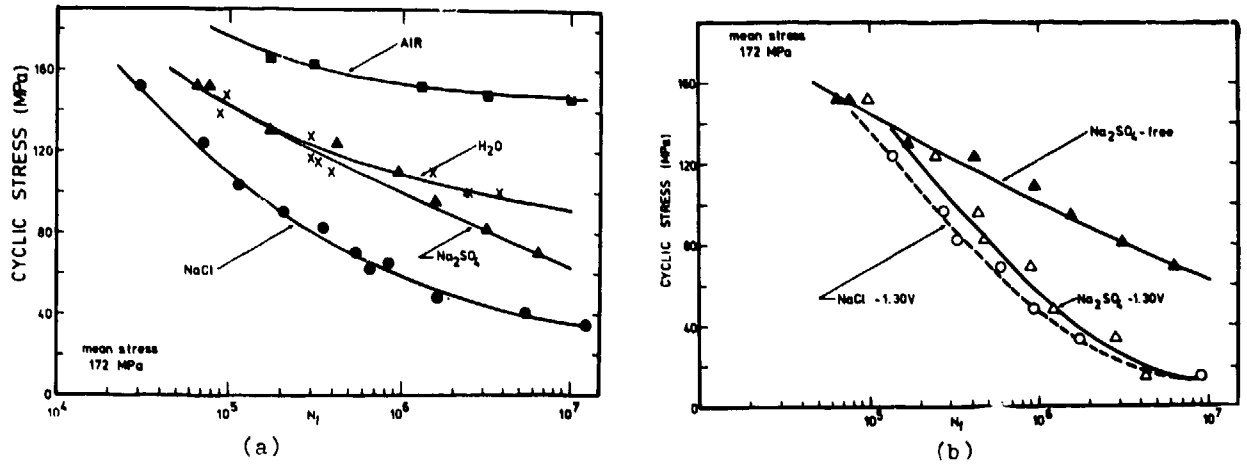

Figure 7. a) Fatigue behavior of 7075-T6 exposed to air, H_2O and 0.5 N Na_2SO_4 and 0.5 N NaCl. H_2O and Na_2SO_4 solutions show similar behavior (see Figure 2).

b) Effect of cathodic polarization of 7075-T6 in 0.5 N NaCl and 0.5 N Na_2SO_4 showing essentially identical behavior for either anion.

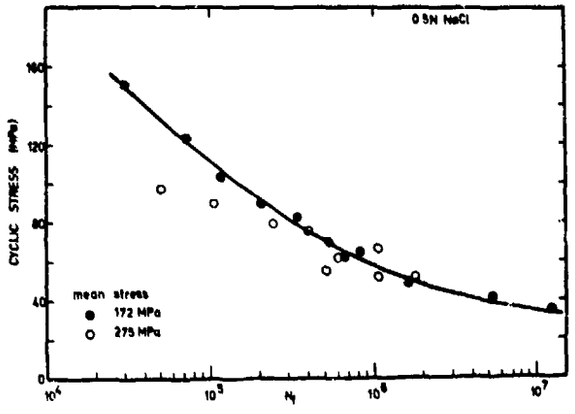

Figure 8.

Figure 8. Effect of mean stress on the corrosion fatigue behavior of 7075-T6 in 0.5 N NaCl solution showing that, except at very large cyclic stresses (above σ_{YS}) mean stress has virtually no effect on fatigue resistance.

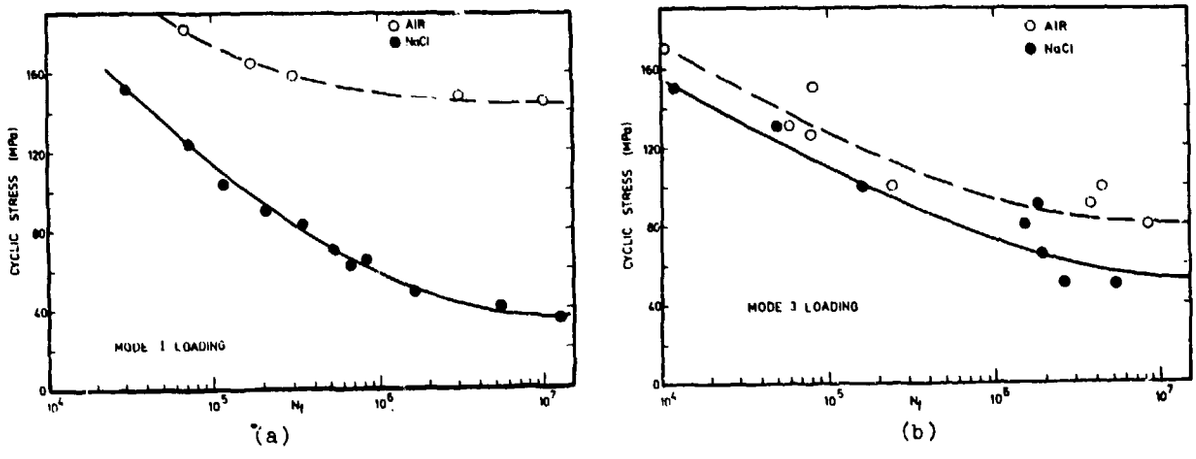

Figure 9. The effect of loading mode on fatigue resistance of 7075-T6 in 0.5 N NaCl solution. These data show that loading in shear has little effect on corrosion fatigue susceptibility when compared with tensile loading. The slight decrease in resistance which is observed in Mode III loading can probably be explained by the non-isotropic nature of the alloy.

FRACTURE MECHANICS BASED MODELLING OF THE CORROSION FATIGUE PROCESS

by

David W. Hoeppner,* Ph.D., P.Eng.
Douglas Mann,** BASc.
J. Weekes**

*Cockburn Professor of Engineering Design and
Director-Structural Integrity Laboratories
Department of Mechanical Engineering
University of Toronto
5 King's College Road
Toronto, Ontario M5S 1A4

**Mr. Mann and Mr. Weekes are graduate research assistants in Mechanical Engineering at the University of Toronto. Mr. Mann is an NSERC (Natural Sciences and Engineering Research Council) Fellow.

Prepared for presentation at Specialist Meeting on Corrosion Fatigue NATO-AGARD (Advisory Group for Aerospace Research and Development), 52nd Meeting of the Structures and Materials Panel, 1981:04:05-10, Cesme, Turkey.

Acknowledgement: The authors are grateful to the NSERC and Department of Energy, Mines and Resources (Canada) for support.

Dedication: To the memory of John Dunsby. John stimulated many of the ideas contained herein.

Abstract: Corrosion fatigue of structural elements involves a synergism between cyclic load and a chemical environment involving both time and temperature as rate-controlling parameters. Thus, it is very complex to understand mechanistically. Furthermore, the development of rational life prediction methods is hampered by both the lack of mechanistic understanding, the large number of corrosion-fatigue synergisms, and the inadequacies of fracture mechanics based models in both pre mode I fatigue cracking and initial mode I cracking. Aspects of mechanisms related to the formulation of corrosion fatigue life prediction models will be discussed in relation to micromechanical modelling based on fracture mechanics. Emphasis will be placed on the formation of mode I fatigue cracks from pits, and fretting surface damage. A discussion of the needs in this area will be presented. It is believed that with further analytical and experimental information the models presented can be verified and provide useful guidance to engineers and scientists attempting to deal with corrosion and fretting fatigue.

NOMENCLATURE:

- A = Stress Ratio (R sometimes preferred), ratio of alternating stress to mean stress, R is the ratio of the minimum stress to the maximum stress, thus, $R = (1-A)/(1+A)$ and $A = (1-R)/(1+R)$.
- a = Surface crack depth, units of length.
- a_i = Minimum inspectable discontinuity size for a given material for a given non-destructive inspection technique and procedure, units of length.
- a_{i_e} = Minimum inspectable discontinuity size for a given environmental exposure, units of length.
- a_o = Original discontinuity size in a material, units of length.
- b = parameter in pitting equation, experimental.
- $2c$ = Surface crack length, units of length.
- C = The ratio of the number of cycles of load to produce a crack of size a_i or a_o to the number of cycles of load that would cause failure at the same load or stress value; (N_i/N_f).
- C = Parameter in pitting equation, experimental.
- C_b = Same as C above except for a baseline condition.
- C_e = Same as C above except for a given environment.
- d = Pit depth, units of length.

E = Young's Modulus of Elasticity, psi (Mpa)

e = Threshold parameter for crack propagation data.

K = Stress intensity factor , psi$\sqrt{\text{in}}$ (or Ksi $\sqrt{\text{in}}$) (Mpa$\sqrt{\text{m}}$)

K_i = Initial stress intensity factor, psi $\sqrt{\text{in}}$ (Mpa$\sqrt{\text{m}}$)

K_{i_e} = Initial stress intensity factor for a given environment, psi $\sqrt{\text{in}}$ (Mpa$\sqrt{\text{m}}$)

K_{Ib} = Instability parameter in crack growth fitting function, psi $\sqrt{\text{in}}$ (Mpa$\sqrt{\text{m}}$)

K_{Ic} = Plane strain-stress intensity factor for the tensile (Mode I) mode of crack opening, psi $\sqrt{\text{in}}$ (Mpa$\sqrt{\text{m}}$)

K_c = Plane stress-stress intensity factor, psi $\sqrt{\text{in}}$ (Mpa$\sqrt{\text{m}}$)

ΔK = Range in stress intensity in a fatigue loading cycle, $\Delta K = (K_{max} - K_{min})$, psi $\sqrt{\text{in}}$ (Mpa$\sqrt{\text{m}}$).

K_{th} or ΔK_{th} = Threshold value of stress intensity below which no detectable flaw growth is observed in the fatigue loading cycles applied, psi $\sqrt{\text{in}}$ (Mpa$\sqrt{\text{m}}$), Mode I threshold unless otherwise specified.

h = Shape parameter for curve fitting.

N = Number of load cycles to failure (general case)

N_i = Number of cycles to initiate a crack of specified size at a specified stress level or stress intensity level.

N_{i_e} = Same as N_i except in a given environment.

N_f = Number of cycles to failure at a given stress level.

NDI = Non-destructive inspection.

NDT = Non-destructive testing; e.g. proof testing.

P_f = The applied fatigue load.

R = Stress ratio, defined under A above.

S_a = Alternating stress amplitude ($S_r/2$ where S_r is the stress range), psi(Mpa)

S_{mean} = Mean stress in a fatigue cycle, $(S_{max} + S_{min})/2$, psi(Mpa)

S_{max} = The highest algebraic value of stress in the stress cycle, psi(Mpa)

S_{min} = The lowest algebraic value of the stress in the stress cycle, psi(Mpa)

ΔS = The total stress range, used for S_r, psi(Mpa)

S_{net} = The net section stress based on the net section area, psi(Mpa)

t = Time for pit to develop.

v = Characteristic value for crack propagation data.

da/dN = The crack growth rate per cycle, in/cycle (usually μ in cycle or mm/cycle)

da/dt = The crack growth rate in a unit of time, in/sec or cm/sec

ω = Frequency, cps or hz.

INTRODUCTION

The challenge of fatigue design is dealt with by using the "safe-life" and "damage-tolerant" fatigue design philosophies. Frequently the safe-life concept is based on idealized elasticity and plasticity concepts with no-cracks or crack-like discontinuities allowed because of the simplistic assumptions. Thus, the safe-life concept, employing S-N, ε-N, and constant life fatigue diagrams, frequently has been used to estimate time to "first cracking" in a structure. However, it is well known that crack-like discontinuities can exist in the initial "state" of the structure or be created during the use cycle. Thus, fracture mechanics has been developed to aid in the design of aircraft structures of all types to tolerate the presense of either the inherent discontinuities or those created in the use cycle. Numerous conferences in the last fifteen years have aided in the formalization of fracture mechanics analysis procedures and data generation procedures to complement the already existing structural design methods. Several NATO-AGARD publications are available that discuss several aspects of this challenge to the aircraft structural design engineers (1-3). In addition to aircraft these concepts can be applied to ships and other structures (4). Figure 1 is a summary of the various aspects of fracture mechanics analysis that constitute a significant part of damage tolerant design today. These concepts are expanded in Figure 2(5). As part of the sub-critical growth stage (middle column of Figure 2) the anticipated service stresses and environments (thermal, chemical, and radiation) are needed to make a "life" estimate.

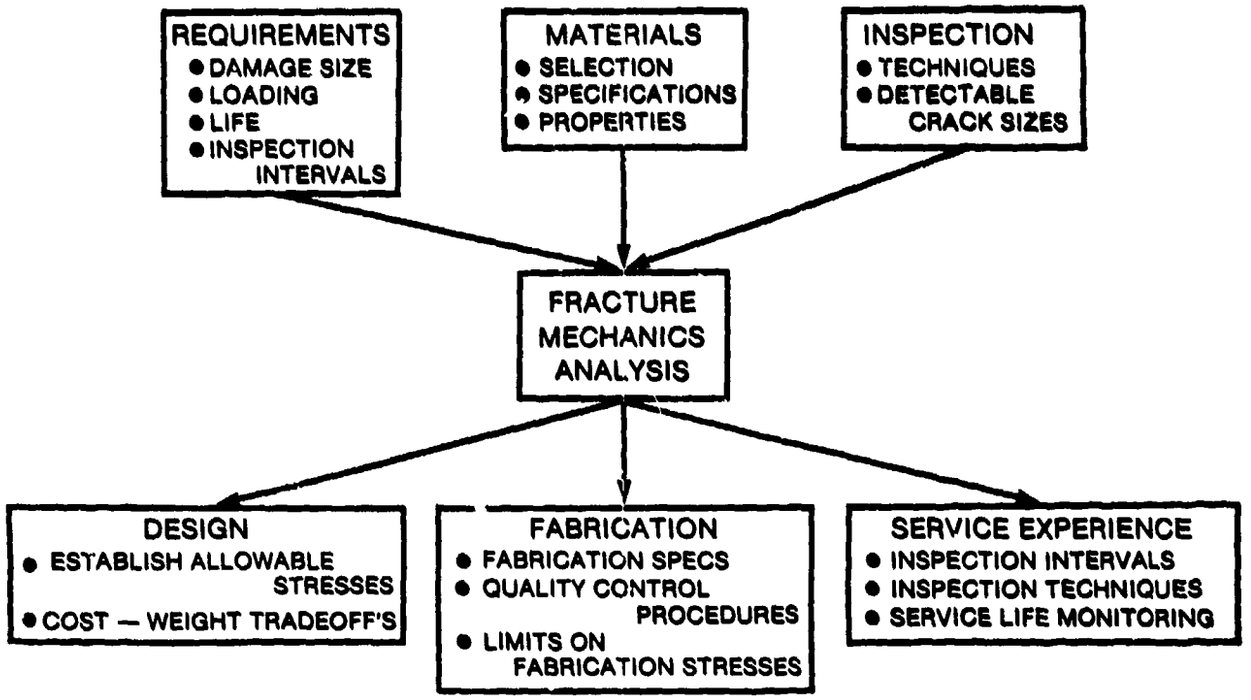

Figure 1 - Elements of Fracture Mechanics Design Methodology Used in Damage Tolerant Design of Aircraft, Surface Ship, Submersible, Spacecraft, Piping, and Power Generation Structures.

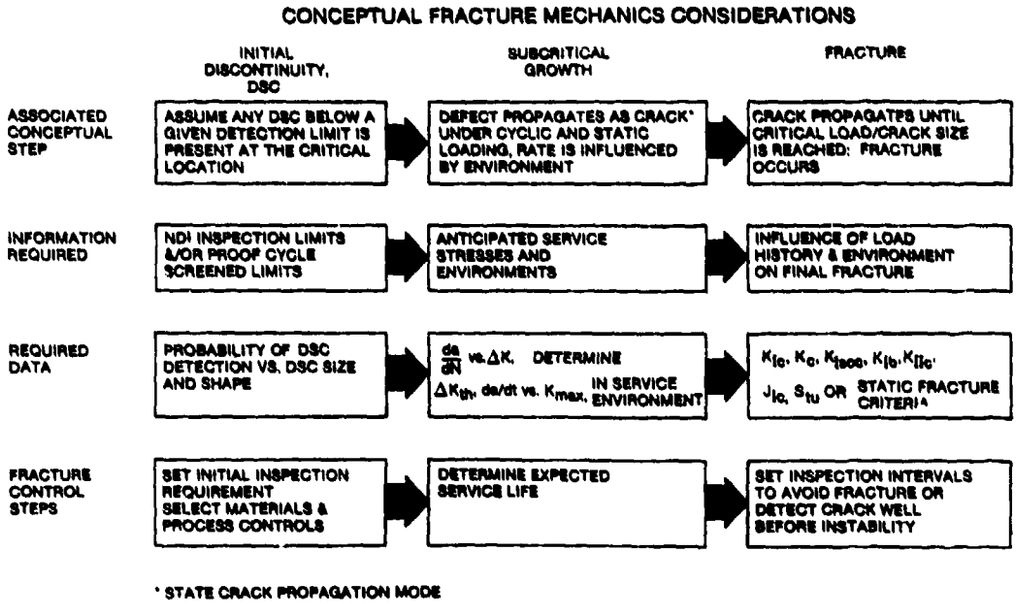

Figure 2 - Conceptual Fracture Mechanics Considerations in Design (5 - by permission)

In addition, data on crack extension rates in the environment are desired for the component and/or system in question.

The engineer, always faced with the exciting prospect of configuring the component to do the job intended (perform the function/mission) must now formally deal with the potential for inherent crack-like discontinuities. These inherent discontinuities can be any one of the following types:

INHERENT MATERIAL DISCONTINUITY

INHERENT MANUFACTURING AND ASSEMBLY DISCONTINUITIES

INHERENT GEOMETRIC DISCONTINUITY.

Given that a discontinuity is inherent an estimate of fatigue life can be made by application of reasonably well established procedures based on extension of the inherent discontinuity by fatigue crack growth under the conditions-of-interest to the structure (6-9).

Even though this may appear to be a straight forward problem it is not! W. Schütz (8) discussed some of the aspects of this great challenge previously: "The effect of environment on the materials properties must be investigated thoroughly. First, a definition of the actual environment is necessary. Is a test in 3.5 per cent NaCl actually a close enough simulation of an aircraft environment?

Second, corrosion is assumed to be a time-dependent phenomenon. However, the combined action of time and load, especially if the latter is variable, can reverse this effect, as reported in (10) and shown by IABG results ----. Here, tests under variable (8-step programme) loading demonstrated a much smaller effect of a salt-water environment than the latter. How can this be explained?

Third, a possibility must be found of shortening the testing time compared to actual service time, otherwise the tests take too long, are too expensive, and their results come too late". (Ref. 8 p 759)

Based on the extensive needs to find reliable and reasonably economical test methods and methods to transfer data to estimate inspection/repair/replacement intervals, numerous test programs are under way to develop a standardized test procedure to rank materials for their environmental fatigue resistance. In partial recognition of this need programs were initiated in 1968 by the U.S.A.F. that had the specific objective of providing information related to evaluating specific environments, establishing test procedures, producing data evaluation and presentation techniques in relation to material behavior of airframe, landing gear, and engine materials (11, 12). One of the results of both of the extensive studies cited was that much further work was needed. It is pleasing to thus participate in this meeting which is, in part, related to filling these great needs of the engineer/scientist to deal with the corrosion fatigue challenge.

Notwithstanding the significant progress being made in our ability to deal with environmentally assisted mode I crack growth, there is a large area of the problem of damage tolerant design that needs a great deal of attention. This is the area that deals with the production of localized "damage" in structures during the use cycle (including inspection, maintenance, repair, and replacement induced "damage"). Thus, even though crack-like discontinuities can be inherent as described, discontinuities can be created during the use cycle that may become more significant than the inherent discontinuities. This situation is represented conceptually in Figure 3. The items on the left indicate mechanisms of generation of a localized discontinuity (damage) from which a mode I crack may extend as indicated in the Figure.

This paper describes researches that have been underway to utilize fracture mechanics concepts to deal with the left side of Figure 3 as it relates to corrosion pitting fatigue and fretting fatigue. In the sections that follow the concepts being utilized are described. It is not our attempt here to go over all details of the work completed to date either in the Structural Integrity Laboratories of the University of Toronto or elsewhere. Rather, the concepts being developed will be described and reference made to recent researches that are relevant.

Dealing with Corrosion Fatigue from an Engineering Perspective

In 1971 a view of Corrosion Fatigue Considerations in materials selection and engineering design was presented (13). Figures 4-6 (from Ref. 13) suggested several important aspects of both the corrosion fatigue challenge and the fretting fatigue challenge that should be given consideration. Figure 4 provides guidance as to the various aspects that should be considered in a systems context. Clearly the aspects listed will have a synergistic interaction that is difficult to deal with Figure 5 presents the elements of the conceptual physical/chemical model presented in 1971(13) that are the basis for much of the research being done now to attempt to estimate the extent of life reduction related to the development of a mode I discontinuity or the propagation of a mode I discontinuity under conditions where the chemical environment is having a significant influence. This figure forms the basis of the discussion in the next section.

Figure 6 presents suggested engineering guidelines for dealing with the corrosion fatigue challenge. The portion on the left headed "initiation" deals with initiation of a given chemical

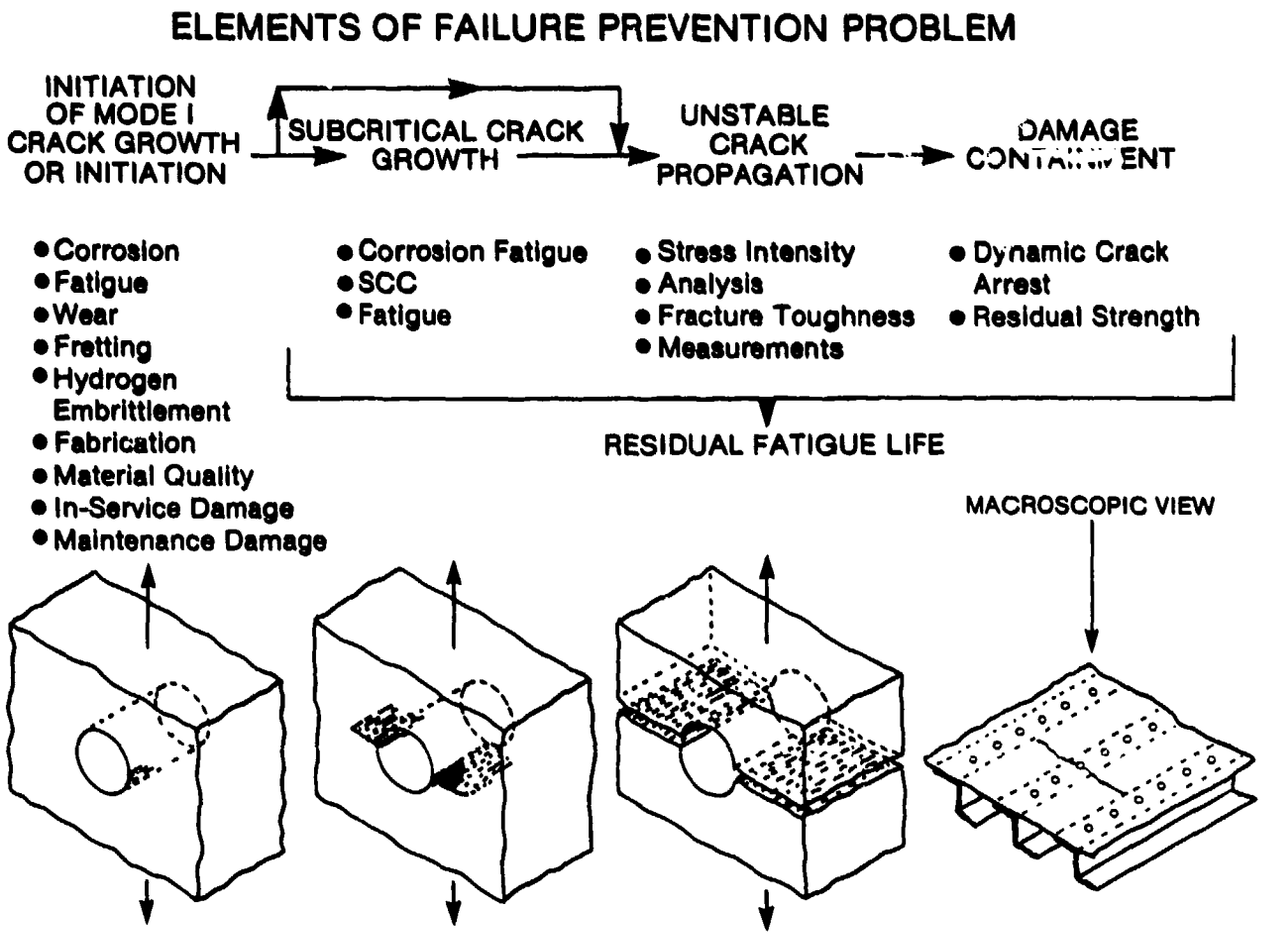

Figure 3 - Conceptual representation of elements of the failure prevention problem. [Crack-like discontinuities can be created during use by the processes indicated on the left. They may become large enough to produce a mode I crack that extends to produce fracture instability or be detected by either malfunction or inspection].

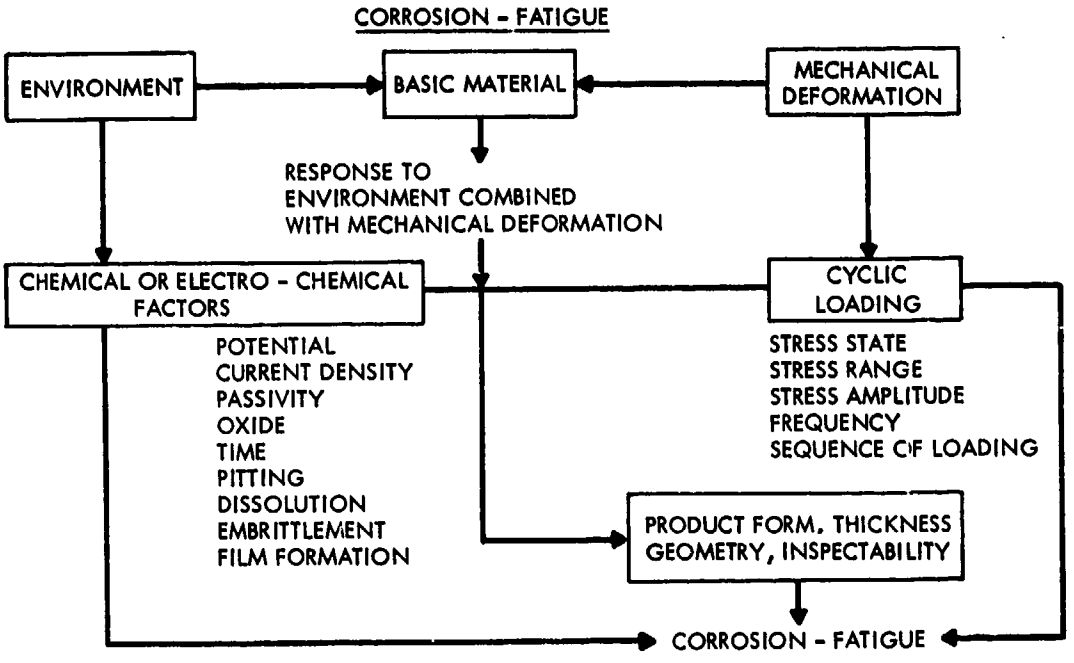

Figure 4 - The various aspects of the problem that should be considered in a systems context related to corrosion fatigue (13).

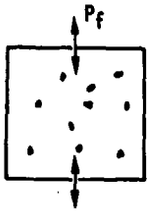

1 CORROSIVE ATTACK UNDER CYCLIC LOADING

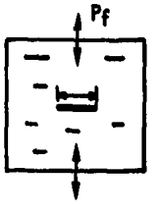

2 GENERATION OF A CRACK OF INITIAL, INSPECTABLE SIZE, a_i

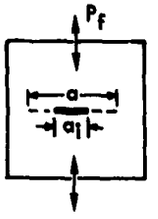

3 ENVIRONMENTALLY ENHANCED FATIGUE - CRACK PROPAGATION

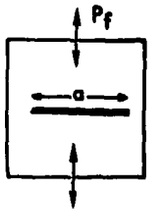

4 STRESS INTENSITY DOMINATED FATIGUE - CRACK GROWTH

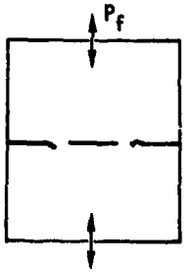

5 UNSTABLE FRACTURE

Figure 5 - The conceptual model presented in 1971(13) that has been expanded in recent years related to corrosion pitting fatigue.

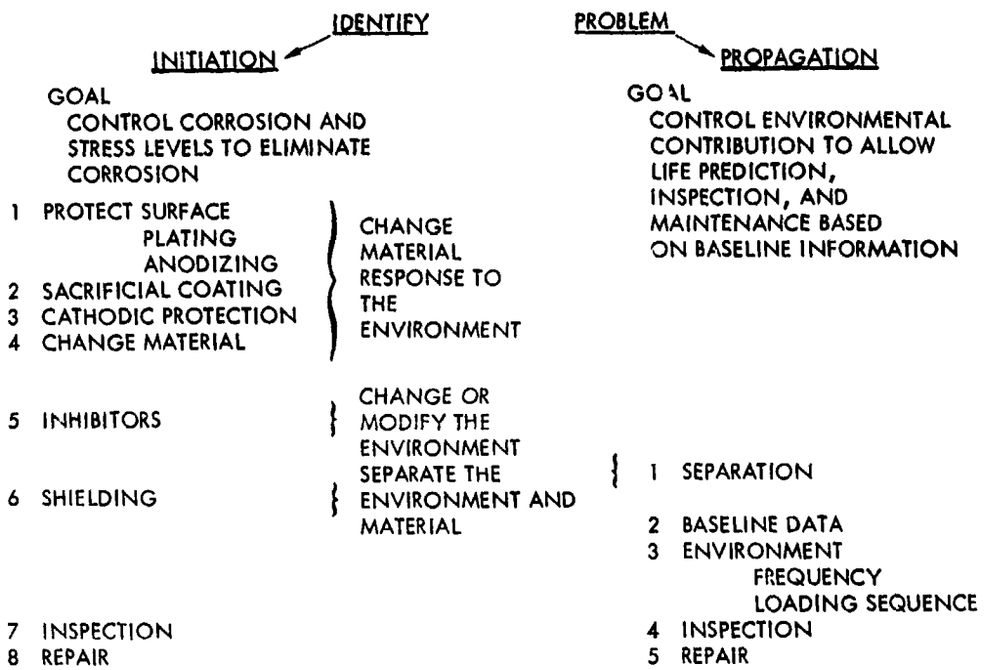

I OBTAIN BASELINE INFORMATION AND EFFECT OF ENVIRONMENT FOR FOR CONDITIONS OF INTEREST
II CHANGE MATERIAL RESPONSE TO THE ENVIRONMENT
III CHANGE OR MODIFY THE ENVIRONMENT
IV SEPARATE THE ENVIRONMENT AND MATERIAL
V OBTAIN PROPAGATION INFORMATION AND SET INSPECTION INTERVALS

Figure 6 - Suggested guideline for eliminating the corrosion fatigue challenge or alleviating it to an extent (13). Upper portion deals with initiation of pitting (or other corrosion form) under dynamic loading and the lower portion deals with crack propagation.

interaction with dynamic loading to produce physical discontinuities. As the column suggests the most desirable situation would be to eliminate corrosion so that its (or other corrosive forms) would not be "initiated". The left column of Figure 6 suggests ways that the problem is typically dealt with to prevent or eliminate the generation of discontinuities during the use cycle. If this is accomplished then no need would exist for using fracture mechanics to model the corrosion fatigue (or fretting fatigue) challenge, as exists for inherent discontinuities. The right side of Figure 6 suggested various ways to deal with propagation of mode I discontinuities. These aspects have been explored considerably and undoubtedly this research will continue.

In engineering other methods of dealing with the corrosion fatigue challenge exist. Anderson (14) suggested that lead the fleet articles be examined for corrosion fatigue as the "structure corrodes away". He also suggests that the full-scale fatigue test has dubious value since the compressed time under which it is conducted cannot simulate the corrosion aspect. [Even though we conduct full-scale fatigue tests for other reasons (notably identification of structural hot-spots) we agree with some of Anderson's assertions]. Crichlow (15), in the same AGARD document suggested fatigue life reduction factors (R_E) for three environmental exposures on the airframe for some common airframe materials as follows:

Material	Fatigue Life Reduction for Environmental Exposure Indicated (R_E)		
	Internal Structure Unexposed	External Structure - Exposed Normal Atmosphere	Active Environment*
Aluminum alloys Steel " Titanium "	1.25	2.0	4.0
Magnesium "	(4.0)	(8.0)	(10.0)

*Active environments include fuel sump water, food and human waste products, engine exhaust gases, and others more active than normal sea coast atmosphere (15).

Using the various approaches suggested, we have been able to cope with many aspects of both the corrosion fatigue and fretting fatigue challenge.

However, if as suggested in 1971(13) and in other publications on fretting fatigue a damage threshold exists, which, when crossed suggests that a mode I fatigue crack is propagating, the corrosion (or fretting) only has an influence to the extent that it may accelerate mode I crack growth. In many practical situations where we are not able to eliminate either corrosion pitting or fretting it is desirable to know the extent of either pitting or fretting that can be tolerated before repair or replacement action are taken. This is one of the main reasons for continuing the pursuit of the fracture mechanics modelling of corrosion pitting fatigue and fretting initiated fatigue.

Fracture Mechanics Modelling

The elements of the conceptual model for corrosion pitting fatigue are presented in Figure 7. The Figure should be viewed left to right. Basically, an attempt is made to evaluate the corrosion pit depth using pitting theory. Then, using knowledge of the fatigue-crack growth threshold in the environment under consideration the depth at which the pit converts from a pit to a mode I crack is estimated. The pit has been modelled as a surface "flaw" as indicated below:

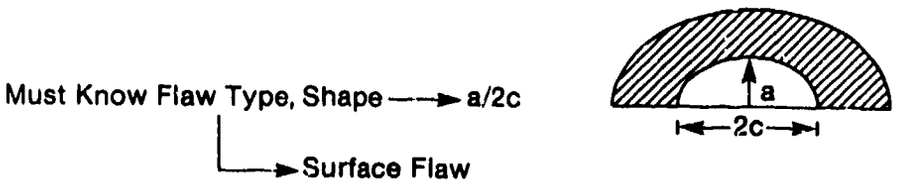

This turns out to be an oversimplification for numerous pit morphologies, but represents a starting point. Several of these concepts were significantly influenced by the contributions and stimulating interaction with Dr. G. Bowie. References 16 - 18 further coverage of the detailed concepts of the model are presented in References (16-18). Mayfield(19), Cox(20) and Weekes (21) all have conducted experimental research to continue the model verifications. The former workers conducted research on 2024-T851 and 2124-T851. Weekes conducted research on AISIC1045 Steel. For the materials evaluated to date (7075-T6, pipeline steels, 2024-T3, 2024-T851, 4340(280Ksi = Stu), Ti-6Al-4V[M A], and AISIC1045), the model offers some promise of providing estimation capability.

Several problem areas have been found to exist to date. These are:

1) The utilization of surface flaw equations provides simplicity but does not model many pit morphologies. The work of Cox(20)

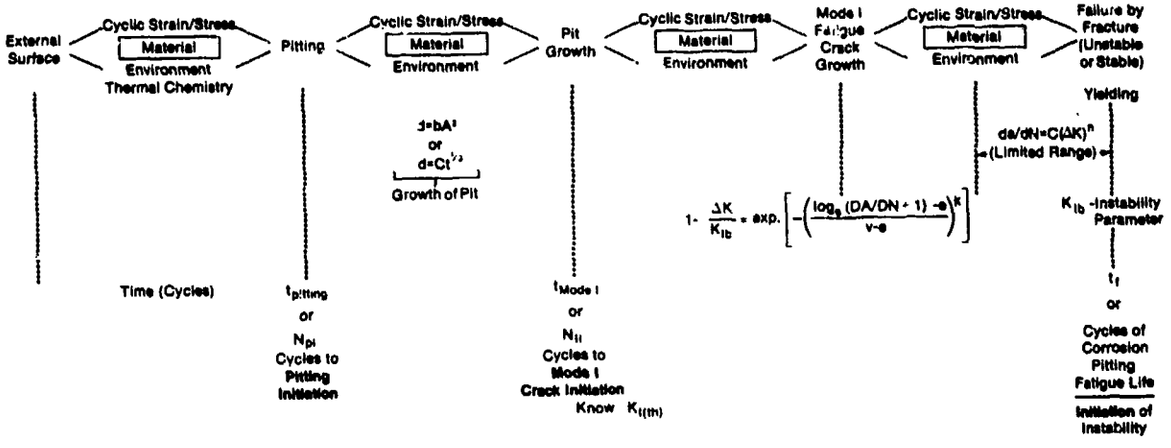

Figure 7 - Elements of Fracture Mechanics Modelling of Corrosion Pitting Fatigue (13, 16-18)

and Weekes (21), as well as Ebara (22, 23) and Kitigawa et al (24) indicate some variance of the pit morphology. The significance of this needs extensive evaluation.

2) Numerous small cracks have been observed by investigators to form within the pits. The transition of these multiple cracks within the pits to a mode I type crack needs much further study. An example of the type pit encountered in steel (21) is shown in Figure 8.

3) Statistical aspects of pit formation must be dealt with more extensively. Kitigawa (24) has approached this problem to some extent.

4) In the model use is made of the fatigue crack growth threshold determined by testing either compact tension or modified wedge opening loading specimens according to the ASTM practise. This is an expensive and time consuming procedure but must be done since the threshold of mode I crack growth is a critical parameter in the model. Cox(20) conducted tests on 2124-T851 in lab air and salt water. His results indicated a shift in threshold as shown in Figure 9. He determined the fatigue-crack growth threshold by fitting a Weibul survivorship function (16) to the data determined (indicated by the solid lines in Figure 9) and extrapolating to obtain the threshold as indicated by the equation below:

$K_{I(th)}$ = Mode I Fatigue Crack Growth Threshold

$$K_{I(th)} = K_{Ib}\left[1-\exp.\left(-\left[\frac{-e}{v-e}\right]\right)^{k}\right]$$

$$e = 0,\ K_{I(th)} = 0$$
$$e < 0,\ K_{I(th)} > 0$$

e-Threshold Parameter
v-Characteristic Value
k-Shape Parameter
} from test data

Establish $K_{I(th)}$ from data on the material for the conditions of interest

The fit of the function is critically dependent on the amount of data obtained in the environment over the full range of interest. Data are critically needed in the threshold regime and upper instability regime. These data do not exist to any really useful extent and this is a critical need.

5) The use of threshold data determined from CT or Mod WOL specimens needs to be compared from threshold data using preexisting cracks of the order of the pit - mode I transition crack size. (Many would refer to these as "small cracks".)

To date the use of this fracture mechanics model of corrosion fatigue has been encouraging with respect to the experimental verification. Furthermore it provides guidance and direction. Much greater emphasis probably should be given to this area best, as Anderson (14) suggested, we simply "corrode our aircraft away". Additional research is underway to provide additional understanding of the challenge. Similar concepts have been applied to fretting fatigue. This aspect will be discussed briefly related to fretting fatigue.

Fracture Mechanics Modelling of Fretting Fatigue

Fretting fatigue has been the subject of a previous AGARD meeting (25) and much information was provided at that meeting. Several recent references on fretting fatigue provide valuable guidance to dealing with it in structural design (26-28). Environmental aspects of fretting fatigue are discussed in references (29-32) as well as the excellent book by R. Waterhouse (Fretting Corrosion). Numerous researches are underway that are attempting to use similar concepts to those presented earlier to fretting. This is in part due to the hypothesis and verification of a fretting fatigue damage threshold by both Waterhouse and Hoeppner independently.

Figure 8 - An example of a corrosion fatigue pit wi·h small cracks in pit at various locations (21).

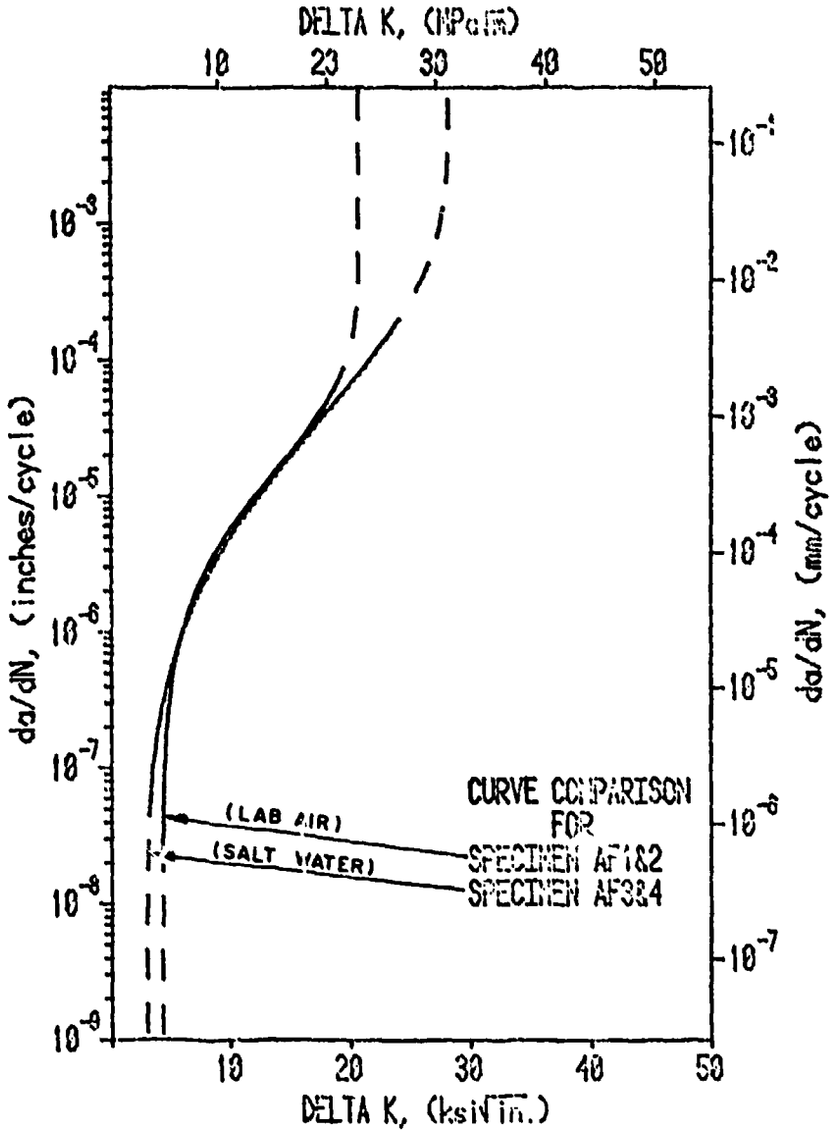

Figure 9 - FCP Curve Comparison Lab Air - Salt Water (20).

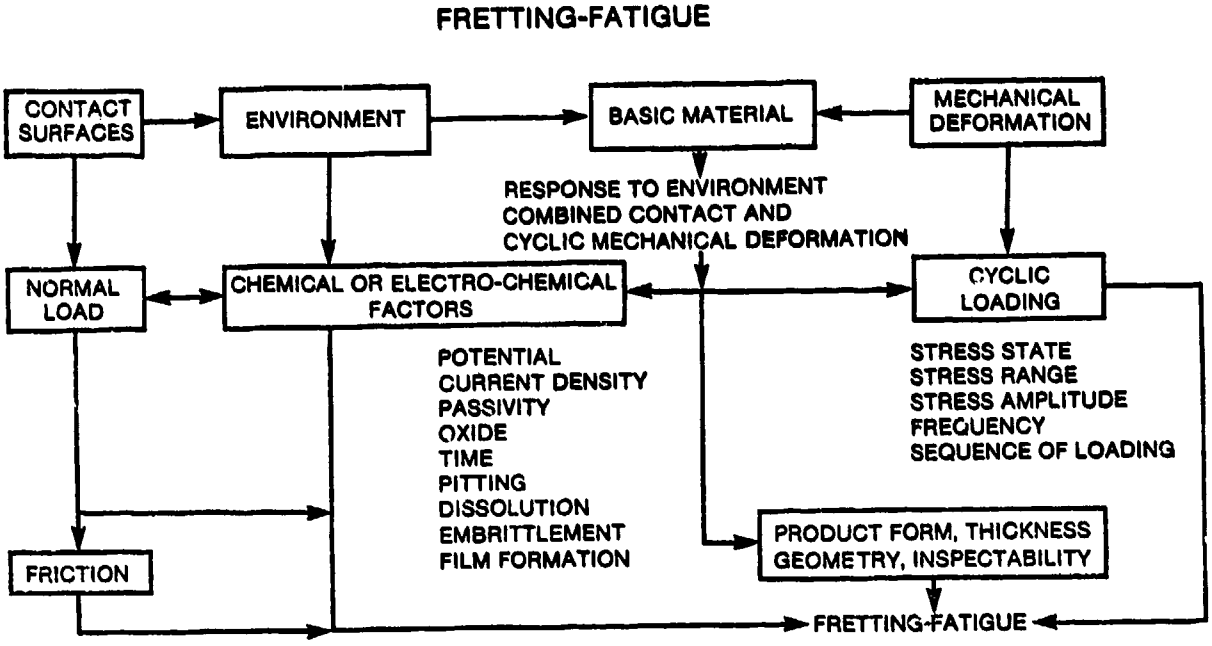

Figure 10 - Aspects that must be considered in the fretting fatigue system (32).

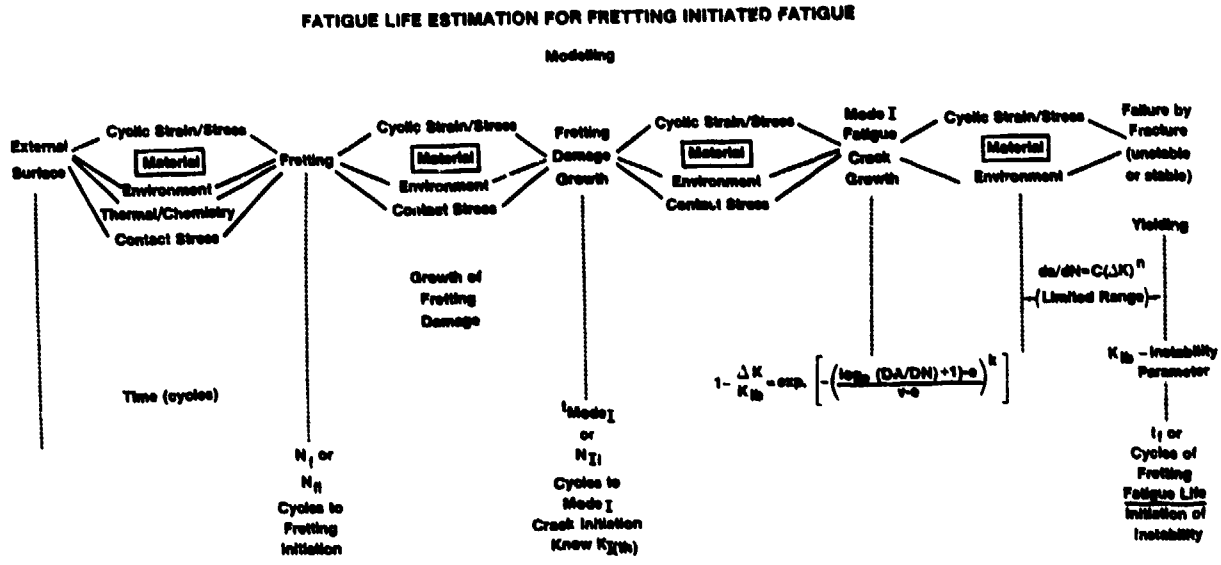

Figure 11 - A conceptual model for fretting fatigue similar to the one for corrosion fatigue (33).

Figure 10 presents the various factors that must be dealt with in consideration of fretting fatigue (32, 33). In addition, a conceptual model has been presented to deal with fretting fatigue (32-34). The model is presented in Figure 11. Reeves (29) and Poon (30) did extensive experimental work to verify this model and the success was encouraging. Recently D. Mann conducted a brief experiment to evaluate applicability of the model (35). He used starting discontinuities induced by both fretting damage and corrosion pits. The results from his research are extremely encouraging and we are continuing our efforts in this area.

All of the concerns related to the corrosion fatigue model can be expressed for fretting fatigue as well.

Closure

This paper briefly reviewed the use of fracture mechanics in modelling the corrosion fatigue and fretting fatigue challenges. Much insight has been gained in recent years to aid this procedure but a great deal remains to be accomplished. Nonetheless the ideas presented appear to offer guidance to engineers who are attempting to alleviate, eliminate or modify these two challenging failure modes.

References

1. AGARD Manual No.8 (Reprint)
   Advisory Group for Aerospace Research and
   Development, NATO
   MANUAL ON FATIGUE OF STRUCTURES:
   Fundamental and Physical Aspects (Reprint)
   W.G. Barrois
   1st published June 1970, reprinted June 1973

2. AGARDograph No.257
   Advisory Group for Aerospace Research and Development, NATO
   PRACTICAL APPLICATIONS OF FRACTURE MECHANICS
   Edited by H. Liebowitz
   Published May 1980

3. AGARDograph No.176
   Advisory Group for Aerospace Research and Development, NATO
   FRACTURE MECHANICS OF AIRCRAFT STRUCTURES
   Edited by: H.Liebowitz
   Published January 1974

4. Sorkin, G., Pohler, C., Stavovy, A., Borriello, F.,
   "An Overview of Fatigue and Fracture for Design and Certification
   of Advanced High Performance Ships", Engineering Fracture Mechanics,
   1973, Vol 5, pp 307-352.

5. Hoeppner, D.W., Figure from forthcoming book, "Structural Integrity Principles
   Applied to Engineering Design", to be published by John Wiley Interscience, by
   permission. This figure resulted from collective discussion and interaction
   with D. Pettit and W. Krupp in 1970 at Lockheed California Co. Burbank Calif.

6. D.W. Hoeppner, W.E. Krupp, "Prediction of Component Life by Application of
   Fatigue-Crack Growth Knowledge", Engineering Fracture Mechanics, 1974
   Vol 6, pp 47-70.

7. Barrois W., "The Strength of Structures and the Application of the Fracture Mechanics",
   Engineering Fracture Mechanics, 1978, Vol 10, pp 109-114.

8. Schütz, W., "Fatigue Life Prediction of Aircraft Structures - Past, Present and Future",
   Engineering Fracture Mechanics, 1974, Vol 6, pp 745-773.

9. Hoeppner, D.W., Ekvall, J., McCammond, D., Poon, C., Venter, R.
   "Aircraft Structural Fatigue, Course Notes for Course on Aircraft
   Structural Fatigue prepared for U.S. Federal Aviation Administration",
   1979, revised 1980, 3rd revision 1981. pp 552-565, 580-616.

10. Anderson, W.E., "Engineering Utility and Significance of Stress Corrosion Cracking Data",
    AGARD Conference Proceedings No.98,
    North Atlanta Treaty Organization, Advisory Group for Aerospace Research
    and Development,
    SPECIALIST MEETING ON STRESS CORROSION TESTING METHODS
    Published January 1972.

11. Hall, L.R., Finger, R.W., Spurr, W.F.
    "Corrosion Fatigue Crack Growth in Aircraft Structural Materials."
    AFML-TR-73-204, September 1973.

12. Pettit, D.E., Ryder, J.T. Krupp, W.E., Hoeppner, D.W.,
"Investigation of the Effects of Stress and Chemical Environments on the Prediction of Fracture in Aircraft Structural Materials",
AFML-TR-183, December 1974.

13. Hoeppner, D.W., "Corrosion Fatigue Considerations and Engineering Design",
Corrosion Fatigue: Chemistry, Mechanics and Microstructure.
O.Devereux, A.J. McEvily, R.W. Staehle,
Editors, NACE-2, 1972
National Association of Corrosion Engineers, pp 3-11.

14. Anderson, W.E., "Corrosion Fatigue-or How-to Replace the Full-Scale Fatigue Test",
AGARD Lecture Series No.62
Advisory Group for Aerospace Research and Development, NATO
FATIGUE LIFE PREDICTION FOR AIRCRAFT STRUCTURES AND MATERIALS
W. Schütz (Lecture Series Director)
Published May 1973

15. Crichlow, W.J., "On Fatigue Analysis and Testing for the Design of the Airframe",
AGARD Lecture Series No.62
Advisory Group for Aerospace Research and Development, NATO
FATIGUE LIFE PREDICTION FOR AIRCRAFT STRUCTURES AND MATERIALS
W. Schütz (lecture Series Director)
Published May 1973.

16. Bowie, F., Hoeppner, D.W., "Numerical Modelling of Fatigue and Crack Propagation Test Results",
Computer Simulation For Materials Applications, Nuclear Metallurgy,
Edited by R. Arsenault, J. Beeler, Jr., J. Simmons, Vol 20, part 2,
1976 pp 1171-1178.

17. Bowie, G., Besari, M., Weber, K., VanOrden, J., Pettit, D.,
"Correlation of Failure Analysis Data: Pitting Corrosion",
Lockheed California Co. Report LR27399, Dec 1975.

18. Hoeppner, D.W., "Model for Prediction of Fatigue Lives Based Upon a Pitting Corrosion Fatigue Process", Fatigue Mechanisms, ASTM-STP675, J.T.Fong, Editor.
1979, pp 841-870.

19. Mayfield, M.E., "Corrosion Assisted Fatigue in 2024-T851 Aluminum Alloy",
May 1978, M.S. Thesis, U.of Missouri-Columbia.
David W. Hoeppner, Thesis Supervisor.

20. Cox, James M., "Pitting and Fatigue-Crack Initiation of 2124-T851 Aluminum in 35% NaCl Solution", M.S. Thesis, U.of Missouri-Columbia, David W. Hoeppner, Thesis Supervisor, (Limited copies available from D.Hoeppner on request) 1979.

21. Weekes, J.R., "An Investigation Into the Initiation of Propagation of Fatigue Cracks from Corrosion Pits in AISI C 1045 Steel", B.A.Sc. Thesis, March 1981, University of Toronto, Department of Mechanical Engineering, D. Hoeppner, Supervisor.

22. Ebara, R., Kai-T., Inque-K., "Corrosion-Fatigue Behavior of 13Cr Stainless Steel in Sodium-Chloride Aqueous Solution and Steam Environment",
Corrosion Fatigue Technology, ASTM STP 642,
H.L. Craig, Jr., T.W. Crooker, D.W. Hoeppner, Editors
American Society for Testing and Materials, 1978, pp 155-168.

23. Ebara, R., Kai,T., Inque, K., "Long Life Corrosion Fatigue Behavior of 13 Cr Stainless Steel in NaCl Acqueous Solution", Proceedings of the 21st Japan Congress on Materials Research, Society of Materials Science, Japan, 1978.

24. Kitigawa, H., Fujita, T., Miyazawa, K., "Small Randomly Distributed Cracks in Corrosion Fatigue", Corrosion Fatigue Technology, ASTM STP 642, H.L. Craig, T.W. Crooker, D.W. Hoeppner, Editors, American Society for Testing and Materials, 1978, pp 98-114.

25. AGARD Conference Proceedings No. 161
Advisory Group for Aerospace Research and Development, NATO
FRETTING IN AIRCRAFT SYSTEMS
Published January 1975.

26. CONTROL OF FRETTING FATIGUE, National Materials Advisory Board (NMAB), National Research Council, National Academy of Sciences, NMAB 333, Washington. D.C., 1977.

27. Hoeppner, D.W., Gates, F., "Fretting Fatigue Considerations in Engineering Design",
To be published in WEAR, 1981.

28. Barrois, W., "Repeated plastic deformation as a cause of mechanical surface damage in fatigue, wear, fretting-fatigue, and rolling fatigue", International Journal of Fatigue,
Vol 1, No 4, Oct. 1979, pp 167-189

29. Reeves, R.K., Hoeppner, D.W., "Microstructural and Environmental Effects on Fretting Fatigue", WEAR, 47(1978) 221-229.

30. Poon, Cheung Jarm, "Environmental Effects on the Mechanism of Fretting Fatigue in 7075-T6 Aluminum", Ph.D. Dissertation, UM-Columbia, 1978 Columbia Mo.

31. Poon, Cheung Jarm, Hoeppner, D.W., "The Effect of Environment on the Mechanism of Fretting Fatigue", WEAR, 52 (1979) 175-191

32. Hoeppner D.W., "Environmental Effects in Fretting Fatigue", in Fretting Fatigue, R. Waterhouse, Editor, Applied Science Publishers. 1981, pp 143-158

33. Hoeppner D.W., Structural Integrity Principles Applied to Engineering Design, to be published Wiley-Interscience.

34. Mann D., "Stress Intensity Factor Verification Using Crack Propagation Data for Surface Cracks Under Fretting Conditions", Special Project Assignment for Fracture Mechanics MEC1304F, 1981.

CORROSION FATIGUE BEHAVIOUR OF SOME ALUMINIUM ALLOYS

by

D. Aliaga and E. Budillon
Aerospatiale , Laboratoire Central
12, rue Pasteur 92152 Suresnes

ABSTRACT

The present study deals with the evaluation of corrosion fatigue strength of aluminum alloys currently used in the aeronautical industry.

Crack propagation was evaluated in various different environments (dry argon, wet air, salt water). The effect of frequency, of test specimen thickness, and of ratio R

$$\left(R = \frac{K_{min}}{K_{max}} \right)$$ were investigated

And the effect of these various environments on the endurance limit at 10^7 cycles was likewise studied and some surface protections evaluated.

1 - INTRODUCTION

In fatigue the tests carried out at the laboratory are not always representative of the real conditions encountered in service. In particular the effect of the environment which can be considerable should not be neglected at structure design level. To this end the intent of the present survey is to compare the response in fatigue of various aluminum alloys used in the aeronautical construction.

The environments studied are the following : dry argon, wet air and salt-water. They were retained so as to simulate and amplify the more or less aggressive nature of these environments in which aircraft can find themselves both on the ground or in the air. In this survey the two major aspects of corrosion fatigue namely crack initiation and crack propagation were studied with an emphasis on in-service behaviour.

The importance of the corrosion fatigue phenomenon has been evaluated in various alloys. As far as crack propagation was concerned the environmental effect on the Paris law has been identified for rates ranging from 10^{-4} to 10^{-2} mm/cycle. But on the contrary, the theoretical aspects of those mechanisms involved in corrosion fatigue have not been studied. As far as crack initiation is concerned some surface treatments and protections currently used in aeronautics have been examined in various environmental conditions.

2 - MATERIALS AND EXPERIMENTAL PROCEDURES

To study crack propagation type 2024, 2214, 2618, 6061, 7175, 7575, 7050 alloys have been evaluated with an emphasis in type 2618 A and 7175 alloys. To study crack initiations the two last alloys only were examined under the following test conditions :

- without surface treatment,
- with chromic acid anodizing,
- with an aircraft type protection

2.1 - Materials studied

The materials and semi-finished products we studied are given in the following table :

Materials	Direction	R_{O2}-MPa	R-MPa	Originating products
2024 T 351	T	332	486	Plate 60 mm thick
2214 T 651	T	437	504	Plate 45 mm thick
2618 A T 851	T	417	460	Plate 55 mm thick
6061 T 6	T	295	327	Extruded spar
7050 T 73651	T	446	514	Plate 90 mm thick
7175 T 7351	T	428	489	Plate 50 mm thick
7475 T 7351	T	426	494	Plate 60 mm thick

2.2 - Test specimens

To study crack propagation, two different types of test specimens with different thicknesses have been retained to evaluate the possible effect of this parameter on their behaviour :

- a compact tension specimen (CT, 75 mm wide 10 mm thick)
- center crack tension specimen (CCT, 600 x 200, 1.6 mm thick)

Crack initiation has been studied in "Moore" type specimens taken from the transverse direction using a conventional rotating-bending machine and after having received the various following surface treatments :

A- as machined (no protection)

B- alochrome (Alodine 1200) and a paint coat (Airbus type)

C- chromic acid anodizing (see appendix for detailed process)

D- chromic acid anodizing plus shot peening

2.3 - Methods and test conditions

The test set-ups are shown in appendix. The test enclosure is made of plexiglass and the assembly sealing is ensured by plastic seals bonded in-between the enclosure and the test specimen. During crack propagation, the measurement of crack length is carried out with the help of gages bonded to the CCT specimens and visually with an hand magnifying glass on the CT specimens.

In rotating-bending tests endurance limits were determined at 10^7 cycles by the so-called "staircase method" each increment being of 10 MPa ; 15 test specimens were used for each limit. Because of the number of cycles which is relatively high (10^7) it has been decided to consider negligible the ratio existing between propagation rate cycle number and life duration, consequently the endurance limit so noted is most typical of crack initiation status. Tests were carried out at a frequency of 50 Hz which corresponds to exposure periods of about 56 hours.

The three different environments which we studied are as follows :

- Dry argon - The composition of which is as follows :

A	99.995 %
O_2	5 ppm
H_2O	5 ppm
N_2	40 ppm

The argon flow into the test cell was 2 l/min.

- Wet air - The production of water vapor was obtained by bubbling compressed air through water. An hygrometer was used to control the relative humidity into the cell which should range from 85 to 95 % during test.

- Salt-water - The solution used (type A3) contained per liter of demineralized water :

30 g	NaCl Sodium chloride
0.19 g	Disodium phosphate
1.25 g	Boric acid

The solution pH was adjusted to 8 with sodium carbonate. The solution has been changed as soon as the pH value was no more meeting the adequate requirement.

3 - TEST RESULTS

All the results are shown in Fig. 1 to 20 for crack propagation and in Fig 21 for crack initiation.

3.1 - Crack propagation

2618 A T 851 Alloy

- Effect of environment

Fig. 4 shows that propagation rates are quite similar in both salt-water and wet air. On the contrary there is a significant deviation between the above rates and rates measured in dry argon. It should be noted moreover that said deviation is the more important, the propagation rates are lower and ratio R is lower.

- Effect of test frequency

The effect of test frequency was evaluated between 0.1 and 25 Hz in three different environments. The results are shown in Fig. 10,11 and 12. It appeared that for this alloy the test frequency has little effect.

- Effect of test specimen thickness

No particular effect appeared to be entailed by specimen thickness for tests conducted with R = 0.01. Conversely where R is greater (for example R = 0.5) propagation rates appeared to be higher in CCT specimens 1.6mm thick (see Fig. 1, 2 and 3).

7175 T 7351 Alloy

- Effect of the environment

Fig. 8 and 9 show that in this alloy the effect of the environment is considerable. Between 10 and 15 MPa$\sqrt{m}$ rates recorded in salt water are 5 to 10 times more important than in argon. In-between these 2 environments wet air produces intermediate rates. The same comment applies as for 2618 A : the effect of the environment is the more important, the propagation rates are lower and ratio R value is lower. However the effect is much more important on alloy 7075 than on 2618.

- Effect of test frequency

The effect of test frequency is most marked in salt water between 1 and 25 Hz (see Fig 15). But it is relatively low in wet air and practically nil in dry argon (see fig. 13 and 14). The effect of test frequency between 25 and 1 Hz shows that these mechanisms generated by corrosion fatigue have little effect at 25 Hz.

- Effect of test specimen thickness

Just as for alloy 2618 A, it appeared that test specimen thickness has a slight effect when R = 0.5 and when propagation rates are low (see Fig. 6 and 7).

2024 T 351 and 2214 T 351 alloys

The results shown in fig. 16 and 17 demonstrate that there is no marked effect of the environment on these alloys. The slight difference noted at low rates between the argon and A3 solution (see Fig 17) is in line with the comments made on alloy 2618 A.

7050 T 73651 and 7475 T 7351 alloys

The results show (fig.19 and 20) that these alloys are sensitive to the environment. They both have an almost similar behaviour to that of alloy 7175. The effect of salt water is the less important, the propagation rates are higher.

6061 T6 Alloy

Fig. 18 shows that this alloy has a sensitivity to environments which is intermediate to that of the 2000 and 7000 series alloys.

— Conclusions — In general as far as crack propagation is concerned, the environment can have a substantial effect on material behaviour, the more aggresive being salt water and to a lesser degree wet air. The alloys belonging to the 2000 séries (2024, 2618A, 2214) are less sensitive and have a common response ; in other words they are sensitive to the environment when ΔK is greater than 20 MPa$\sqrt{m}$. Conversely, at 15 MPa$\sqrt{m}$ crack propagation rates are multiplied by a factor 5, when passing from dry argon to salt water. The results obtained in wet air are always very close to those obtained in salt water.

The alloys belonging to the 7000 series(7175, 7475, 7050) are much more sensitive to the various environments. It should be noted however that the environment has little effect when rates reach 10^{-2} mm per cycle (ΔK in the vicinity of 30 to 40 MPa$\sqrt{m}$). From 15 to 20 MPa$\sqrt{m}$, propagation rates are multiplied by 10 when passing from dry argon to salt water. For the 3 alloys, the rate values evaluated in wet air or ambient air are closer to those obtained in dry argon than to those obtained in salt-water.

3.2 - Results concerning crack initiation

Only specimens from alloys 2618 A and 7175 were examined. The results shown in fig. 21 can be summarized as follows :

A. Effect of wet air and salt-water

While humidity has no effect at all on crack initiation, salt-water on the contrary can divide endurance limit by a factor of 2 to 4 depending upon the case considered. In wet air and ambient air the two materials we examined show an equivalent fatigue strength but conversely in salt-water the endurance limit noted for 2618 A are always greater than for 7175, the average deviation being approximately 25 %.

B. Effect of protections and surface treatment

In an environment which is not very aggressive (for instance humid air or ambiant air) chromic acid anodizing appeared to decrease by 20 % the fatigue properties of the materials but such decrease could be attenuated by a previous shot peening. After exposure to salt water the alochrome plus a paint coat application prove to be the best way to decrease substantially the aggressivity of this environment.

4 - CONCLUSIONS

To study crack propagation a wide range of aluminum alloys has been evaluated in various environments : dry argon, ambient air, wet air, salt-water. The results show that the 2000 serie alloy on one side and the 7000 series alloys on the other side have different behaviours. For the 2000 series alloys (2024, 2618, 2214) the environment has little effect. At 20 MPa$\sqrt{m}$, crack propagation rates are identical whatever is the environment. But on the contrary at 15 MPa$\sqrt{m}$, rates are approximately by 5 times higher in salt-water than in dry argon. The 7000 series alloys (7475, 7175, 7550) are more sensitive than the above alloys to environmental effects. When factor K amplitude varies from 15 to 20 MPa$\sqrt{m}$, rates are 10 times higher in salt water than in argon.

To study crack initiation, endurance limits at 10^7 cycles have been evaluated at a frequency of 50 Hz, which corresponds to an exposure time of 56 hours to the environment. Here again, the sensitivity of the 7175 T 3351 alloy to salt water is greater than that of 2618 A-T851. Among the various protections which have been assessed the application of alodine (alochrome) plus a paint coat appeared to be the most effective.

APPENDIX

- Chromic Acid Anodizing

The surface treatment consists in the following process :

. Degreasing with trichlorethylene vapor,

. Pickling, Composition : Na_2CO_3 : 44.5 g/l
Na_3PO_4 : 18.6 g/l
Duration : 5 minutes
Temperature : 60°C

. Rinsing in tap water : 5 minutes

Sulfochromic etching

. Composition : CrO_3 : 46.6 g/l
H_2SO_4 free : 263.1 g/l
H_2SO_4 combined : 39.2 g/l

. Duration : 25 minutes

. Temperature : 63°C

. Rinsing in tap water : 3 minutes.

Chromic Acid Anodizing

. Bath composition : CrO_3 free 40.5 g/l
CrO_3 total 56.5 g/l

. Cycle : Bengough

. Duration : 50 minutes

. Temperature : 40°C

. Rinsing in tap water : 5 minutes.

Sealing

. Bath composition : 30 mg/l : $K_2Cr_2O_7$

. Duration : 40 minutes

. Temperature : 97°C

Drying : Hot air oven : 50°C

Measurement of crack propagation in C.T. specimens

CCT specimen test set-up

Rotating bending machine

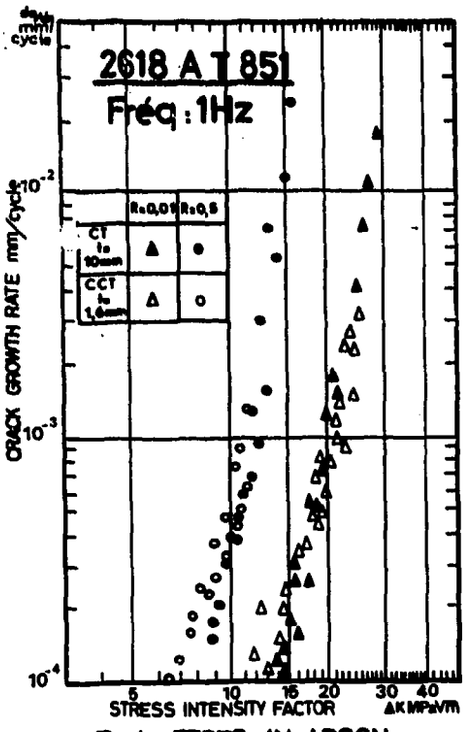

Fig 1 - TESTS IN ARGON

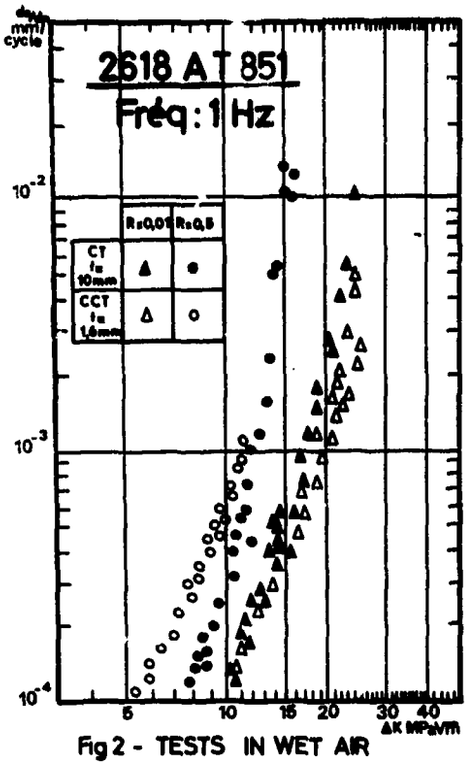

Fig 2 - TESTS IN WET AIR

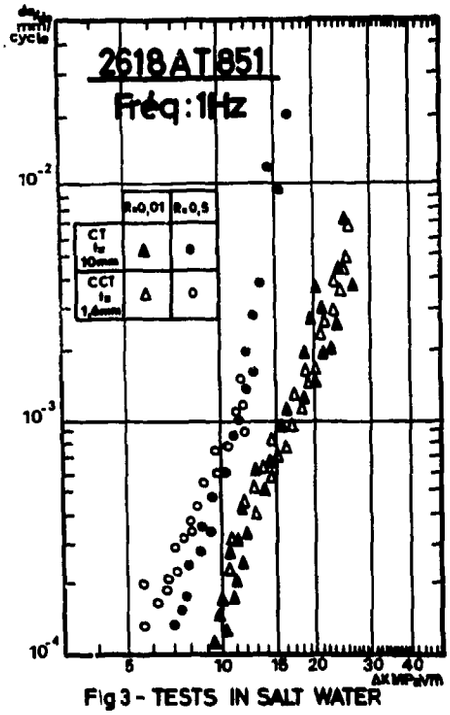

Fig 3 - TESTS IN SALT WATER

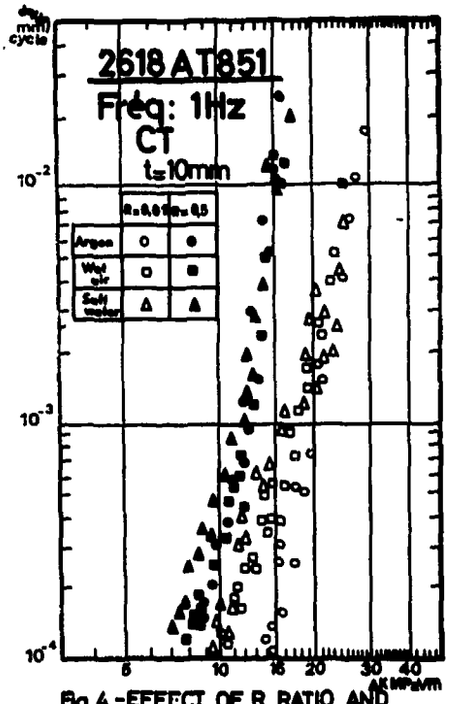

Fig 4 - EFFECT OF R RATIO AND ENVIRONMENT

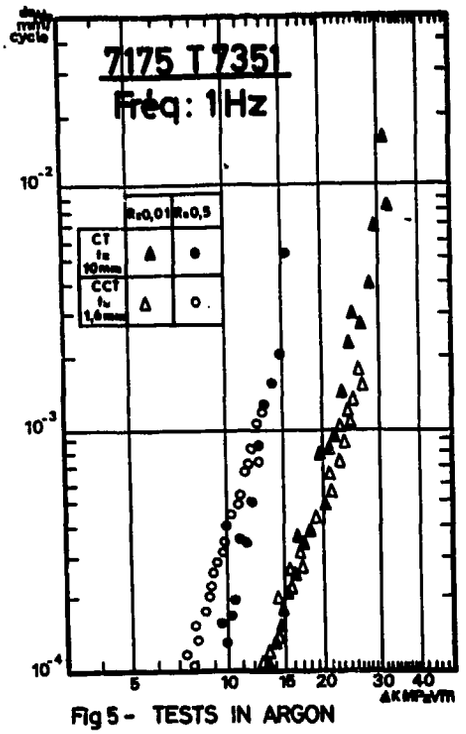

Fig 5 - TESTS IN ARGON

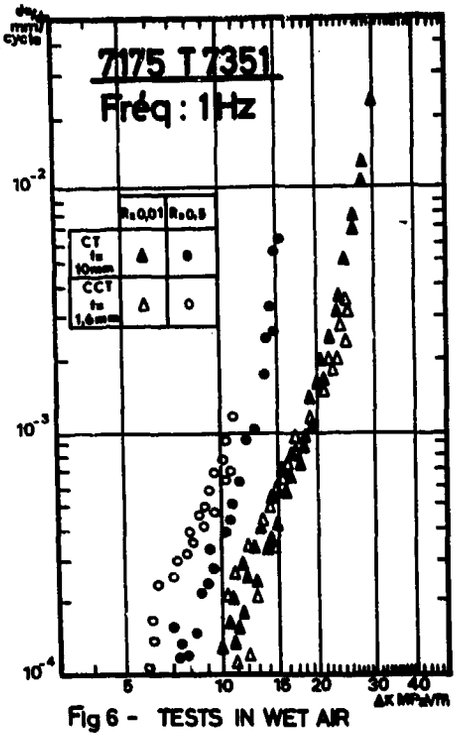

Fig 6 - TESTS IN WET AIR

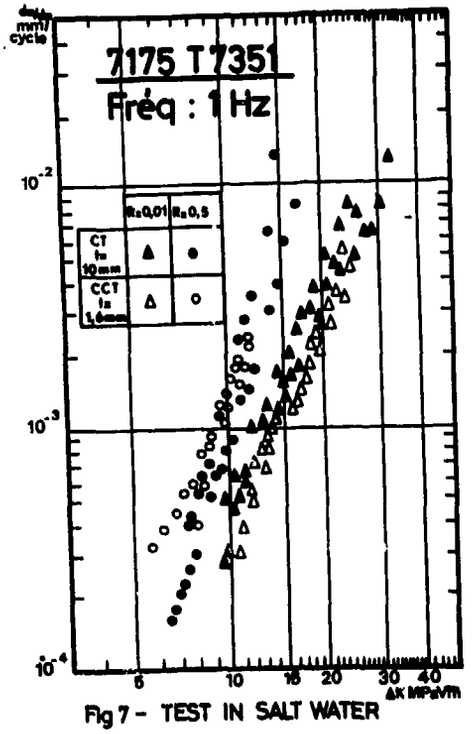

Fig 7 - TEST IN SALT WATER

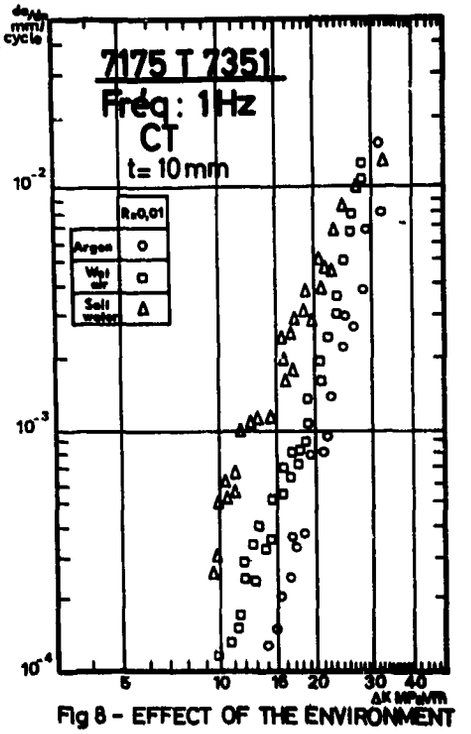

Fig 8 - EFFECT OF THE ENVIRONMENT

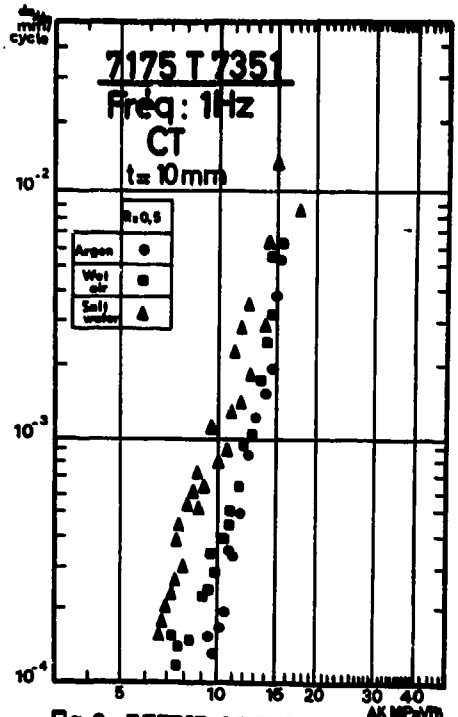

Fig 9 - EFFECT OF THE ENVIRONMENT

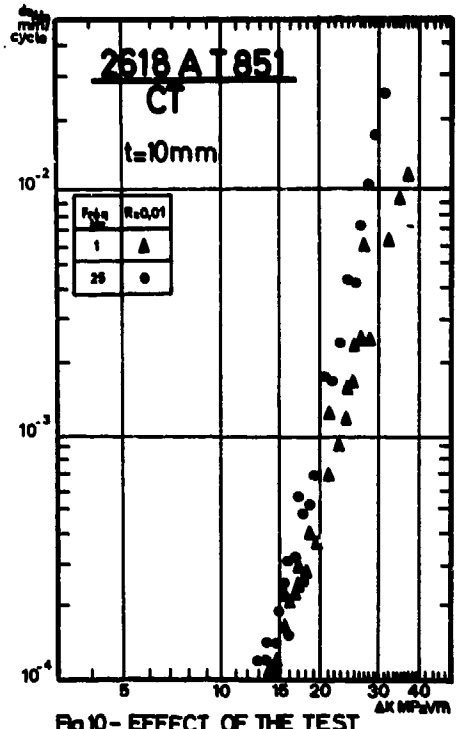

Fig 10 - EFFECT OF THE TEST FREQUENCY IN ARGON

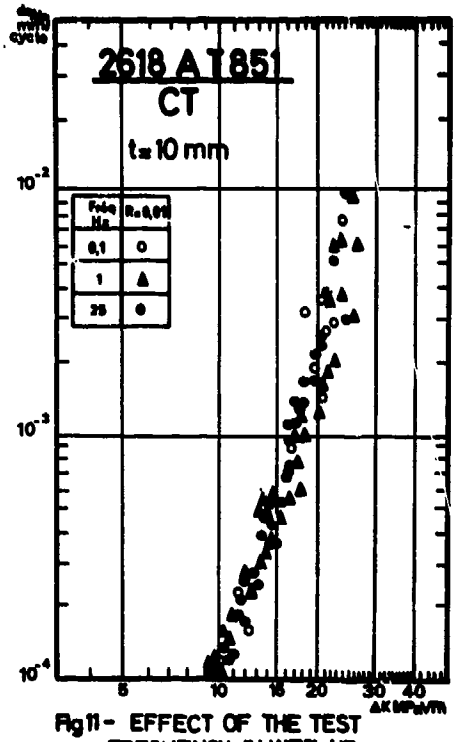

Fig 11 - EFFECT OF THE TEST FREQUENCY IN WET AIR

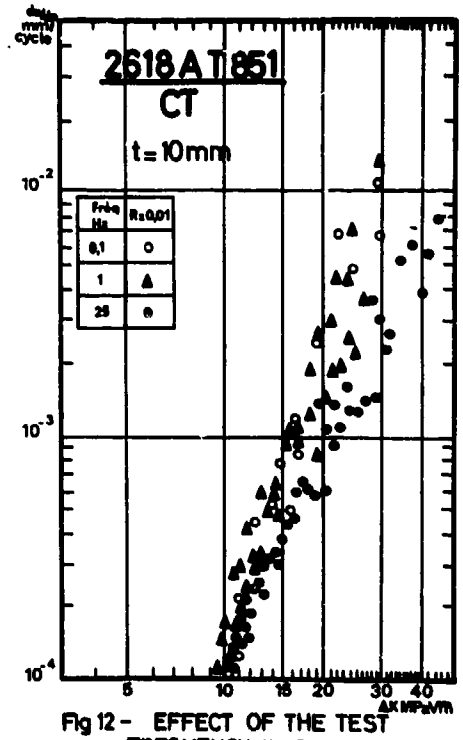

Fig 12 - EFFECT OF THE TEST FREQUENCY IN SALT WATER

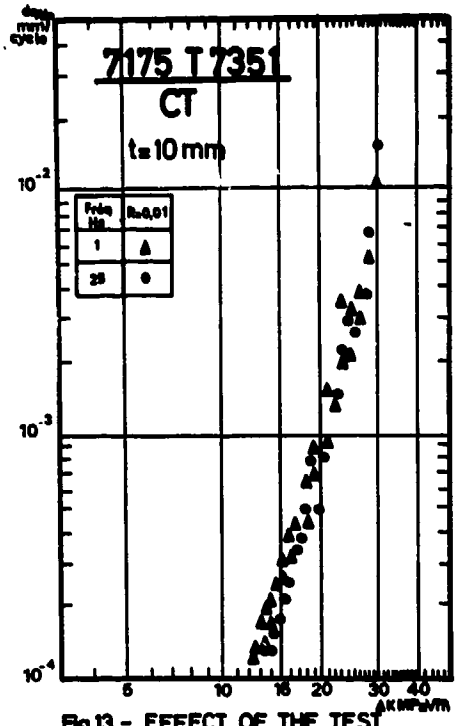

Fig 13 - EFFECT OF THE TEST FREQUENCY IN ARGON

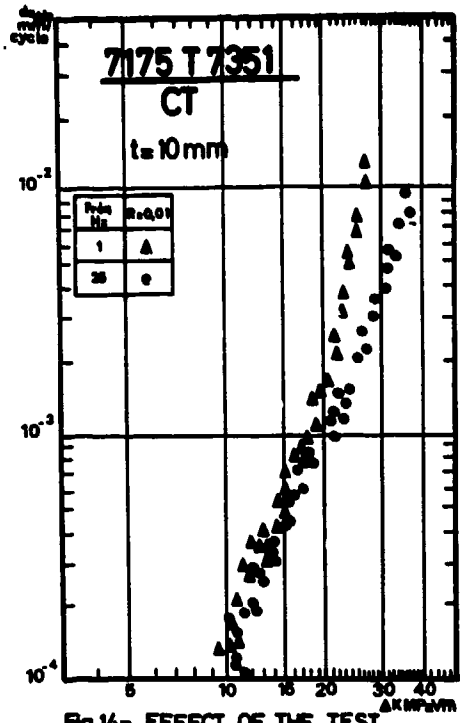

Fig 14- EFFECT OF THE TEST FREQUENCY IN WET AIR

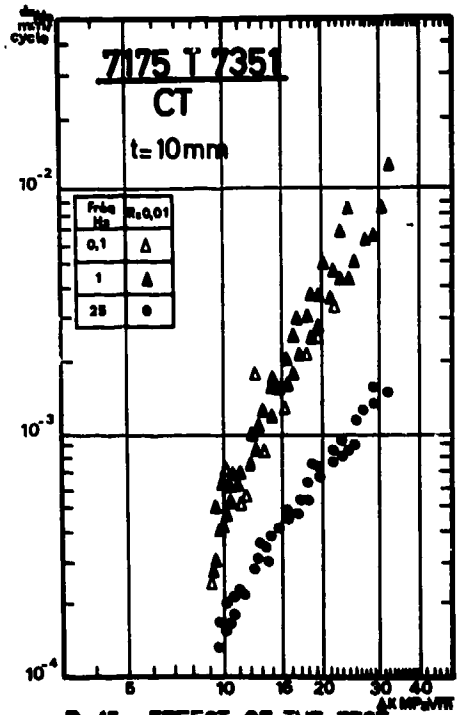

Fig 15 - EFFECT OF THE TEST FREQUENCY IN SALT WATER

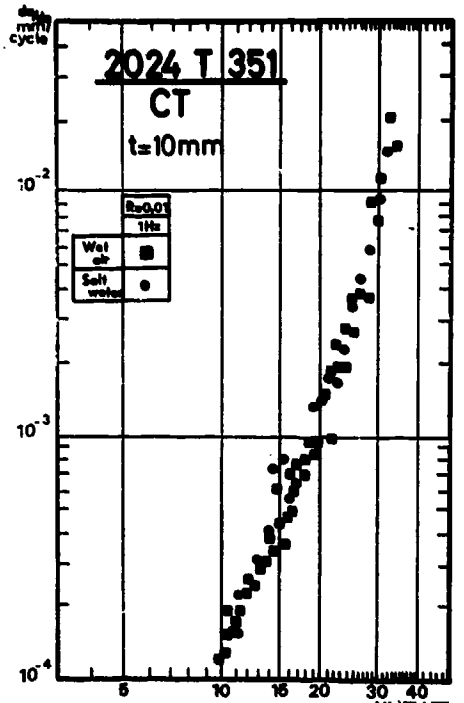

Fig 16 - EFFECT OF THE ENVIRONMENT

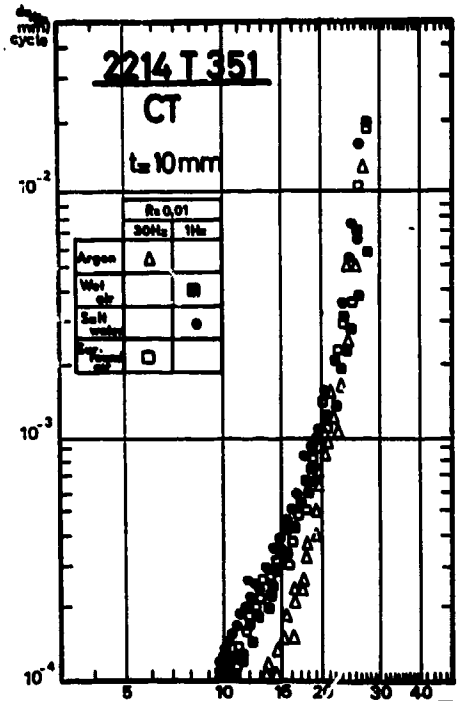

Fig 17 - EFFECT OF THE ENVIRONMENT

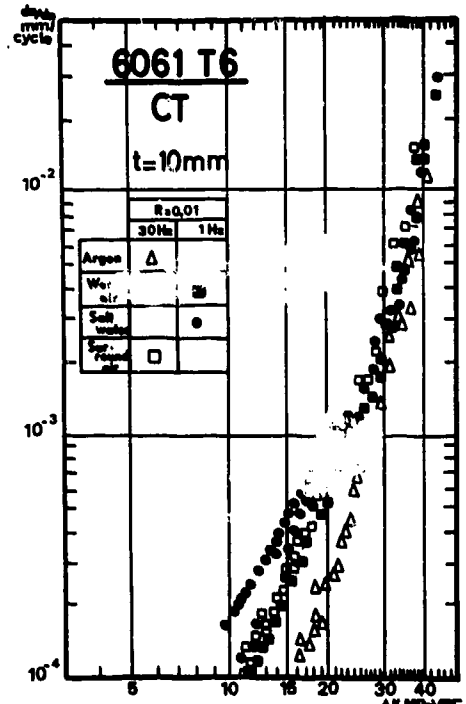

Fig 18 - EFFECT OF THE ENVIRONMENT

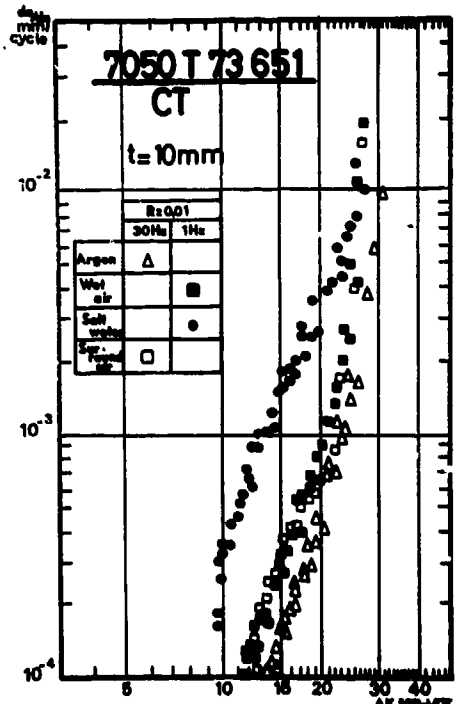

Fig 19 - EFFECT OF THE ENVIRONMENT

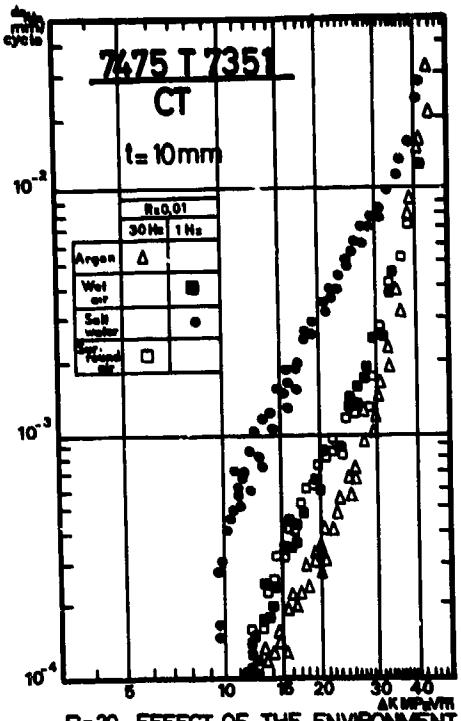

Fig 20 - EFFECT OF THE ENVIRONMENT

Fig 21 - VARIATION OF ENDURANCE LIMIT AT 10^7 CYCLES VERSUS COMBINED EFFECT OF ENVIRONMENT AND PROTECTION

Rotating bending tests - Exposure : 56 hours

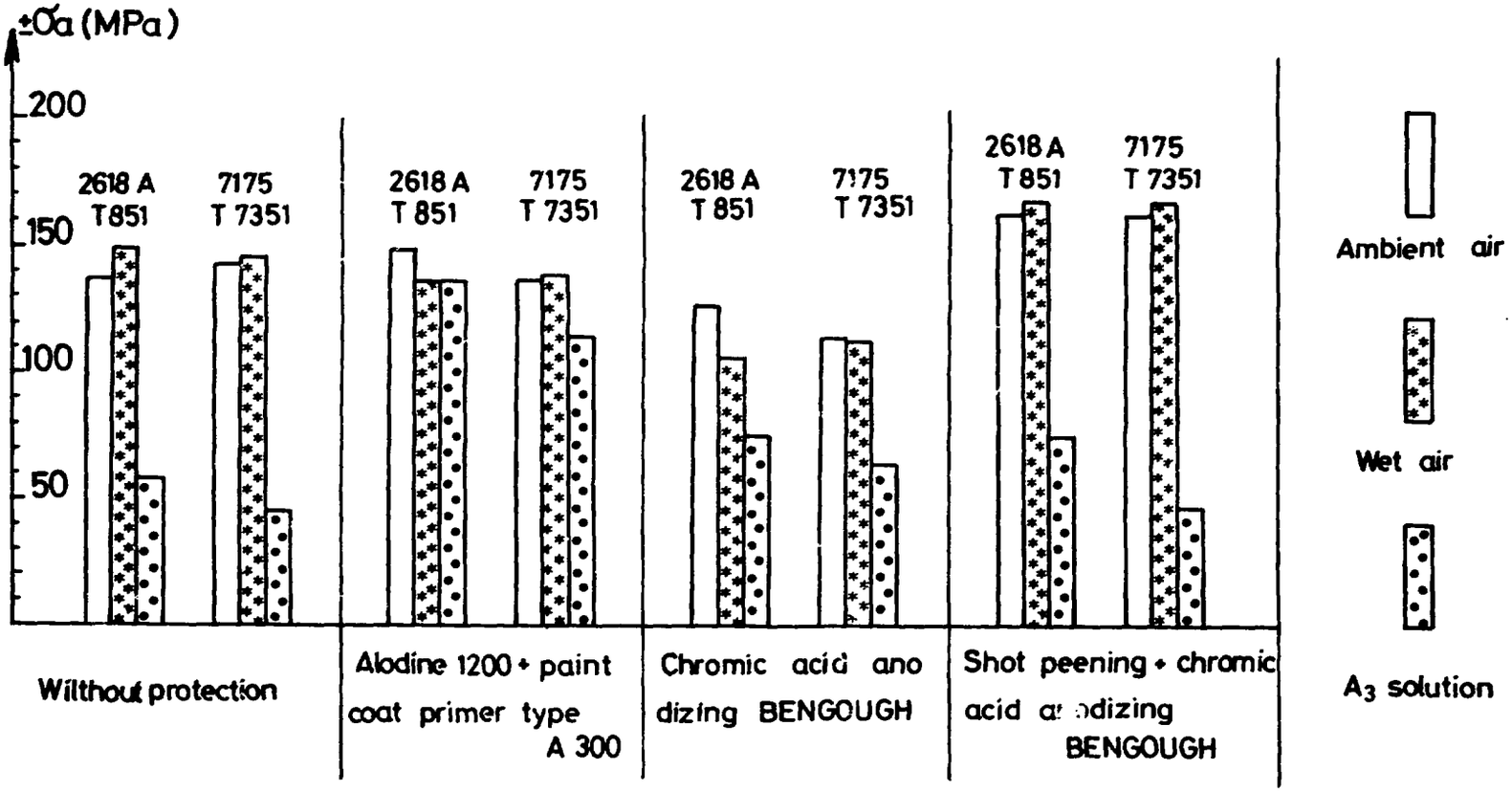

CORROSION FATIGUE OF OFFSHORE AND SHIP-BUILDING STEELS

by

Dr.-Ing. Walter Schütz

Industrieanlagen-Betriebsgesellschaft mbH
Einsteinstraße 20, 8012 Ottobrunn, Germany

SUMMARY

The results of several test programs on various steels are discussed where in addition to realistic variable loads a corrosive environment was simulated. For comparison, constant amplitude tests were also carried out as well as test in air. It is shown that under constant amplitude loading the damaging effect of corrosion was always greater than under realistic loading. In addition, test frequency appears to be not so important as in constant amplitude test; this means that tests under variable amplitude can be carried out at normal test frequencies of the order of 10 Hz, saving time and costs. Finally the results of a research program on welded tubular joints in seawater are described in which the above conclusions were incorporated.

1. INTRODUCTION

The service fatigue loads of most structures are a complex mixture of stochastically and deterministically variable stresses, Figure 1.

It has been known for many years /1 - 18/ - at least in the aircraft fatigue community - that to get realistic results you have to do realistic fatigue tests. This means a quite accurate simulation of the actual load sequence; for aircraft this means flight-by-flight tests.

This is the state-of-the-art in many laboratories in the western countries; the servo-hydraulic machines (including computer control) required for such tests are available, as well as the necessary expertise; a large number of test programs, most of them for aircraft purposes, have been reported in the literature /9 - 40/. This is true at least for tests in a laboratory atmosphere; as soon as additional environmental effects are considered - be they temperature or corrosion or both - the problems become considerably more complex and very few data are available: In the case of elevated temperatures the well known "Concorde" - and SST-programs have resulted in some very complex tests and interesting results /25, 26, 38, 39/.

In the case of marine corrosion the author is aware of very few papers, in which a seawater environment was superimposed on a realistic load sequence. The bulk of the corrosion fatigue tests on materials and components (including those for aircraft purposes) available today consists of constant amplitude tests; thus the load sequence applied was not realistic, and usually, neither was the effect of the environment realistically simulated, because of too short testing times.

2. PROBLEMS IN CORROSION FATIGUE TESTING

More than any other fatigue test, a corrosion fatigue test is a compromise. Figure 2 shows the main parameters which have to be accounted for. Obviously it is not possible to simulate all of them realistically; therefore the first problem of the researcher is where to put the main emphasis of the test. If he considers corrosion fatigue to be "just another type of corrosion" he will opt for the "corrosion" parameters (enumerated in the left column, Figure 2) and more or less neglect the others shown in the right column. Thus his preferred test will most probably be a constant amplitude test at low frequency but high stresses in order to arrive at practical testing times.

If the researcher considers corrosion fatigue as "just another type of fatigue" he will try to simulate the "stress" side of the parameters (right hand column in Figure 2). But he will then have to use an increased, unrealistic test frequency in order to arrive at practical test times. In both cases one parameter cannot be realistically simulated and that is the time in the environment.

As mentioned in the introduction, most tests up to now have been of the first category. For example, in the 1978 seminar on the large cooperative offshore steels research program of the European Coal and Steel Community /41/ only two papers contain random tests in seawater, while in fourteen papers constant amplitude tests are described. Another example: None of the many reports in the annual Offshore Technology Conferences in Houston from 1970 to 1975 are on corrosion fatigue tests with realistic load sequences.

3. TEST PROGRAMS

In 1970 the author's firm was asked to carry out comparative fatigue tests on two different amagnetic steels to be used for special purpose ships. The tests in air will not be reported on in any detail here, except to say that SN-tests as well as 8-step program tests with two different spectra (straight-line distribution simulating a wave spectrum and Normal distribution) were performed in large numbers on the three different specimen types shown in Figures 3 to 5.

The two steels are characterised in Table 1. As will be noted, the steel PN 18 So 2 was of the stainless type, the other steel was a chronium-free manganese type. Both have similar tensile strengths (quite high for ship structural steels) and a large difference between the 0.2 percent yield strength and the tensile strength.

Using the same materials and specimen types corrosion fatigue tests were carried out in 1971, the results of which will be described in somewhat more detail, as they substantially influenced all subsequent corrosion fatigue tests carried out by the author. Again, the two different load spectra mentioned above and shown in Figures 6 and 7 were employed. The straight line distribution will be called G.V., the Normal distribution N.V. in subsequent figures. It was desired to simulate 30 years of navy service in these tests, corresponding to about 10^8 cycles. Therefore the tests under the straight line distribution were extended to more than $5 \cdot 10^7$ cycles; the time the specimens spent in the corrosive environment at this number of cycles was 115 to 145 hours. In addition the SN-curves for the three specimens were determined from about 10^5 to 10^7 cycles. Because of the lower number of cycles to failure and the much higher test frequencies (see below) the maximum time the constant amplitude specimens spent in the corrosive environment was only 16,5 to 18,5 hours. The SN-tests will be called E.V. in subsequent figures.

Two different types of test machines were employed: For the SN-tests an Amsler Vibrophore, running at about 120 - 160 Hz, for the program tests Schenck resonance machines running at about 50 Hz in the resonance mode and at about 1 Hz in the mechanical mode (necessary for steps 1 to 4 or 5 of the programs shown in Figures 6 and 7).

Artificial seawater according to DIN 50900 was used as corrosion agent; its pH-value was constant at 7,2 ± 0,3, its temperature at 15 ± 1° C. The water level was intermittently raised and lowered; at the low water level the salt deposit on the specimen was dried by the same air jet which at the high water level saturated the saltwater with oxygen. The specimens were also precorroded for one hundred hours in a salt spray chamber at 25° C.

The results are summarized in Figure 8:

- The damaging effect of the artificial seawater was much greater in constant amplitude tests than in program tests for both steels and for all three specimen types. This despite the fact that the time in the corrosive environment was from three times to about eight times longer in the program tests than in the constant amplitude tests, as shown in Figure 8.

- In the case of the stainless steel no damage at all was done by the corrosive environment in the notched, unwelded condition in both types of program test. However, under constant amplitudes (E.V. in Figure 8) there was a pronounced damaging effect even though the time in the environment was only about one eight of that in the program test (G.V.).

- The fatigue strengths in seawater of the stainless steel PN 18 So 2 in both welded specimen types on the average were no better than those of the non-stainless steel B 967. This is true for program tests and constant amplitude tests and can be described to the well known chromium depletion due to welding.

- However, the SN-curve of B 967 had a quite steep slope up to and beyound 10^7 cycles, while the slope of the SN-curve of the stainless steel decreased beyond about 10^6 cycle, see Figure 9. That is the fatigue limit in seawater was not reached at 10^7 cycles for the non-stainless steel - if it exists at all - while for the stainless steel it was at least approached at that number of cycles, see Figure 9.

- The percentage of the fatigue life to failure spent in crack propagation was <u>larger</u> in the corrosive environment than in air for the program tests.

- Miner's rule predicted the fatigue life under corrosion reasonably well - at least better than the life in air, see Figure 10.

These admittedly unexpected results were discussed with many fatigue and corrosion experts. No convincing explanation for the less damaging effect of corrosion under program loading inspite of longer times in the environment was ound. However, if one assumes that the residual compressive stresses set upt by the high stress cycles of the program test are <u>more</u> beneficial under corrosion than in air, most of the results can be explained, at least qualitatively; for example: In the notched specimen with a $K_t = 3,6$ there was a damaging effect of seawater corrosion to the stainless steel in constant amplitudes. Local stresses at the root of the notch are below the yield strength. Under program loading, the peak loads of the spectrum result in local strains far above yield (at the notch root), see Figure 8; thus, residual compressive stresses are set up, counteracting the damaging effect of corrosion, which is present in the constant amplitude tests; thus

residual compressive stresses are set up, counteracting the damaging effect of corrosion, which is present in the constant amplitude tests; thus the end result of the synergistic effects of variable amplitudes and corrosion is zero additional damage due to corrosion.

The geometrical stress concentration factor of the longitudinal stiffener was measured by strain gages to be $K_t = 1,7$; this alone is not sufficiently high to exceed, under the maximum loads of the spectrum, the yield strength locally. However, in welded joints residual tensile stresses are always present and it can therefore be assumed that these, together with the local stresses due to the external loads, exceeded the yield strength.

Several objections can be raised against the test program described above:

- Different frequencies were used in constant and variable amplitude tests.
- The variable amplitude test was of a blocked, not a random sequence.
- The test frequencies were (too) high.

A new test program was therefore carried out in 1977 - 1978 in which the above objections were taken into account as far as possible:

- The test frequencies in constant and variable amplitude tests were equal at 5 Hz under corrosion and at 20 Hz in air. This resulted in equal times in the corrosive environment at equal numbers of cycles to failure. The tests were extended to about $5 \cdot 10^6$ cycles in both constant and variable amplitude tests, giving a maximum of about 250 hours ≙ 11 days in the corrosive environment.
- The standardised random sequence developed by the LBF and the IABG /43/ was employed, resulting a Normal distribution; the irregularity factor $J = N_O/N_1 = 0,99$ was used. Figure 11 shows an example of the load sequence.

To make the corrosive environment more severe artificial seawater according to ASTM-D-1141 was used, but with a tripled NaCl content. The temperature was controlled at $15 \pm 1,0^{\circ}$ C, the pH-value however, was $8,1 \pm 0,1$; oxygen saturation was obtained by bubbling air through the water; the specimens were kept constantly immersed. Notched and longitudinal stiffener specimens according to Figures 3 and 4 were used.

Instead of the amagnetic non-stainless steel B 967 a so-called "high strength structural ship steel" D 36 was used, which had a tensile strength of 580 N/mm^2 and a 0.2 percent yield strength of 440 N/mm^2.

The quantitative results of this investigation are still proprietary, but some qualitative results can be disclosed:

- Again the corrosive environment was far more damaging under constant amplitude loading than under realistic loading for both steels and for both specimen types.
- Also, in the welded specimens the damaging effect of corrosion was more pronounced in both steels than in the notched specimens.
- The random tests gave shorter lives than the blocked program tests. This was true under corrosion - where it might be ascribed to the more severe corrosion conditions - but also in air.
- Miner's rule again predicted the fatigue life in the corrosive environment slightly better, that is with a smaller scatter than in air, but 6 out of 8 predictions were unconservative, see Figure 12.
- In the welded condition, both steels showed very similar fatigue behavior in seawater.

Thus, the conclusions from the early test program were completely confirmed.

A large cooperative research program on the corrosion fatigue strength of offshore steels has been underway for about three years for the European Community of Steel and Coal (ECSC); first results were presented in 1978 at a meeting in Cambridge /41/. Although most of the data obtained are for constant amplitude loading, the two German laboratories taking part - LBF and IABG - in view of the experience described above, decided to do random tests. The results are again proprietary, but some general remarks may be made:

- There was no significant influence of test frequency - be it 10 Hz or 1 Hz - in the random tests, although the longest time in the environment was about 30 days. This has been proved by about 30 tests, both at the LBF and at the IABG with several different steels. A very few tests were even carried out at 0.2 Hz by the LBF, in which the specimen spent more than 100 days in seawater. There was no statistically significant influence of test frequency, meaning that the number of cycles to failure was very similar at the identical stress levels for test frequencies of 10 Hz or 0.2 Hz, see Figure 12 /44/, although the time spent in the environment was about 50 times longer at the lower frequency.

- The additional damage caused by seawater was quite small in the random tests; judging from the constant amplitude results of other participating laboratories it is bigger in constant amplitude tests.

In view of the above results from hundreds of fatigue tests on many different steels, it was decided to carry out tests on welded tubular joints accordingly. These tests will now be described: The necessary data for the simulation of a realistic load sequence were obtained for us by the German Lloyd from one year's measurement on the German research platform "Nordsee".

Each sea state from 1 to 12 results approximately in a Gaussian distribution. This is known from many measurements. The sequence of these Gaussian distributions of different intensities and frequencies results, over a long enough time in a straight line distribution, as the sea conditions can change from the momentary state only to the next higher or lower state, i.e. from six to five or seven, the load sequence was programmed accordingly. It became apparent from the measurement that bad weather occurs mainly during autumn and winter; that is, bad high sea states are not distributed statistically over the whole year. Again, this fact was incorporated in the load sequence. A return period of one year was choosen, because on the average the weather will repeat itself every year. In order to save test time and costs, sea states one to three were left out because it was assumed that the corresponding low stresses would not contribute to the fatigue damage. The welded joints were intermittently immersed in artificial seawater according to ASTM, whose pH-value, temperature and oxygen contents were controlled.

The stress level - one of the important parameters according to Figure 2 - was set so that first cracks would start after 5 to 10 return periods, that is after 5 to 10 simulated years of service. At the test frequencies used, this means a test time of between three and six weeks per tubular joint. The occurence of the crack was noted, as well as its propagation behavior, in order to obtain the basic data needed for a crack propagation calculation using fracture mechanics.

The specimens were welded tubular Y-joints, see Figure 14 and 15, consisting of a large tube of about 400 mm diameter and a brace of about 270 mm diameter. The material for two thirds of the specimens was mild steel TT St 35.11; one third of the specimens was fabricated from the higher strength steel F 36 (yield strength 360 N/mm^2). 8 of the specimens were stressed by axial load in the brace, 16 by bending.

Qualitatively, the results of our tests can be described as follows:

- The yield strength of the materials does not influence the results; this was to be expected, since the welded tubular joint is a severly notched member with a weld in the most highly stressed region.

- The crack propagation curve is highly irregular, see Figure 16 and 17, and does not follow the well known "regular" shape one is accustomed to. Sometimes the crack, as measured on the surface, just stops for more than one return period, corresponding to one million cycles; it then sometimes accelerated to very high crack propagation rates, only to return to a more normal shape again. At the moment no convincing explanation can be given for this behavior.

- Also, there is no direct correlation between stress level and propagation rate; that is, a higher stress level does not automatically result in a faster crack propagation rate. Obviously this is a consequence of the very high scatter in the crack initiation as well as crack propagation phases.

- A further complication is the fact that a long crack initiation period does not automatically guarantee slow crack propagation. On the contrary, these are cases where the crack starts very early and then propagates slowly; there is also the reserve case where it starts very late and propagates quickly.

All this obviously will make the calculation of crack propagation very difficult.

CONCLUSIONS

(It will be understood that the following conclusions are based on results from many different steels and on many hundred fatigue tests in seawater.)

- In a corrosion fatigue test it is absolutely essential - more so than in any other fatigue test - to simulate the load sequence as closely as possible. If at all possible the stress levels should not be increased above those occuring in the actual structure.

- Test frequency is a second order effect, if the sequence is realistic. It is far better to simulate the sequence and the stress level correctly and run the test at an unrealistically high frequency than vice versa.

- The time in the environment also is a second order effect.

- The effect of corrosion is quite small in random tests and is much less than in constant amplitude tests.
- Further investigations are urgently required, especially at large numbers of cycles to failure.

REFERENCES

/ 1 / Melcon, M.A. and A.J. McCulloch: Simulation of Random Aircraft Service Loadings in Fatigue Tests, in: Current Aeronautical Fatigue Problems, 3. ICAF Symposium, Rom, 1963

/ 2 / Melcon, M.A., W.J. Crichlow and A.J. McCulloch: Investigation of the Representation of Aircraft Service Loadings in Fatigue Tests. Technical Report ASD-TR-61-435, Lockheed California Company, 1962

/ 3 / Schijve, J.: The Accumulation of Fatigue Damage in Aircraft Materials and Structures. AGARDograph No. 157, 1972

/ 4 / Jacoby, G.: Comparison of Fatigue Life Estimation Processes for Irregularly Varying Loads. Proc. 3rd Conf. on Dimensioning, Budapest, 1968

/ 5 / Jacoby, G.: Vergleich der Lebensdauer aus Betriebsfestigkeits-, Einzelflug- und digital programmierten Randomversuchen sowie nach der linearen Schadensakkumulationshypothese. Fortschrittsbericht VDI-Z., Reihe 5, Nr. 7, 1969

/ 6 / Branger, J.: Life Estimation and Prediction of Fighter Aircraft, in: International Conference on Structural Safety and Reliability edited by A. Freudenthal, Pergamon Press, 1972

/ 7 / Corbin, P.L. and E.C. Naumann: Influence of Programming Techniques and of Varying Limit Load Factors on Maneuver Load Fatigue Test Results. NASA TN-D3149

/ 8 / Schütz, W.: Fatigue Life Prediction of Aircraft Structures - Past, Present and Future. Engineering Fracture Mechanics, Vol. 6, No. 3, pp. 671 - 699, 1974

/ 9 / Foster, H.W.: Fatigue Testing of Airframe Structural Components, in: ASTM STP 203, 1957

/ 10 / Kowalewski, J.: Über die Beziehungen zwischen der Lebensdauer von Bauteilen bei unregelmäßig schwankenden und bei geordneten Belastungsfolgen. Dt. Versuchsanst. f. Luftfahrt, Mülheim, Bericht Nr. 249, 1963

/ 11 / Sherman, A.C. and R. Steiner: Fatigue Life under Random Loading for Several Power Spectral Shapes. NASA TR R-266, 1967

/ 12 / Naumann, E.C., H.F. Hardrath and D.E. Guthrie: Axial Load Fatigue Tests of 2024-T3 and 7075-T6 Aluminum Alloy Sheet Specimens under Constant- and Variable-Amplitude Loads, NASA TN D-212

/ 13 / Naumann, E.C.: Evaluation of the Influence of Load Randomization Cycles on Fatigue Life. NASA TN D-1584

/ 14 / Schijve, J.: Fatigue Life and Crack Propagation under Random and Programmed Load Sequences, in: Current Aeronautical Fatigue Problems, 3. ICAF-Symposium, Rom 1963

/ 15 / Lipp, W.: Ermittlung einer wirklichkeitsgetreuen Lebensdauerfunktion für Fahrzeugbauteile mit statisch veränderlichen Belastungen. LBF-Bericht 154, 1965

/ 16 / Laudert, H., G. Jacoby, H. Nowack und H.-D. Weber: Einige Möglichkeiten der Ermüdungsprüfung bei Randombeanspruchungen. VDI-Z. Fortschritts-Bericht, Reihe 5, Nr. 7, 1969

/ 17 / Gassner, E. und G. Jacoby: Experimentelle und rechnerische Lebensdauerbeurteilung von Bauteilen mit Start-Lande-Lastwechsel. Luftfahrttechnik-Raumfahrttechnik 11, 138/148, 1965

/ 18 / Gassner, E.: Fatigue Life of Structural Components under Random Loading, in: Fail Safe Aircraft Structures, RAE TR 73183. ICAF-Symposium, London, July 1973

/ 19 / Schütz, W.: The Fatigue Life under Three Different Load Spectra-Tests and Calculations, AGARD CP 118, Symposium on Random Load Fatigue, Lyngby, Denmark, 13. April 1972

/ 20 / Schütz, W. und P. Schrader: Ermittlung der Lebensdauer bauteilähnlicher Proben mit einer standardisierten Lastfolge. IABG-Bericht TF-649, 1977

/ 21 / Schütz, D.: Einzelflugversuche und Einstufenversuche an Augenstäben aus AlZnMgCuAg (3.4354.7) zur Überprüfung der linearen Schadensakkumulation. LBF TM No. 53/70

/ 22 / Branger, J.: Full Scale Test and Service Experience in the Swiss Venom Case, in: Proc. Technical Session 11th ICAF Meeting, Stockholm, May 1969

/ 23 / Dabell, B.J. and P. Watson: Random Load Fatigue of Welded Structures at Long Lives, in: Fatigue Testing and Design, Conference Proceedings, London, April 1976

/ 24 / Schütz, D. und H. Lowak: Zur Verwendung von Bemessungsunterlagen aus Versuchen mit betriebsähnlichen Lastfolgen zur Lebensdauerabschätzung, LBF-Bericht FB-109, 1976

/ 25 / Imig, L.A. and W. Illg: Fatigue of Notched Ti-8Al-1Mo-1V Titanium Alloy at Room Temperature and 550° F (560° K) with Flight-by-Flight Loading Representative of a Supersonic Transport. NASA TN D-5295, 1969

/ 26 / Peterson, J.J.: Fatigue Behaviour of a Fusion Welded Ti-8Al-1Mo-1V Simulated Wing Structure under the Environment of a Supersonic Transport. NASA CR-881, 1970

/ 27 / Booth, R.T. and D.H. Wright: Variable Load Fatigue Testing: Fourth Report, MIRA-Report Nr. 1970/13

/ 28 / Booth, R.T. and D.H. Wright: Variable Load Fatigue Testing: Second Report, MIRA-Report No. 2969/9

/ 29 / Schijve, J., A. Jacobs and P.J. Tromp: Flight Simulation Tests on Notched Elements, NLR TR 74033 U

/ 30 / Edwards, P.R.: Cumulative Damage in Fatigue with Particular Reference to the Effects of Residual Stresses, RAE TR 79237, 1969

/ 31 / Kirkby, W.T. and P.R. Edwards: Variable Amplitude Loading Approach to Material Evaluation, in: Component Testing and its Application to the Design Procedure, 11th ICAF Meeting, Stockholm, May 1969

/ 32 / Gassner, E., H. Lowak und D. Schütz: Bedeutung der Unregelmäßigkeit Gauss'scher Zufallsfolgen für die Betriebsfestigkeit. LBF-Bericht FB-124, 1976

/ 33 / Weissgerber, D. und P. Helm: Lebensdauervorhersage für Kampfflugzeuge, experimentelle und theoretische Untersuchungen zur Überprüfung neuer Lebensdauerberechnungsverfahren. MBB-ZTL-Bericht 2.31.1, 1977

/ 34 / Kirkby, W.T.: Some Effects of Change in Spectrum Severity and Spectrum Shape on Fatigue Behaviour under Random Loading. AGARD CP-118, Symposium on Random Load Fatigue, Lyngby, Denmark, 1972

/ 35 / Schijve, J., F.A. Jacobs and P.J. Tromp: Crack Propagation in Aluminum Alloy Sheet Materials under Flight Simulation Loading. NLR-Report TR 78031 L, Amsterdam, 1968

/ 36 / Schijve, J. and F.A. Jacobs: Crack Propagation in Aluminum Alloy Sheet Materials under Flight Simulation Loading. NLR-Report TR 78066 L, Amsterdam, 1968

/ 37 / Schijve, J. F.A. Jacobs and P.J. Tromp: Crack Propagation in 2024-T3 AlClad under Flight Simulation Loading. - Effect of Truncating High Gust Loads. NLR-Report TR 69050 U, Amsterdam, 1969

/ 38 / Swanson, S.R., F. Cicci and W. Hoppe: Crack Propagation in Clad 7079-T6 Aluminum Alloy Sheet under Constant and Random Amplitude Fatigue Loading, in: ASTM STP 415, 1966

/ 39 / Hearth-Smith, J.R. and F.E. Kiddle: Effects of Heat on Fatigue in Aircraft Structure, in: Proceedings of the 8th ICAF Symposium, Lausanne 1975, J. Branger and F. Berger, eds.

/ 40 / Wilkins, D.J., R.V. Wolf, M. Shinozuha and E.F. Cox: Realism in Fatigue Testing: The Effect of Flight-by-Flight Thermal and Random Load Histories of Composite Bonded Joints, in: ASTM STP 569, 1975

/ 41 / N.N.: Select Seminar: European Offshore Steels Research, 27-29 November 1978. The Welding Institute, Cambridge, UK

/ 42 / Schütz, W. und R. Heidenreich: Die Schwingfestigkeit des amagnetischen chromfreien Manganstahls B 967 und des amagnetischen Chrom-Nickel-Stahls PN 18 So 2 unter Korrosion. IABG-Bericht TFB-229, 1972

/ 43 / Fischer, R., M. Hück, H.G. Köbler und W. Schütz: Eine dem stationären Gauss'schen Prozeß verwandte Beanspruchungszeitfunktion für Betriebsfestigkeitsversuche. Fortschrittsbericht VDI-Z, Reihe 5, Nr. 30, Sept. 1977

/ 44 / Olivier, R. and W. Schütz:
Investigation of Corrosion Fatigue of Offshore Structures, in: Review of Investigations on Aeronautical Fatigue in the Federal Republic of Germany. LBF-Report S-142, 1979

Werkstoff	chemische Zusammensetzung in %									
	C	Si	Mn	P	S	Cr	Ni	C	N	Mo
B 967	0,45	1,42	20	0,053	0,003	0,07	0,06	0,05	0,071	
PN 18 So 2	0,039	0,62	4,97	0,016	0,005	20,06	15,35	-	0,27	3,14

Werkstoff	Kennwerte aus dem Zugversuch		
	$\sigma_{0,2}$ kp/mm^2	σ_B kp/mm^2	δ_S %
B 967	36,8	90,0	71
PN 18 So 2	49,0	84,0	43

TABLE 1

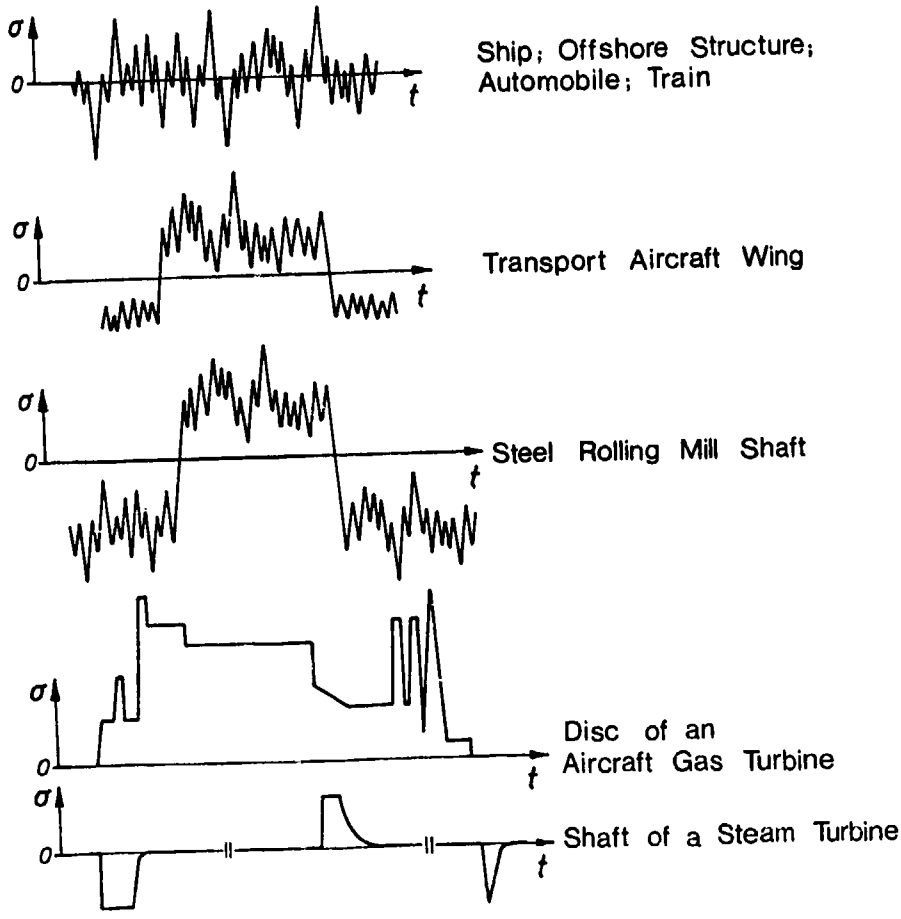

FIGURE 1: Typical Load Sequences (Schematical)

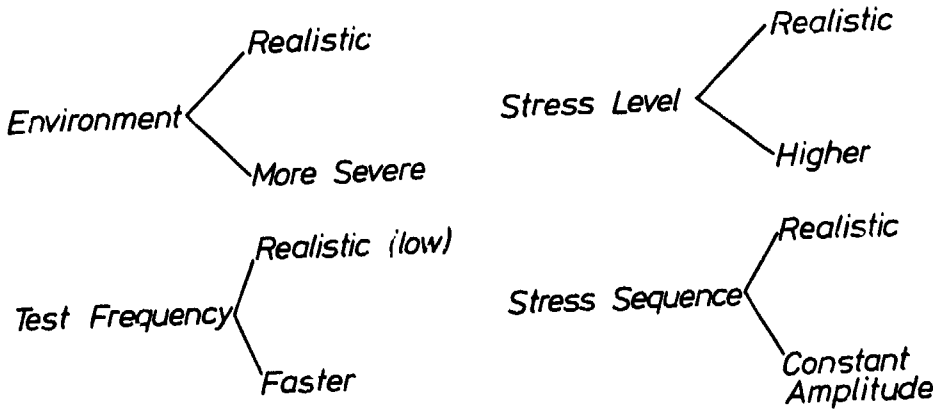

FIGURE 2: Parameters in Corrosion Fatigue Testing

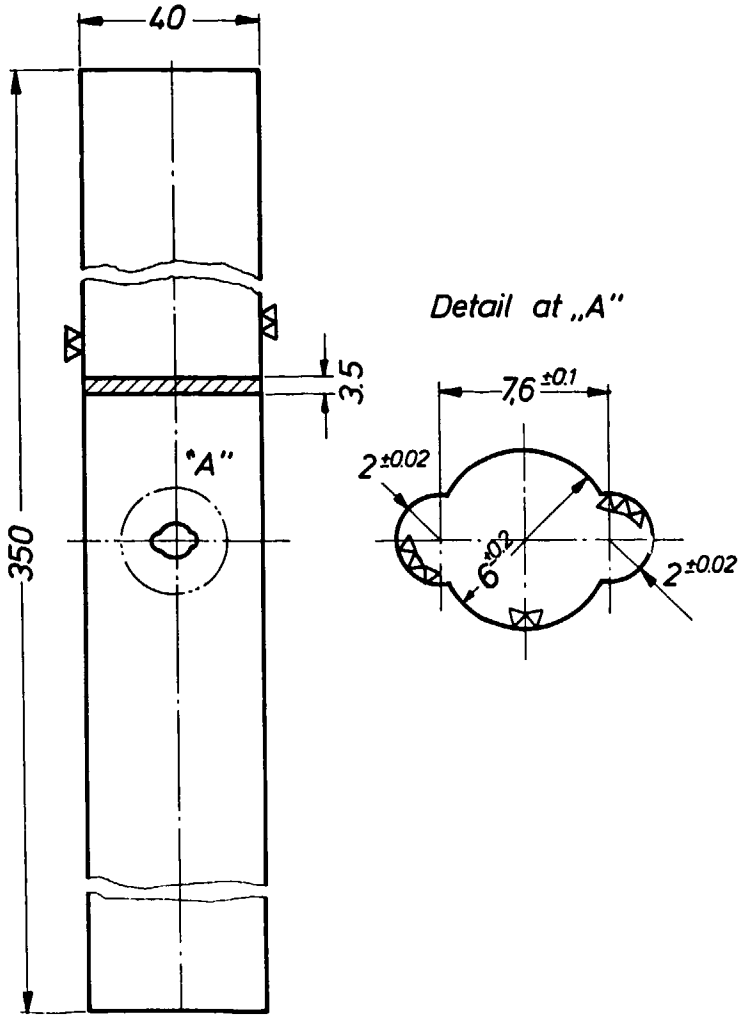

FIGURE 3: Notched Specimen K_t = 3,6

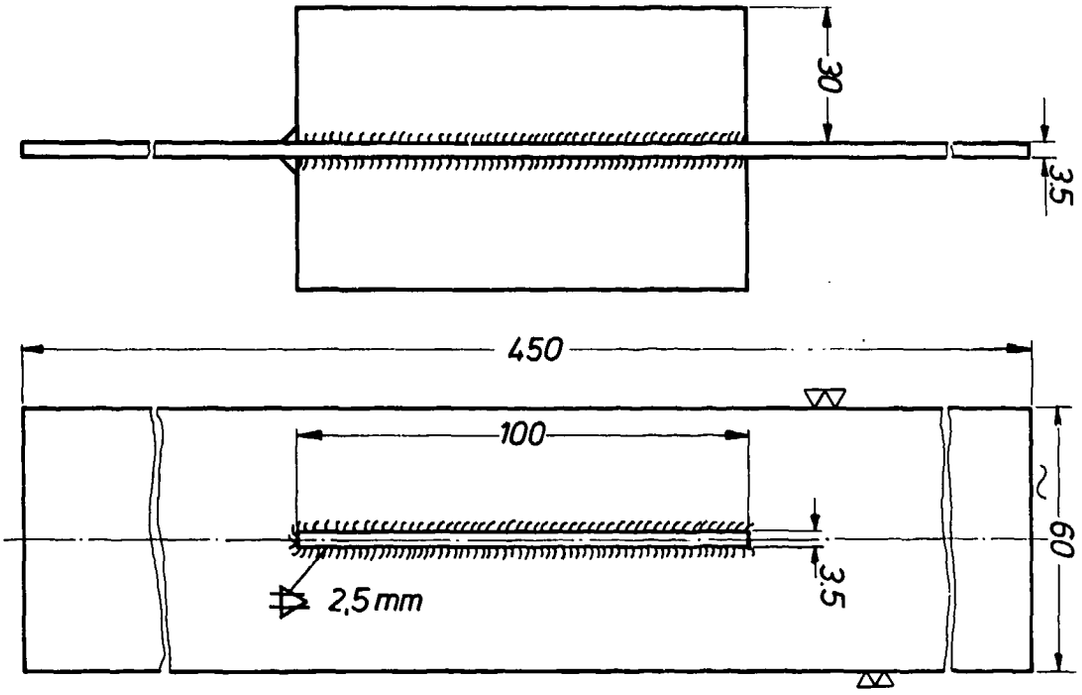

FIGURE 4: Welded Specimen Longitudinal Stiffener

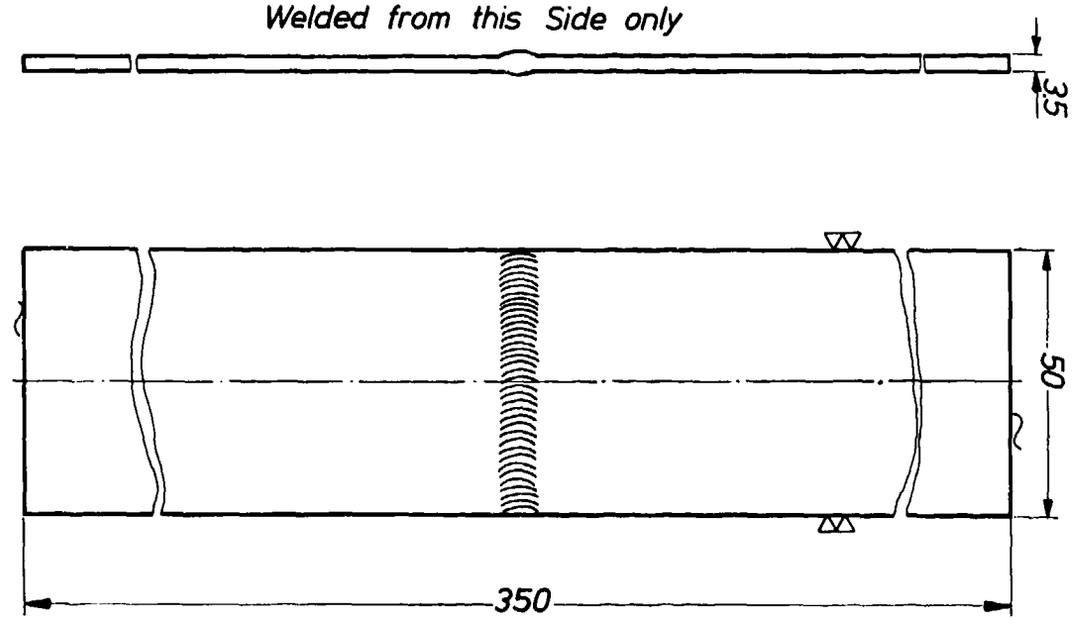

FIGURE 5: Welded Specimen Buttweld

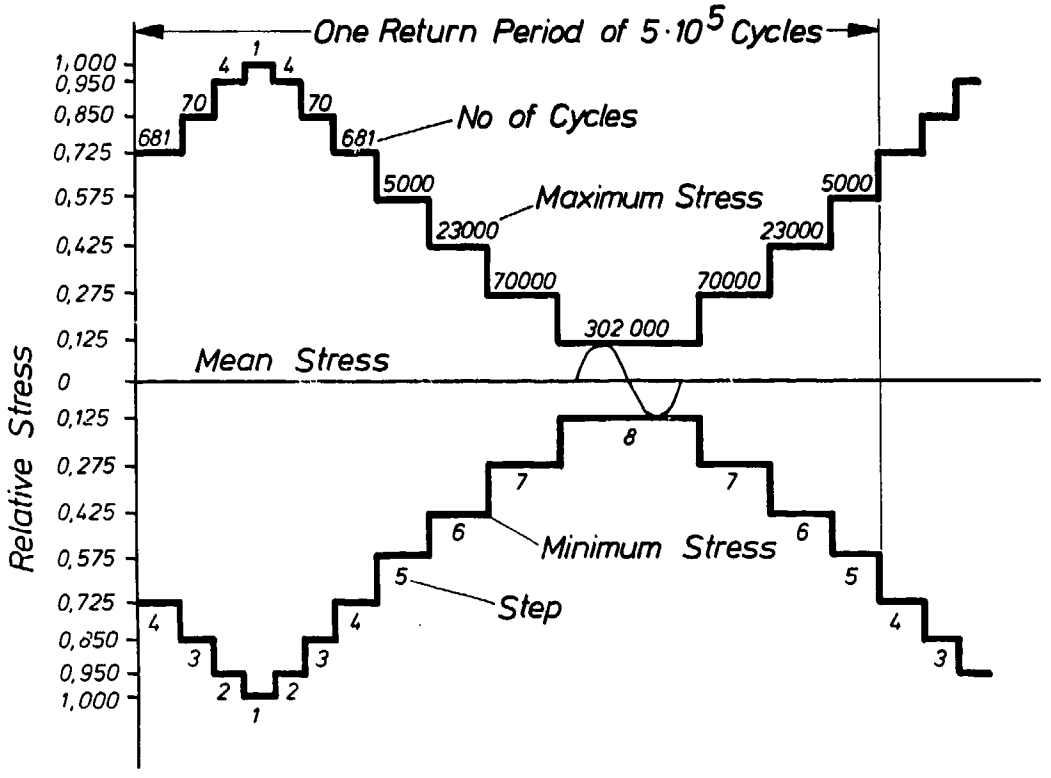

FIGURE 6: 8 Step Test with Normal Distribution

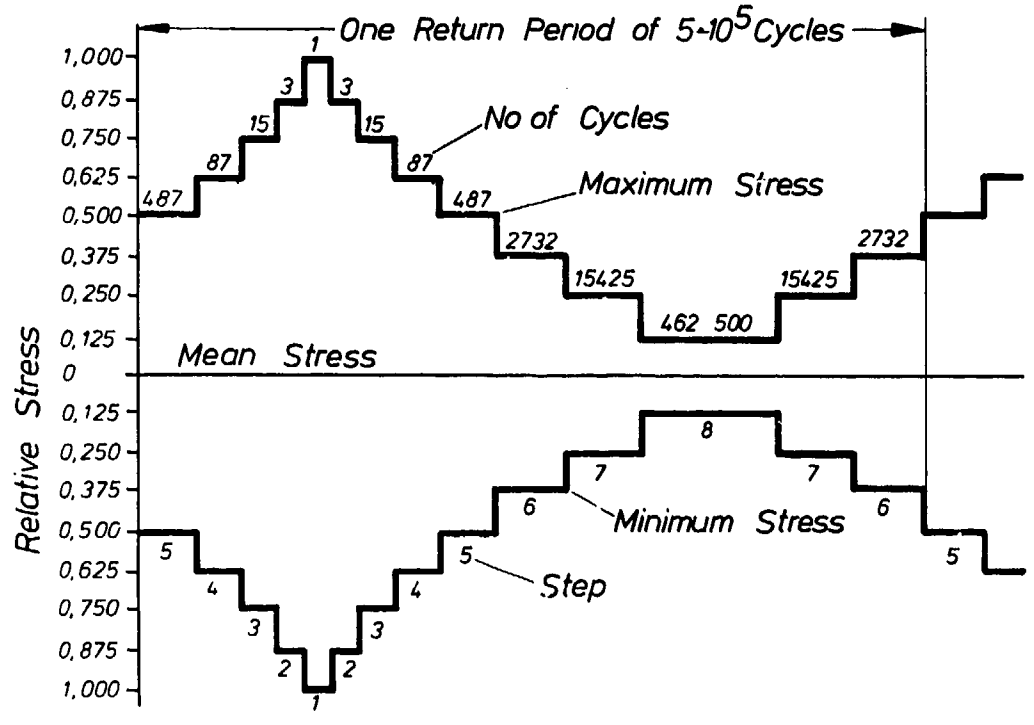

FIGURE 7: 8 Step Test with Straight Line Distribution

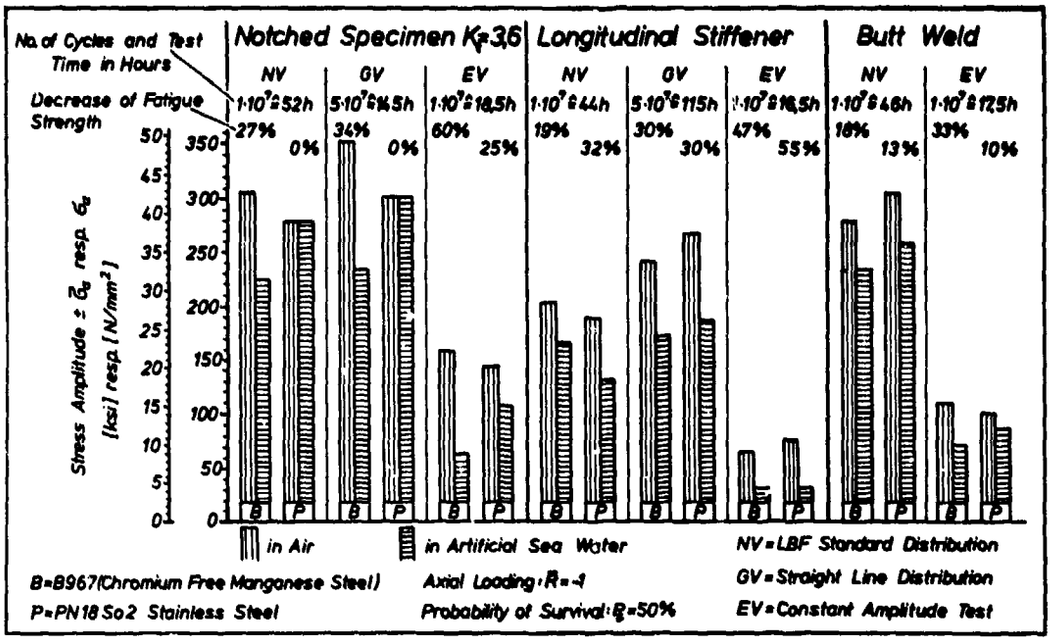

FIGURE 8: Influence of Artifical Seawater on the Fatigue Strength of Amagnetic Steels

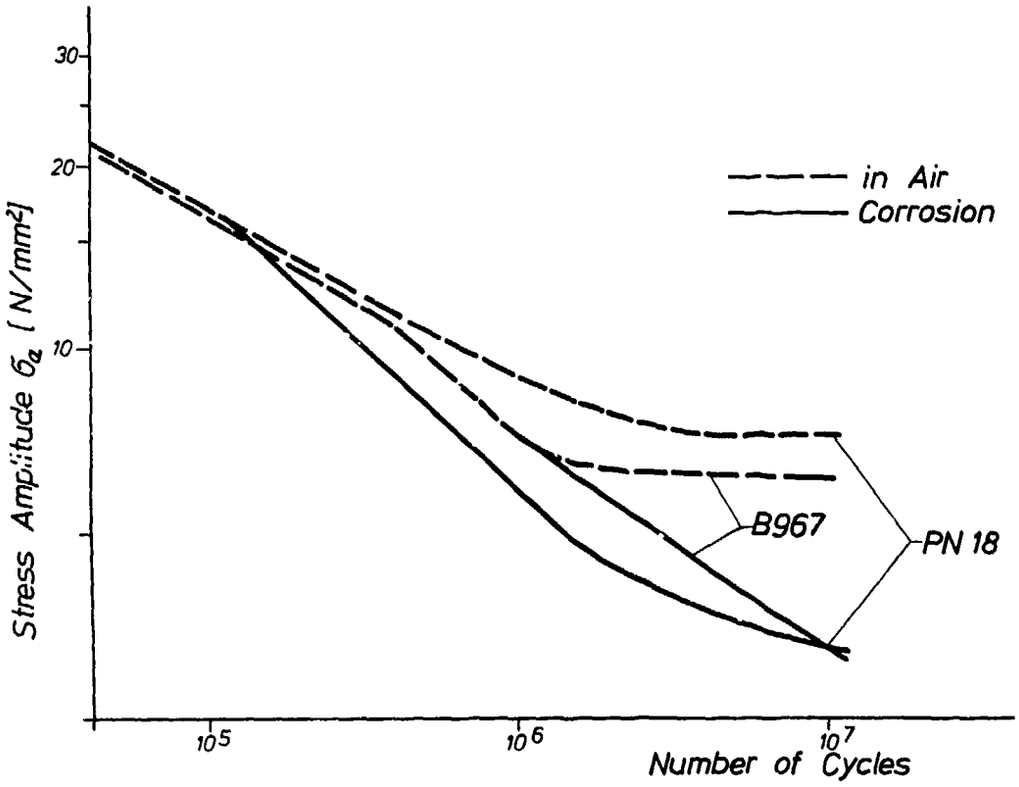

FIGURE 9: SN-Curves Longitudinal Stiffener Specimen

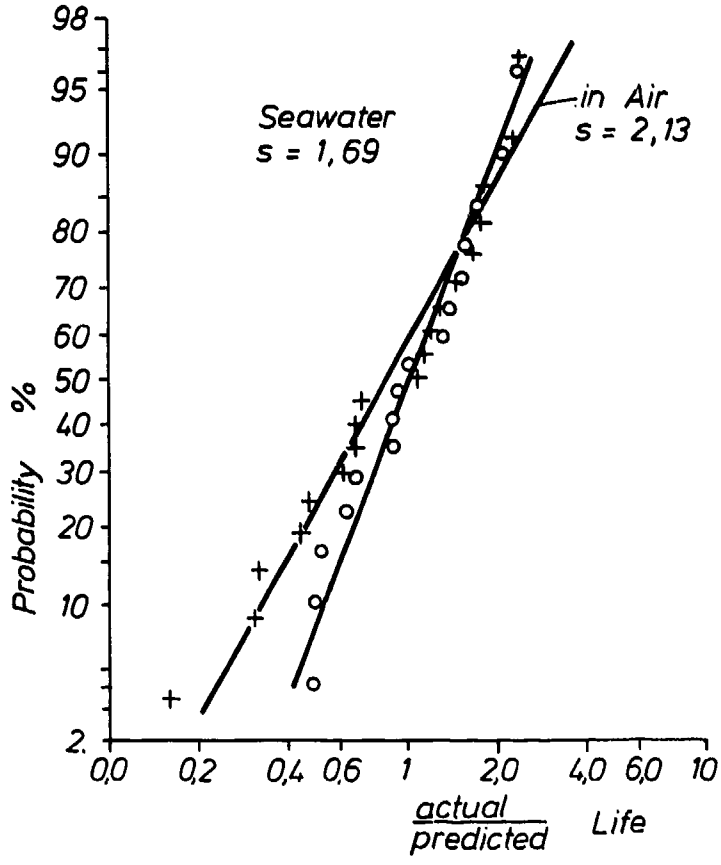

FIGURE 10: Fatigue Life Prediction Using Miner's Rule

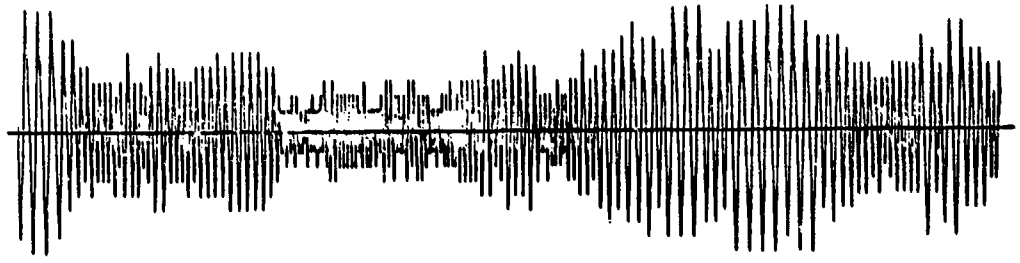

Irregularity Factor $\frac{N_o}{N_1} = 0,99$

FIGURE 11: Stationary Gaussian Random Process

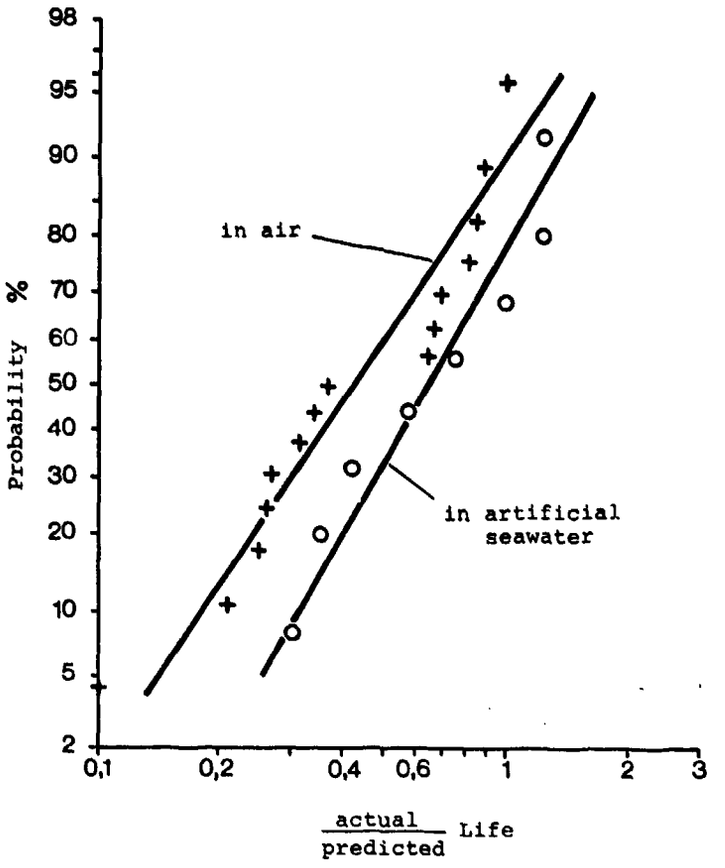

FIGURE 12: Fatigue Life Prediction Using Miner's Rule

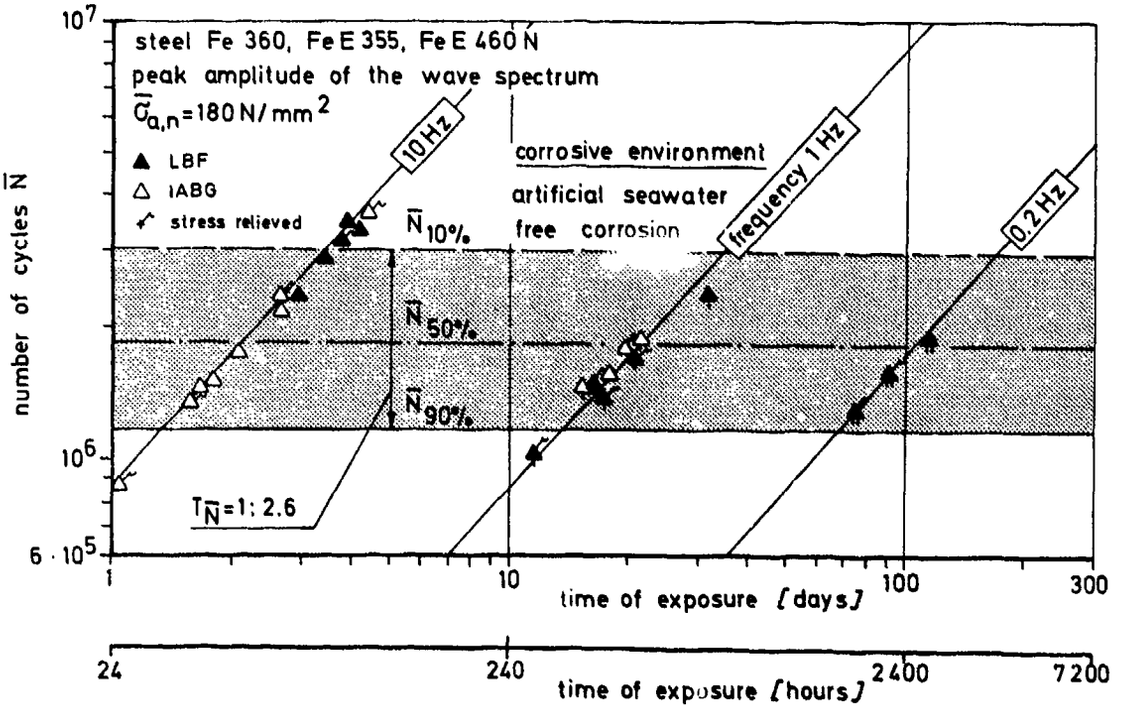

FIGURE 13: Effect of Test Frequency
Random Test Results on angular Fillet Welds

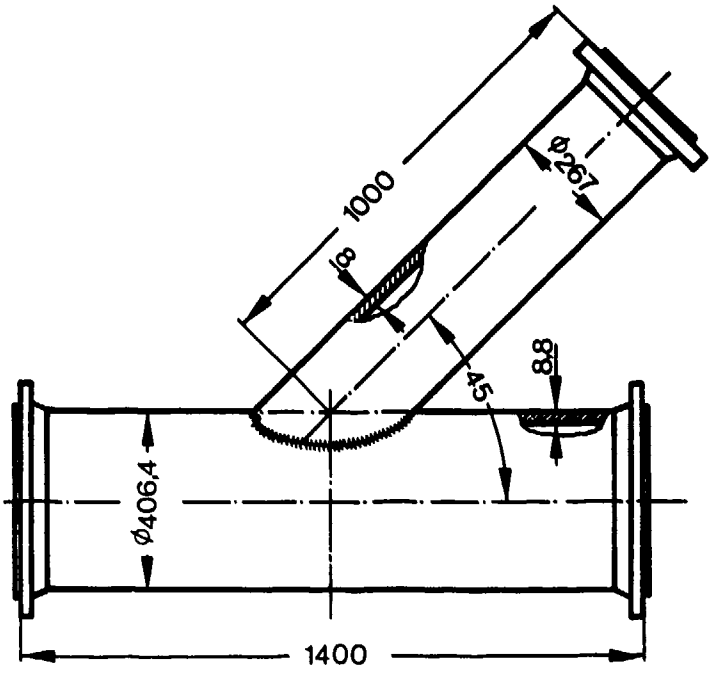

FIGURE 14

FIGURE 15

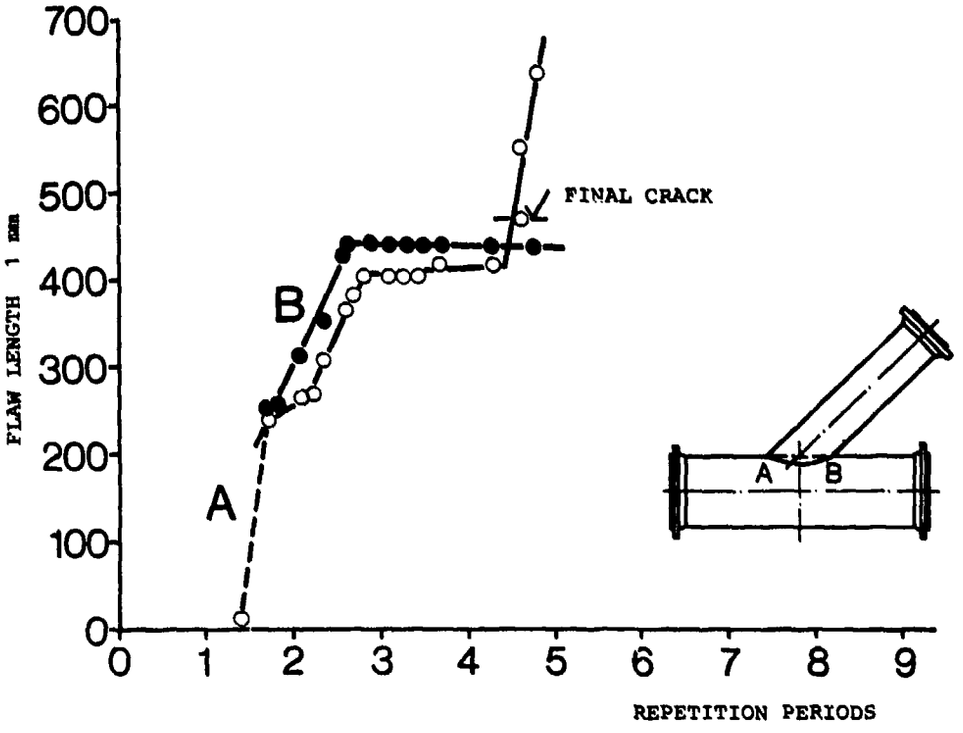

FIGURE 16

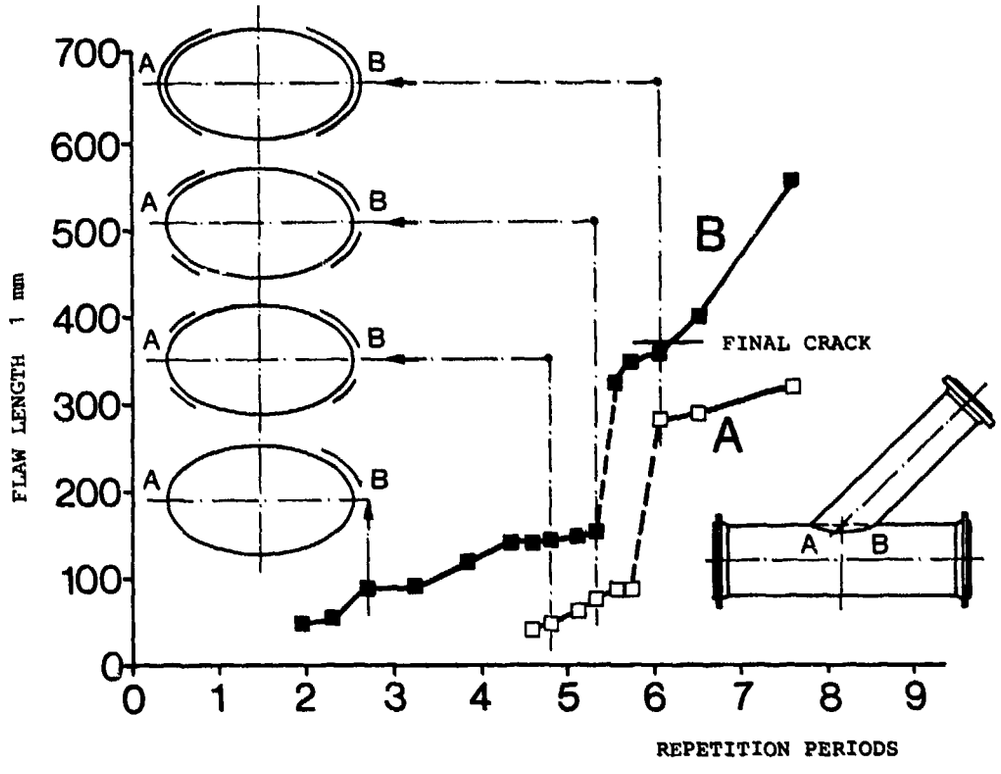

FIGURE 17

VARIABLE AMPLITUDE CORROSION FATIGUE BEHAVIOR OF A LOW CARBON STEEL

R. Gürbüz and M. Doruk
Middle East Technical University, Ankara, Turkey

SUMMARY

The results of an experimental study designed to determine the general characteristics of salt water-enhanced fatigue crack growth under conditions of variable amplitude loading are presented in this paper. The material used was a sheet of 0.22 percent carbon steel. The tests were done on 13 mm thick CT specimens in L-orientation. The crack mouth opening displacement on the loading line (C(M)OD) was varied at a constant rate, whereby the stress intensity factor varied between zero and the maximum value to C(M)OD. Negative stress ratios were eliminated by means of a special control. Comparison crack growth data were obtained by the more conventional constant load amplitude or K-increasing method and also under decreasing load amplitude. The crack growth rates were compared with reference data measured in the laboratory air. It was found that the rates of crack-growth measured at three different rates of displacement do not agree. However from the shift of curves on decreasing the rate it is concluded that the growth rate curves would tend to become stationary.

INTRODUCTION

The engineering approach to fatigue crack growth has dealt with methods of evaluating the crack growth rate as a function of stress or strain cycling. The stress intensity factor, K, has been used successfully to describe the crack propagation behavior particularly in high and medium strength materials. Although the majority of data has been obtained by the more conventional constant load amplitude or K-increasing method, some attention has been devoted also to the constant deflection amplitude and the decreasing load amplitude, in which the stress intensity factor decreases with increasing crack size. Agreement was observed between fatigue crack growth data from K-increasing and K-decreasing techniques for steels tested at different stress ratios [1, 2].

Variable amplitude fatigue testing would also be expected to be important in relation to corrosion fatigue behavior of materials. In addition, there is a need to apply to low strength materials the newer fracture mechanical parameters as the energy-line integral (J-integral), since linear elastic fracture mechanics would be not valid in the case of these materials. In a study of stress corrosion cracking of the same steel as used in the present work, the authors obtained good agreement between crack growth rate and the energy-rate line integral [3]. The evaluation of these parameters is based on the load-extension curves recorded under constant rate of deflection on the loading line.

Pursuing the same approach, the characterization of corrosion fatigue behavior in terms of the energy-rate line integral would require the measurement of the load in dependence of displacement amplitude, where the latter is increased at a constant rate.

The present work was planned basically to obtain information on the effect of this type of test on the crack growth behavior of a low strength steel. The characterization of corrosion fatigue behavior in terms of the energy-rate line integral will be the topic of future work.

EXPERIMENTAL PROCEDURE

Materials

The material used in this study was a hot-rolled 15 mm sheet of ABS Gr.A.3701 steel having a composition of 0.22 percent carbon, 0.70 percent manganese, 0.05 percent silicon, 0.02 percent phosphorus, 0.03 percent sulfur and 0.20 percent copper. The mechanical properties of this steel are as shown in Table 1.

Table 1. Tensile properties of ABS Gr.A.3701 Steel

0.2% Yield Strength, MPa	295
Ultimate Tensile Strength, MPa	450
Fracture Strength, MPa	390
Elongation, %	29
Reduction in Area, %	60
Young's Modulus, MPa	1.76×10^5

Standard 13 mm thick compact tension (CT) specimens were used for crack growth studies. All the specimens were precracked under the action of haversine fatigue loading of R=0 and at a frequency of 10 Hz. The load amplitude was 1000 Kg. 3 to 5 mm length fatigue cracks were obtained for all of them. Two wedging edges were designed to measure the crack mouth opening displacement (C(M)OD) on the loading line by the attachment of a clip-on gage. The crack growth direction was parallel to the rolling direction for all specimens. Dimensions of the compact-tension specimen used in this study are shown in Fig.1.

Testing Equipment

All tests were conducted on a closed-loop hydraulically activated servo-controlled testing machine in the horizontal position. An optical travelling microscope with a

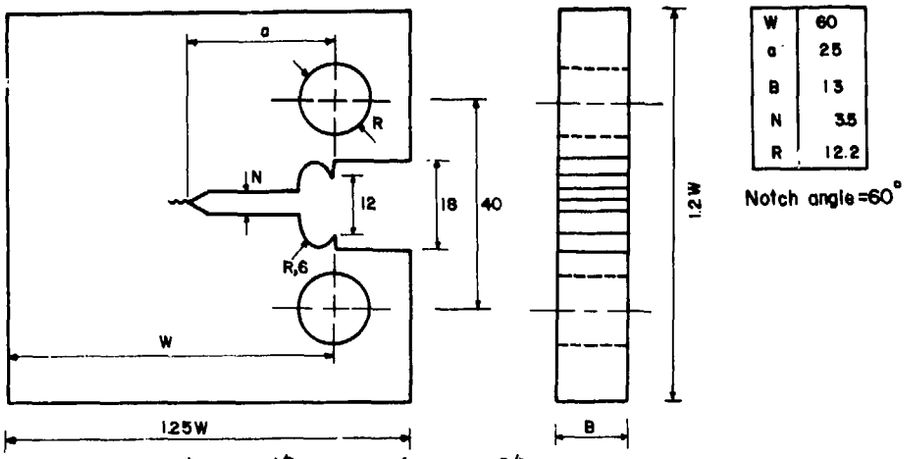

Fig.1. Compact-tension specimen (ASTM E399-72 Designation)

sensitivity of 0.01 mm was used to monitor the instantaneous values of crack length. The increasing displacement and the decreasing load amplitude tests were carried out with the aid of an electro-mechanical scanning device consisting of a helical 10-turn potentiometer and an electrical motor with adjustable speed. A clip-on gage was attached to the wedge edges of the compact tension specimens to measure the instantaneous C(M)OD values. The load vs. displacement or the load vs. C(M)OD curves were taken from the X-Y Recorder on the testing machine

An additional part consisting of a stationary piston and a movable cylinder was designed in order to prevent the compressive stresses during the increasing displacement amplitude tests. Fig.2 shows the cross-sectional view and location of the part in the loading train.

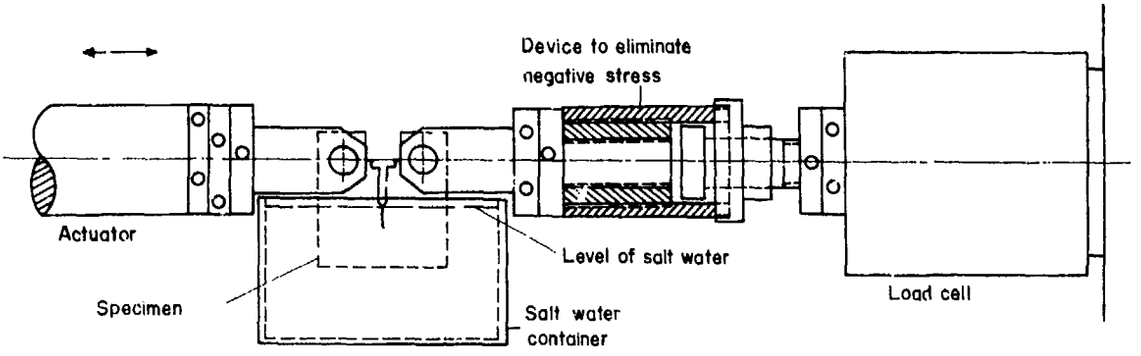

Fig.2. The crossectional view and location of the additional device which prevents the compressive stresses during the increasing displacement amplitude tests.

Testing Program

As shown in Fig.3, the testing program consisted of three sets of experiments carried out under conditions of (1) increasing displacement amplitude, (2) decreasing load amplitude and (3) constant load amplitude. In all tests a sinusoidal type of fatigue loading with a frequency of 1 Hz was applied. In the first set of experiments, the displacement amplitude was increased gradually from zero to higher values at a constant rate. Three different displacement rates (4.467, 2.234 and 1.340×10^{-4} mm/cycle) were used in three experiments in the laboratory air. These tests were then repeated under the same conditions but in a 3.5% NaCl solution at room temperature.

In the second set of experiments two tests were conducted under the condition of decreasing load amplitude with a constant rate from 1200 Kg., first in the laboratory air and second in a 3.5% NaCl solution at room temperature. The load was decreased at a rate of 0.0224 Kg/cycle. The conventional constant load amplitude fatigue test was carried out in 3.5% NaCl solutions at room temperature only. The load amplitude was 1200 Kg.

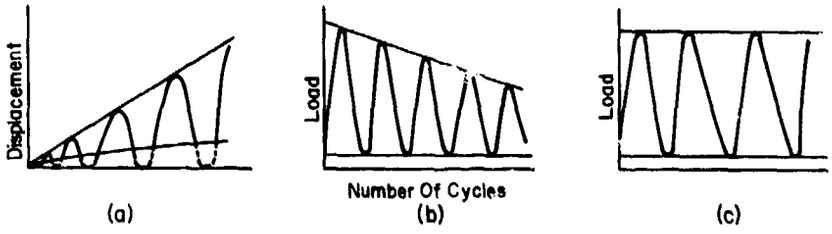

Fig.3. Testing program of (a) increasing displacement amplitude (b) decreasing load amplitude and (c) constant load amplitude tests

A fourth-degree polynomial was fitted to the crack length vs. number of cycles data by using the method of least squares. Instantaneous crack growth rates, da/dN, were calculated by taking the first derivative of the polynomial with respect to N.

RESULTS

Results from the increasing displacement amplitude tests are conveniently presented in terms of the curves shown in Figs.4,6,8,10,12 and 14. The same curves indicating the variation of C(M)OD instead of the variation of load range with number of cycles were plotted for the remaining load controlled experiments (Figs.16,18 and 20). The variation of crack growth rate, da/dN, with respect to the stress intensity range, ΔK, is shown for each experiment on logarithmic scales (Figs.5,7,9,11,13,15,17,19 and 21). Data corresponding to dry and wet experiments under the same conditions were shown on the same figures for comparison (Figs.11,13,15 and 19). Fig.22 shows the change in the crack growth rate with increasing rate of displacement. This figure includes the crack growth data obtained from the more conventional constant load amplitude test for comparison.

DISCUSSION

The results obtained from the increasing displacement amplitude tests are different from those of the conventional constant load amplitude and decreasing load amplitude tests in that a maximum appears in the curves of load range and strees-intensity range vs. the number of cycles. Inspite of the fact that the maxima of load vary over a wide range, the maximum values of stress intensity range show good agreement. This is observed in all experiments conducted in the laboratory air and in the 3.5% NaCl solution as well. Agreement exists also in experiments run with different rates of displacement. Maximum ΔK-values ranging from 209 to 211,1 MPa.$m^{\frac{1}{2}}$ were obtained from experiments in the laboratory air. In the 3.5% NaCl solution, however, the maxima in ΔK showed a slight decrease from 211,1 to 197,5 MPa.$m^{\frac{1}{2}}$ with a decrease in the displacement rate from 4.467 to 1.340×10^{-4} mm/cycle. Maximum ΔK-values measured under conditions of decreasing load and constant load varied between 184.3 and 188.6 MPa.$m^{\frac{1}{2}}$. As shown by the above data, a farreaching agreement exists in relation of the maximum ΔK-values. Thus, an obvious advantage of the increasing displacement tests is that a critical stress intensity range can easily be determined as the maximum in the curves for stress intensity range vs. number of cycles.

As observed for the stress intensity range, the rate of crack growth also goes through a maximum, which corresponds to the maximum stress intensity range. The growth of the crack beyond the K-validity range caused a secondary increase of the crack growth rate in some experiments. This appears to be a serious deviation from crack growth rate vs. stress intensity range curves.

The crack growth rate vs. stress intensity range curves were determined under increasing ΔK. Since the displacement rates were chosen too high,the period taken by increasing ΔK was very short. In fact, the displacement rates need to be chosen much lower than used in this study, in order to obtain reliable data regarding crack growth behavior in corrosion fatigue. As shown in Figs.5,7 and 9, the crack growth rates measured under decreasing ΔK are higher than those under increasing ΔK for experiments conducted in the atmosphere. This appears as a shift of the crack growth rate vs. ΔK curves to lower ΔK. For experiments conducted in 3.5% NaCl solution, however, it is not possible to conclude whether there is any kind of agreement between crack growth rates measured either with increasing or decreasing ΔK.

As shown in Fig.22, the crack growth rate vs. stress intensity range curves are sensitive to the displacement rate. Indeed, the rate of crack growth in corrosion fatigue is controlled by the interaction between the chemical mechanism and mechanical mechanism occurring at the crack tip. It is obvious that the damage caused by the mechanical mechanism will increase with increasing rate of displacement. Thus, on decreasing the displacement rate, the conditions are approached under which the critical interaction between chemical and mechanical factors can take place. This is evident from the shift of curves to higher stress intensity ranges on decreasing the displacement rate (Fig.22). The crack growth rate vs. stress intensity curves are expected to become stationary when the rate of displacement is kept lower than a critical value.

CONCLUSION

The investigation shows the advantage of the constant displacement corrosion fatigue test wherein the crack growth data can be obtained over a wide range from nearly the threshold stress intensity to the critical stress intensity range. At this stage, no conclusion can be reached regarding the utility of the increasing displacement test as an accelerated test.

REFERENCES

[1] Saxena, A., Hudak, S.I., Donald, J.K., and Schmith, D.W., "Computer-Controlled Decreasing Stress Intensity Technique for Low Rate Fatigue Crack Growth Testing." Journal of Testing and Evaluation, Vol.6, No.3, May 1978, pp.167-174.

[2] Stephens, R.I., Benner, P.H., Mauritzson, G., and Tindall, G.W., "Constant and Variable Amplitude Fatigue Behavior of Eight Steels." Journal of Testing and Evalution, Vol.7, No.2, March 1979, pp.68-81.

[3] Utkanlar, N. and Doruk, M., "The Application of Fracture Mechanics to SCC in a Low Strength Steel." (To be sent to the Journal of Engineering Fracture Mechanics for consideration).

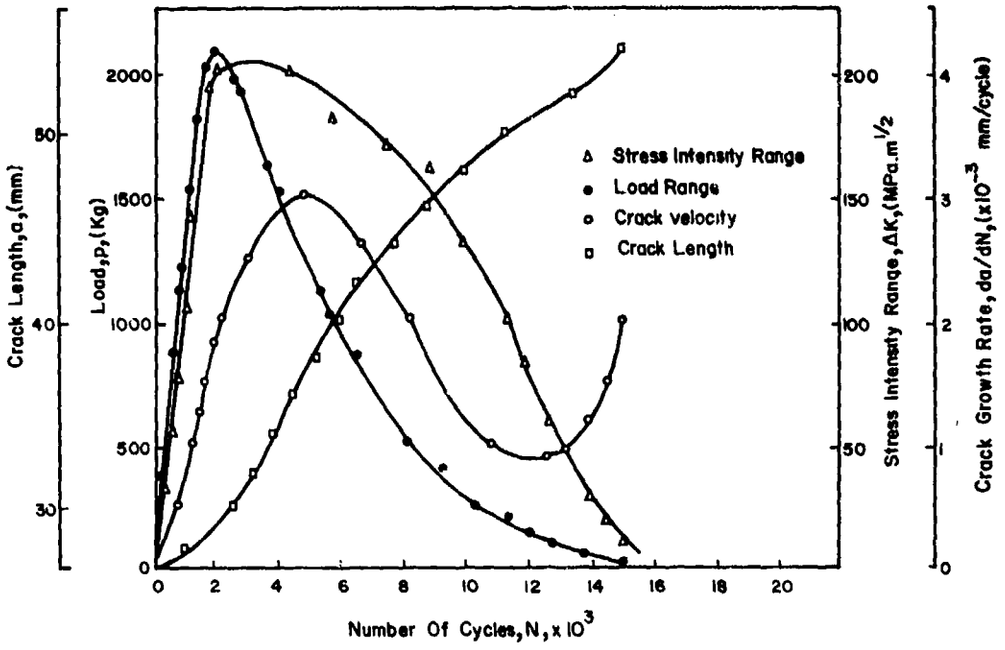

Fig.4. Variations of load range, stress intensity range, crack length and crack growth rate with the number of cycles in the laboratory air (Rate of displacement: 4.467×10^{-4} mm/cycle).

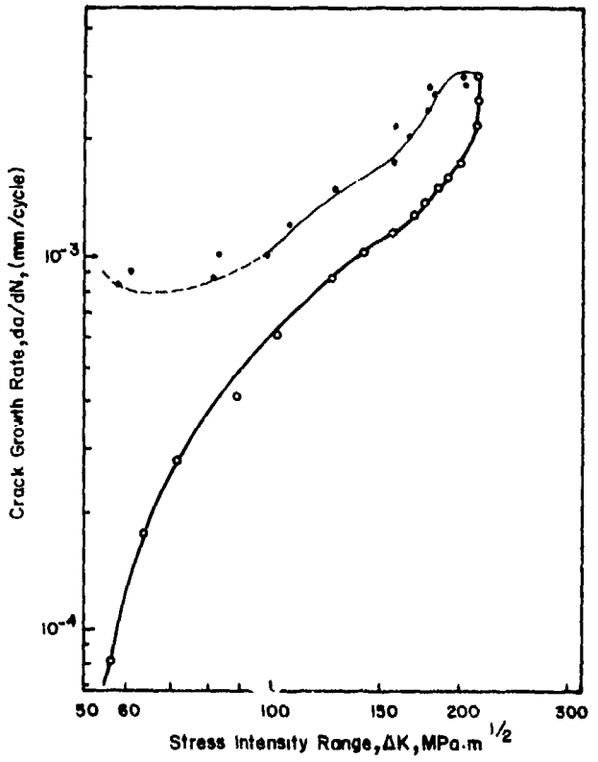

Fig.5. Crack growth rate vs stress intensity range curve in the laboratory air (Rate of displacement: 4.467×10^{-4}mm/cycle).

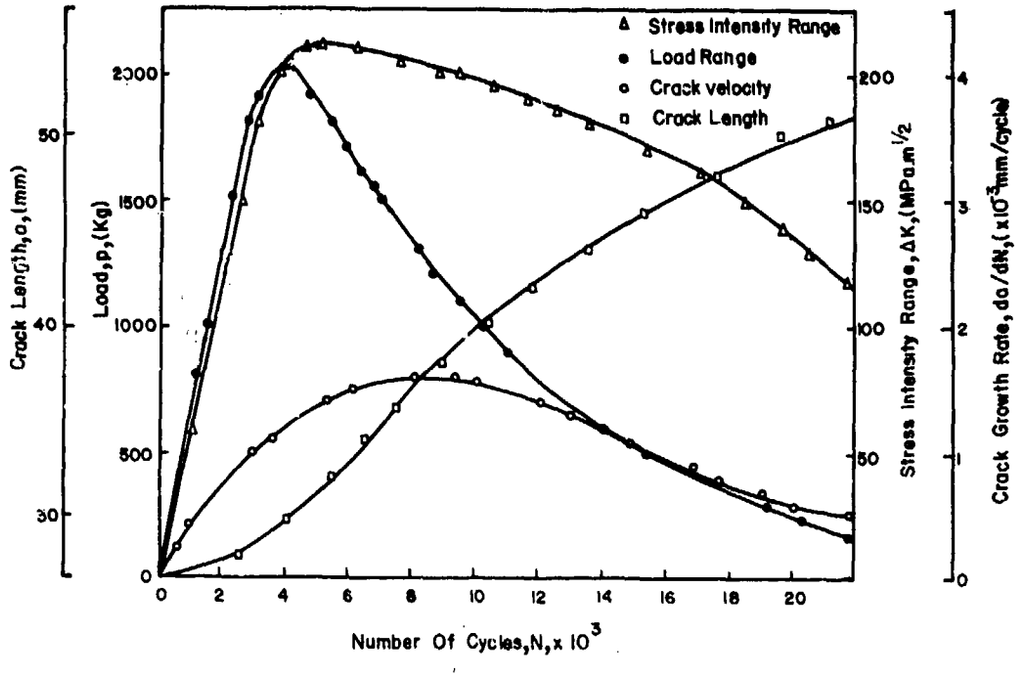

Fig.6. Variations of load range, stress intensity range, crack length and crack growth rate with the number of cycles in the laboratory air (Rate of displacement: 2.234×10^{-4} mm/cycle).

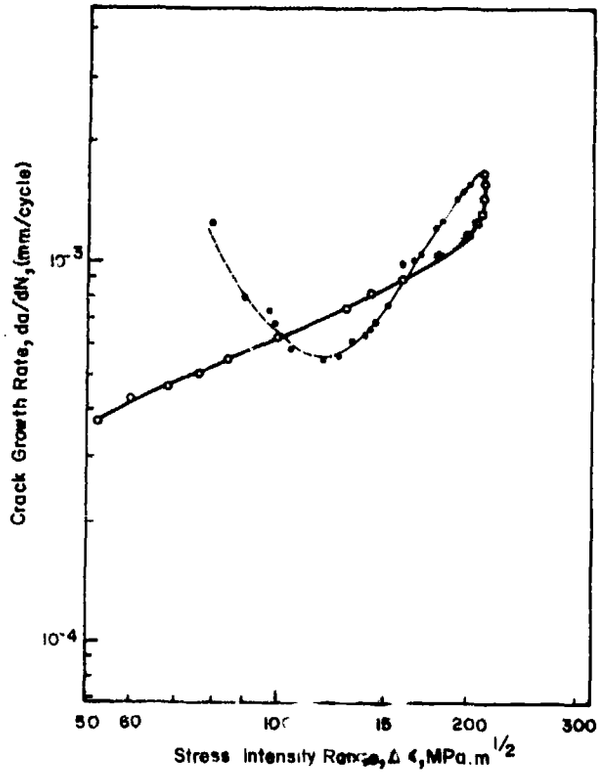

Fig.7. Crack growth rate vs stress intensity range curve in the laboratory air (Rate of displacement: 2.234×10^{-4}mm/cycle).

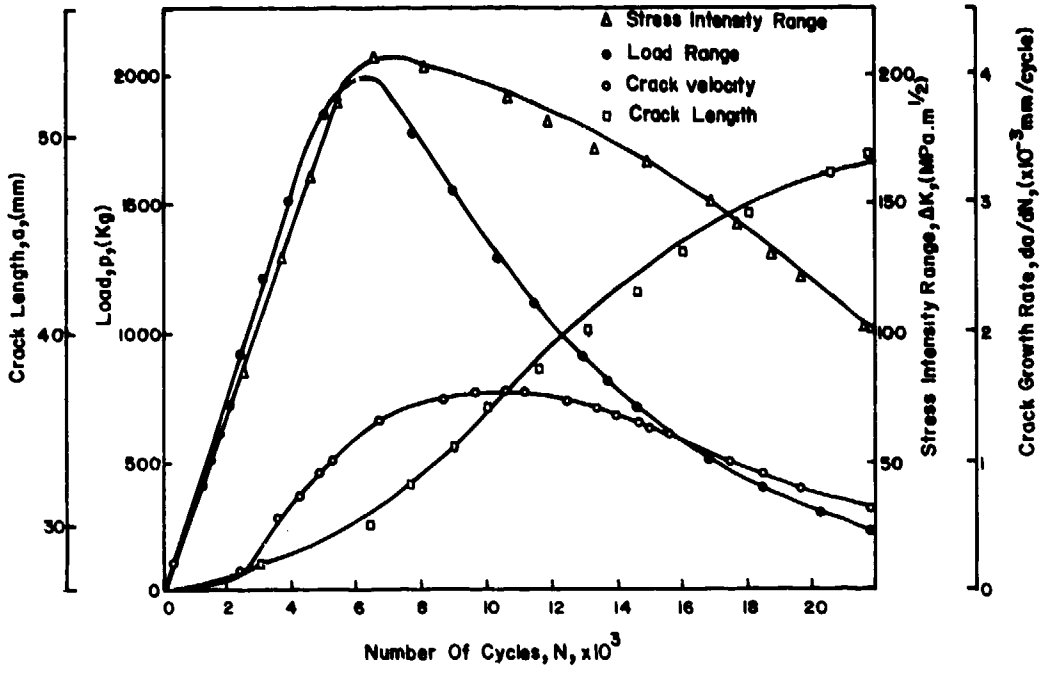

Fig.8. Variations of load range, stress intensity range, crack length and crack growth rate with the number of cycles in the laboratory air (Rate of displacement: 1.340×10^{-4} mm/cycle).

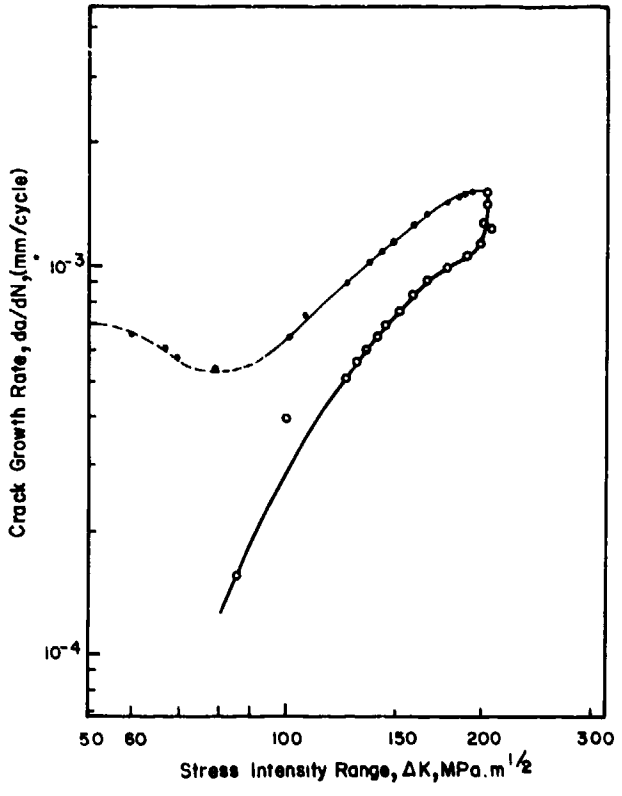

Fig.9. Crack growth rate vs stress intensity range curve in the laboratory air (Rate of displacement: 1.340×10^{-4}mm/cycle).

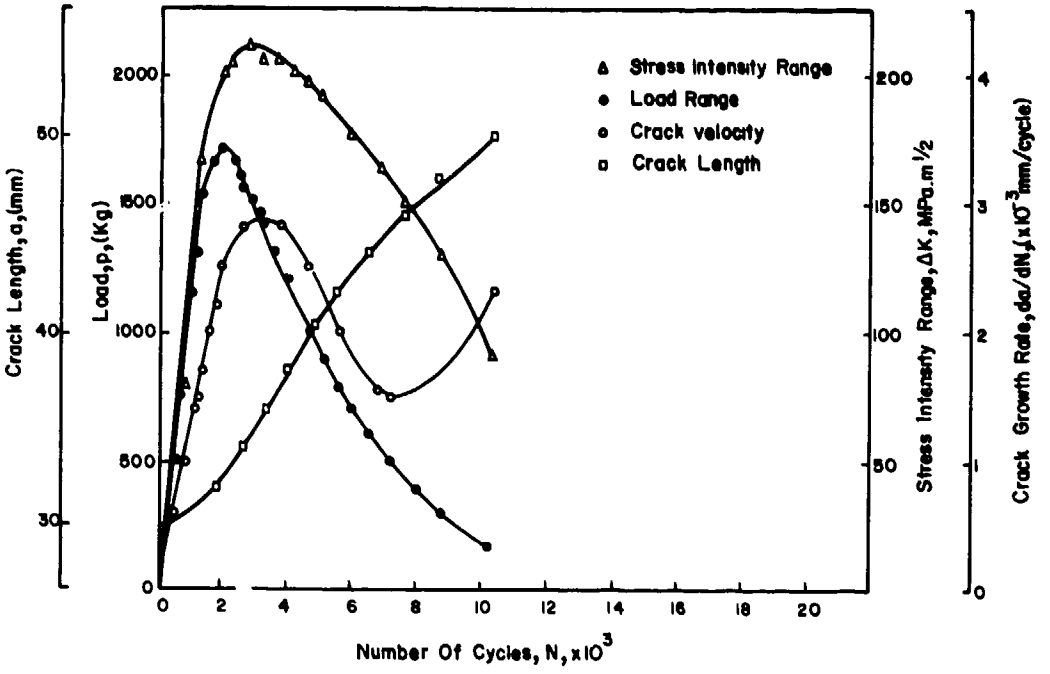

Fig.10. Variation of load range, stress intensity range, crack length and crack growth rate with the number of cycles in 3.5% NaCl (Rate of displacement: 4.467×10^{-4} mm/cycle).

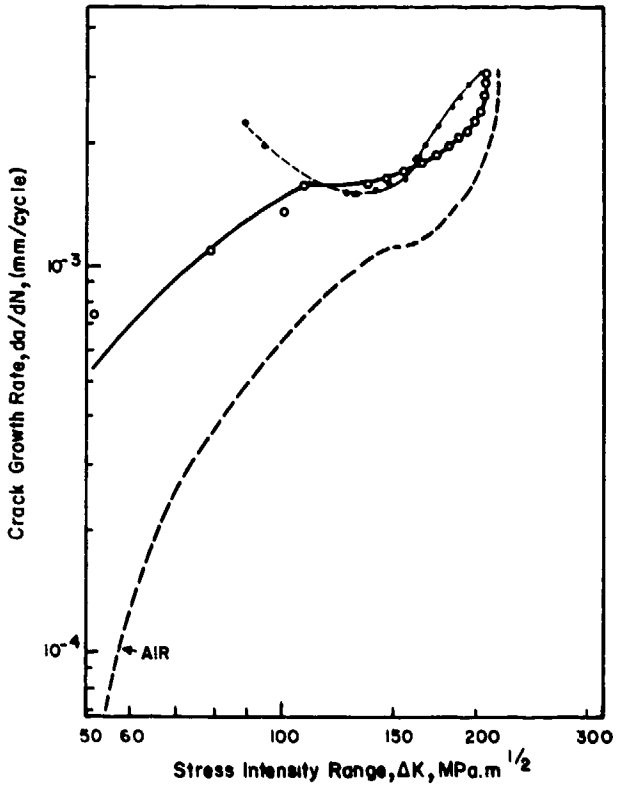

Fig.11. Crack growth rate vs stress intensity range curve in 3.5% NaCl (Rate of displacement: 4.467×10^{-4} mm/cycle).

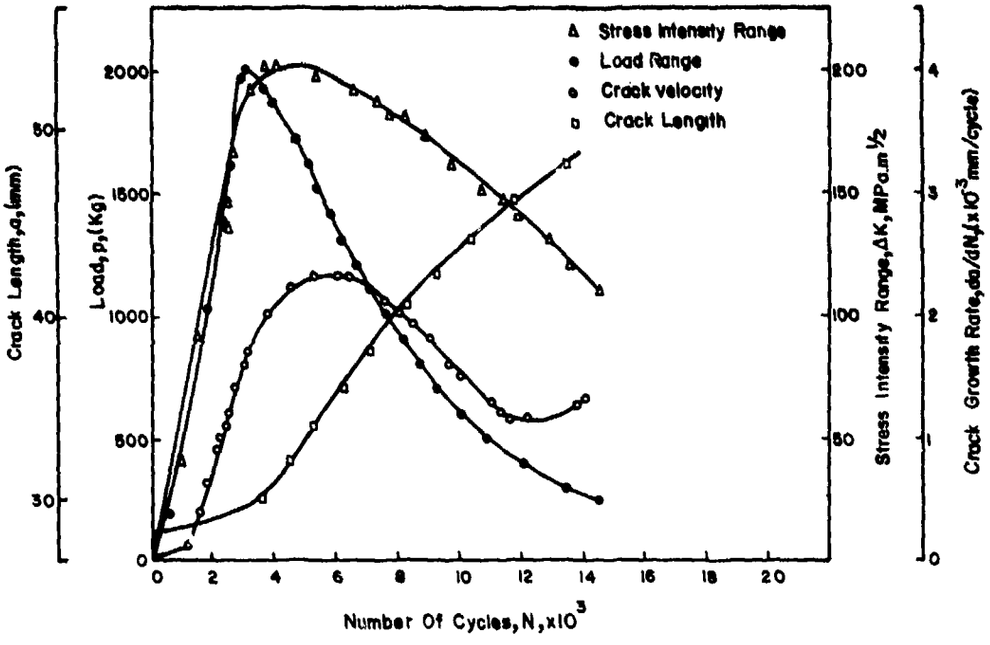

Fig.12. Variation of load range, stress intensity range, crack length and crack growth rate with the number of cycles in 3.5% NaCl (Rate of displacement: 2.234×10^{-4} mm/cycle).

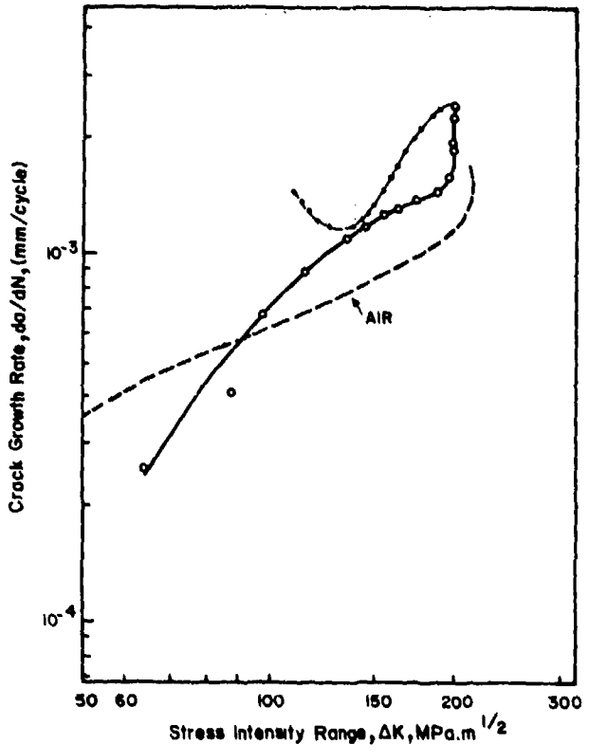

Fig.13. Crack growth rate vs stress intensity range curve in 3.5% NaCl (Rate of displacement: 2.234×10^{-4} mm/cycle).

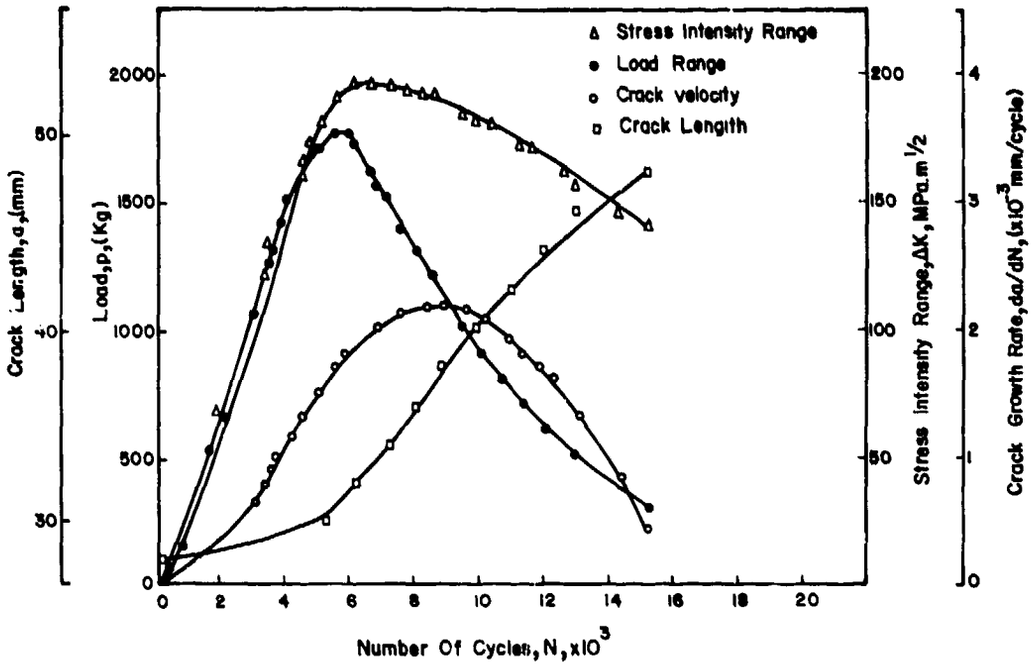

Fig.14. Variation of load range, stress intensity range, crack length and crack growth rate with the number of cycles in 3.5% NaCl (Rate of displacement: 1.340×10^{-4}mm/cycle).

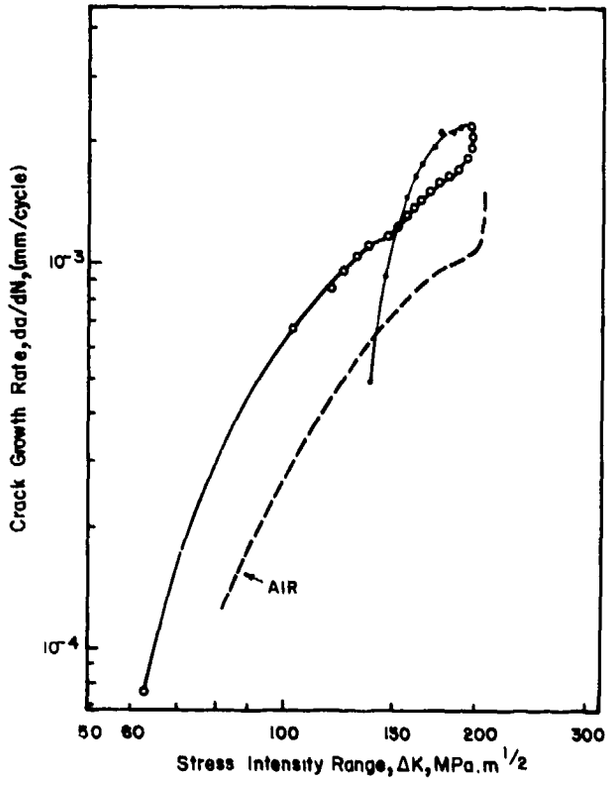

Fig.15. Crack growth rate vs stress intensity range curve in 3.5% NaCl (Rate of displacement: 1.340×10^{-4} mm/cycle).

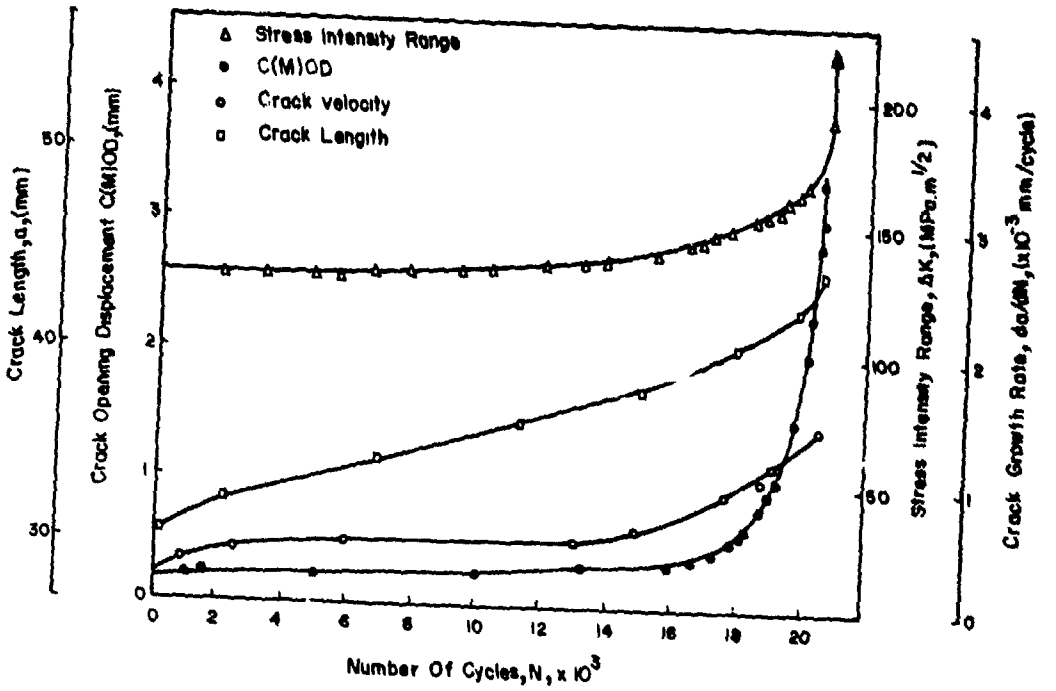

Fig.16. Variation of C(M)OD, stress intensity range, crack length and crack growth rate with the number of cycles in the laboratory air (Load range was decreased from 1200 Kg. with a rate of 0,0224 Kg/cycle whereby the minumum load was kept constant at 60 Kg.).

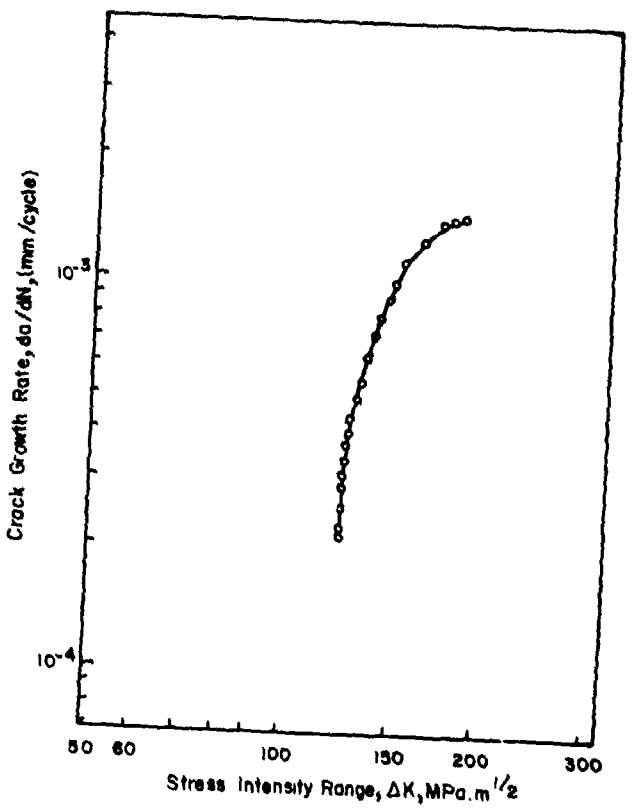

Fig.17. Crack growth rate vs stress intensity range curve in the laboratory air (Load range was decreased from 1200 Kg with a rate of 0,0224 Kg/cycle whereby the minimum load was kept constant at 60 Kg).

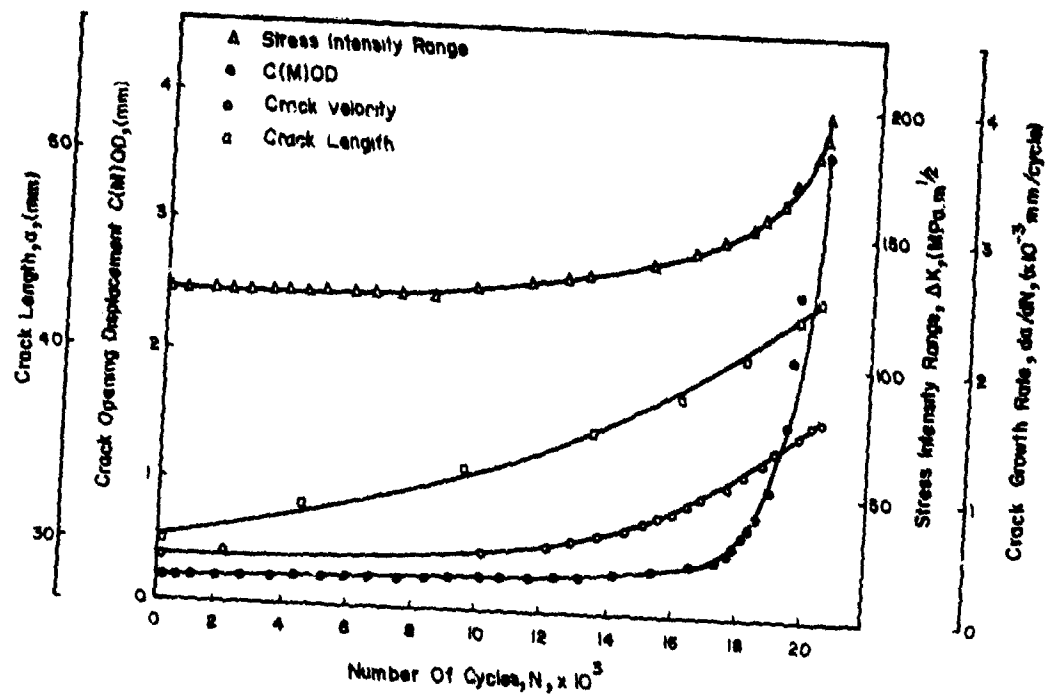

Fig.18. Variation of C(M)OD, stress intensity range, crack length and crack growth rate with the number of cycles in 3.5% NaCl (Load range was decreased from 1200 Kg with a rate of 0,0224 Kg/cycle whereby the minumum load was kept constant at 60 Kg).

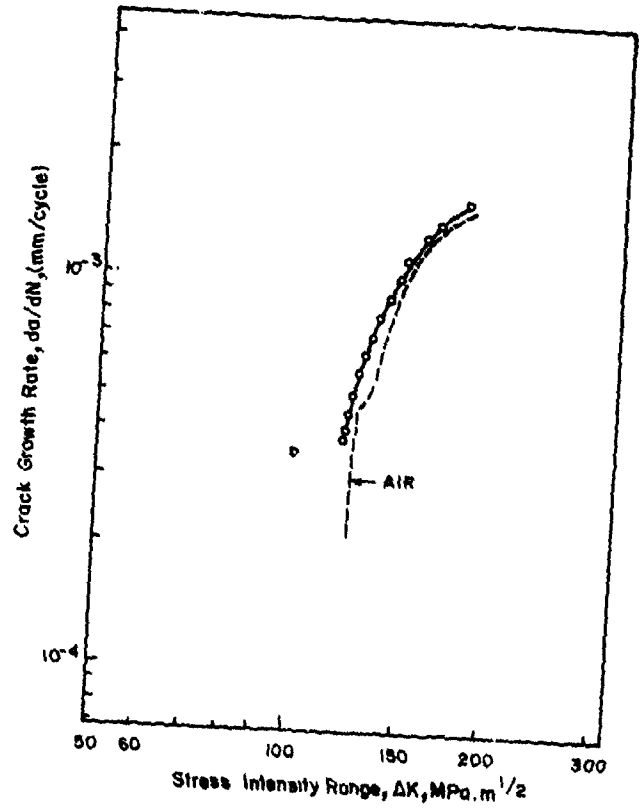

Fig.19. Crack growth rate vs stress intensity range curve in 3.5% NaCl (Load range was decreased from 1200 Kg with a rate of 0,0224 Kg/cycle whereby the minimum load was kept constant at 60 Kg).

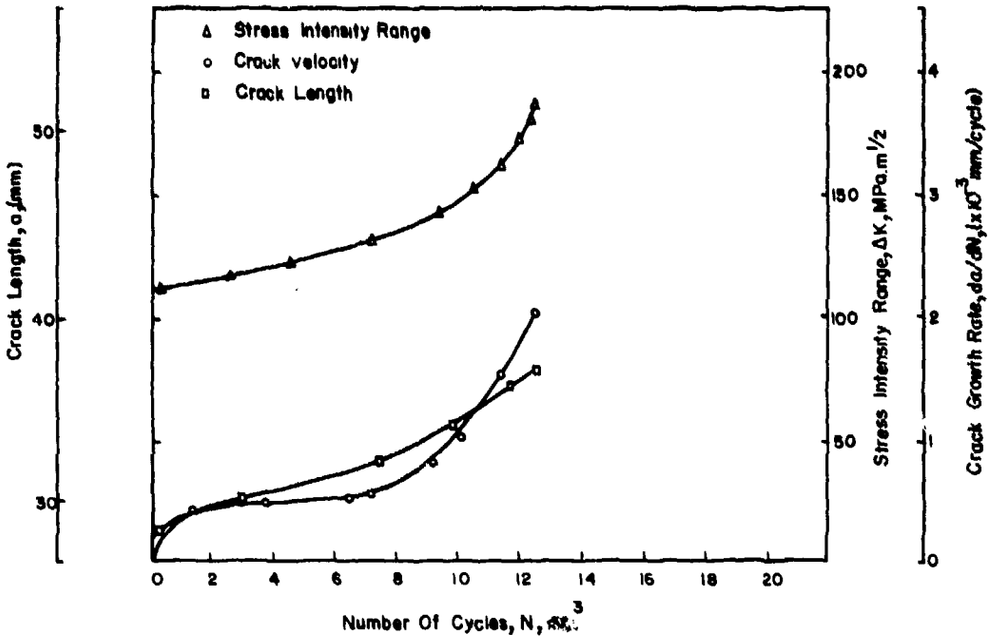

Fig.20. Variation of stress intensity range, crack length and crack growth rate with the number of cycles in 3.5% NaCl (Load range was kept constant at 1200 Kg. at R=0,05).

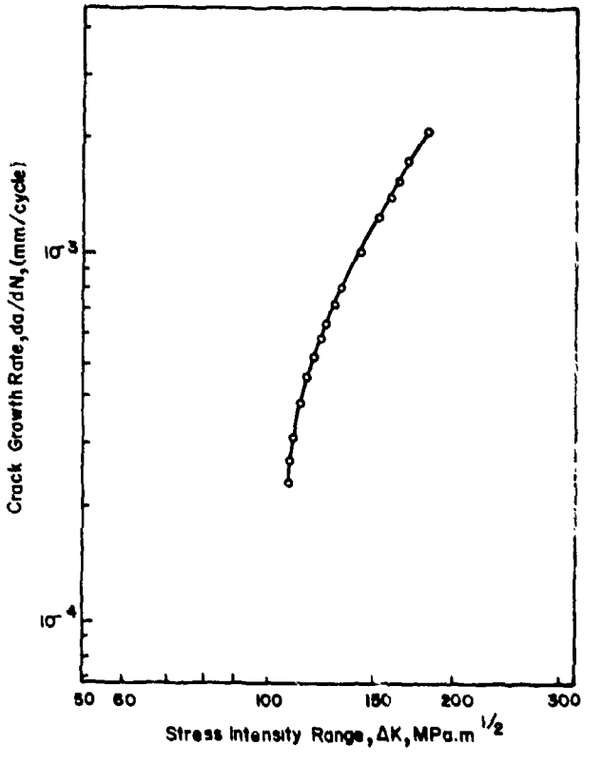

Fig.21. Crack growth rate vs stress intensity range curve in 3.5% NaCl (Load range was kept constant at 1200 Kg at R=0.05).

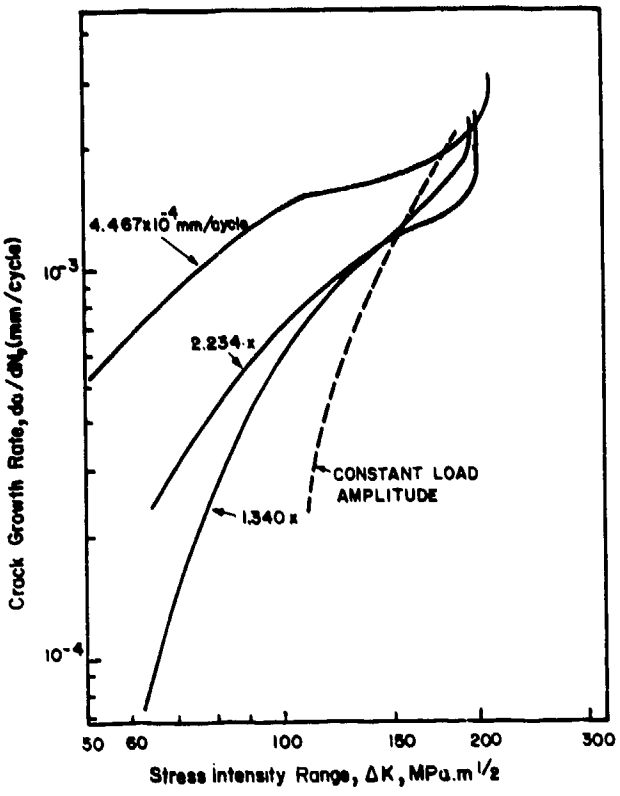

Fig.22. Variation of crack growth rate vs. strees intensity range curves with the rate of displacement compared with the curve obtained from the conventional constant load amplitude test (all in 3.5% NaCl).

FLIGHT-BY-FLIGHT CORROSION FATIGUE TESTS

by

Dr.-Ing. Walter Schütz

Industrieanlagen-Betriebsgesellschaft mbH
Einsteinstraße 20, 8012 Ottobrunn, Germany

1. Introduction

As mentioned in [1], corrosion fatigue tests should be conducted under realistic load sequences. This may be especially important for tests with riveted specimens because the rare high loads of the spectrum may loosen the fasteners, damaging the corrosion protection system and therefore rendering it ineffective. Possibly this does not happen in constant amplitude tests because the loads may not be high enough to crack the protection system.

This is the reasoning behind the test program carried out at the IABG with flight-by-flight tests, this program being part of the supplemental program of the CFCTP. In accordance with this program, it was decided to use the FALSTAFF sequence.

Tests were carried out with two aluminium alloys typical for use in modern and in faying aircraft respectively, namely 7475-T 761 and 7075-T6. The sheet materials were exchanged between the two laboratories of the NLR and the IABG, so that both use materials of the same heats. The specimens used by the NLR and IABG differed, however, in the corrosion protection systems and in the manufacturing of the specimens by different firms.

The present paper is just a status report as of 1 August 1981. Diacussion will be necessarily limited to obvious points. Actual discussion will be contained in the final report to be published in 1982.

2. Test Program

2.1 Materails

Two materials, the high-strength aluminium alloys 7475-T 761 clad and 7075-T 6 bare were used as sheet material of a nominal thickness S = 4.2 mm. Mechanical and chemical properties are given in Table 1. The 7075-T 6 material was from a different heat than that used for the core program specimens.

2.2 Specimen Configurations

The configuration of the IABG specimens was identical to that of the core program specimen, see Figure 1. It is a 1 1/2 dogbone specimen mechanically fastened by a row of two countersunk cadmium-plated steel Hi-Lok fasteners. The fastener fit is a slight press fit for a nominal diameter of 6.306 mm, see Table 2, also nominally identical to that of the core program. The fasteners were also identical to those of the core program, being supplied by VOI-SHAN Corporation.

Manufacturing however, was done not by the US Navy, as for the core program, but by a German aircraft company using the corrosion protection system of a modern European tactical aircraft. This system is applied as follows:

- decreasing with steam
- yellow chromate with "Alodine 1200"
- two-component epoxy primer
- wet assembly with "Celloseel"
- after wet assembly one-component top coat (acrylic Taquer).

When applying "Alodine" and the epoxy primer the fastener holes are not covered. The "Celloseel" is pressed into the fastener holes when wet assembling is done. Further information is not available.

In accordance with the manual for the AGARD - CFCTP all specimens exposed to the corrosive environment are sealed at the side edges of the faying surface and at the Hi-Lok collars of the assembled fatigue specimen in order to get corrosion attack only from the countersunk fastener holes.

The sum up, the configuration and the fasteners were identical, the fastener fit was nominally identical with those of the core program; the manufacturing and corrosion protection scheme were different. One of the materials was nominally identical, but a different heat was used, the other was different from the core program.

In addition a number of core program specimens were supplied by Dr. de Luccia; up to the present, only a few were tested for comparative purposes.

2.3 Environmental Testing

Four different environmental parameters are being used:

- fatigue tests in air
- pre-exposure + fatigue tests in air
- fatigue tests in salt spray
- pre-exposure + fatigue tests in salt spray.

Before environmental exposure and fatige testing all specimens are prestressed in a cold box (Figure 2) at 209 ± 10 K by two cycles to a maximum stress of 238 N/mm^2 (on gross area) in order to crack the paint and primer layers in the fastener hole vicinity. After prestressing the side edges surface and Hi-Lok collars are sealed with silicone rubber.

The pre-exposure is done in the chamber shown in Figure 3. The construction of the chamber and the pre-exposure procedure was as described in the CFCTP manual.

Figure 4 shows the test set-up in the servo-hcydraulic machine, the salt spray equipment and a terminal where the test parameters are input into the computer.

The fatigue tests were conducted at a frequency of 15 Hz in air and 2 Hz in the salt spray environment, again in accordance with the CFCTP manual.

2.? Manoeuver Spectrum Falstaff

FALSTAFF (Fighter Aircraft Loading Standard for Fatigue Evaluation) was established by the Flugzeugwerke Emmen, Switzerland, the NLR, the LBF, and the IABG [2] and is well-known in AGARD circles. It was and is being used, for example, in the critically loaded holes and the fatigue-rated fastener programs of the AGARD SMP. It is considered to be suitable for fatigue investigations of fighter aircraft components. A part of the FALSTAFF sequence is shown in the upper part, the load spectrum for one return period in the lower part of Figure 5.

3. Results

To arrive at fatigue lives relevant [illegible] aircraft, the test loads were set up to obtain failure of the specimens at [illegible] lives of about 4 000 and 10 000 flights.

For a first estimation of these [illegible]ads the NLR published some results of pilot tests with core program specimens (7075-T6) under the "FALSTAFF" sequence. Pilot tests of the IABG using identical test conditions and identical core program specimens showed good agreement with the NLR data (Figure 6) so that the test equipment of both laboratories apparently does not influence the results.

The results obtained up to [illegible] August 1981 are summarized in Figure 7. They will not be discussed in any detail here, because [illegible] program is still underway. However, some interesting results are:

- The fatigue life of the specimens of both materials is quite similar at the high stress level of $\bar{S}_{max}$ = 289 N/mm^2 in air, after pre-exposure, in salt spray and after pre-exposure in salt spray.
- The mean fatigue life of 7475-T761 specimens at $\bar{S}_{max}$ = 289 N/mm^2 decreases from 11 000 flights in air to 8 000 flights after pre-exposure in air to 6 400 flights in salt spray to 4 800 flights after pre-exposure in salt spray. That is, the most damaging corrosive environment decreases the fatigue life by a factor of about 2,5.
- For 7075 T6 this factor is about 3,3.
- However, at the lower stress level $\bar{S}_{max}$ [illegible]24 N/mm^2 pre-exposure plus fatigue in salt spray did not do any additional damage, the fatigue life in air being practically equivalent to that after pre-exposure in [illegible] spray. (This can be said only for the 7075-T6 specimen at the moment.)
- In addition to the 5 primary failure origin found in the core program, the "FALSTAFF"-tests with the German specimens resulted in at least one more origin: Two specimens failed at the faying surface outside of the fastener holes, that is through the gross section, see Figure 8.

The tests will be finished by the spring of 1982.

4. References

[1] Schütz, W.: Corrosion Fatigue of Offshore and Ship-Building Steels. These proceedings

[2] Aicher, W,, J. Branger, G.M. van Dijk, J. Ertelt, M. Hück, H.B. de Jonge, H. Lowack, H. Rhomberg, D. Schütz and W.Schütz: Description of a Fighter Aircraft Loading Standard for Fatigue Evaluation "Falstaff". (Common Report of F+W Emmen, LBG, NLR, IABG, March 1976).

CHEMICAL ANALYSIS

(in per cent maximum unless shown as a range)

Material	Si	Fe	Cu	Mn	Mg	Cr	Zn	Ti	others each	others total
7475-T761 core	0.10	0.12	1.2 - 1.9	0.06	1.9 - 2.6	0.18 - 0.25	5.2 - 6.2	0.06	0.05	0.15
cladding	Si+Fe = 0.7		0.1	0.1	0.1	-	0.8 - 1.3	-	0.05	0.15
7075-T6 bare	0.4	0.5	1.2 - 2.0	0.3	2.1 - 2.9	0.18 - 0.35	5.1 - 6.1	0.2	0.05	0.15

MECHANICAL PROPERTIES

Material	Tensile strength N/mm^2	Yield strength N/mm^2	Elongation %
7475-T761 clad	496 - 500	417 - 427	12.4 - 12.8
7075-T6 bare	524 min	462 min	-

TABLE 1

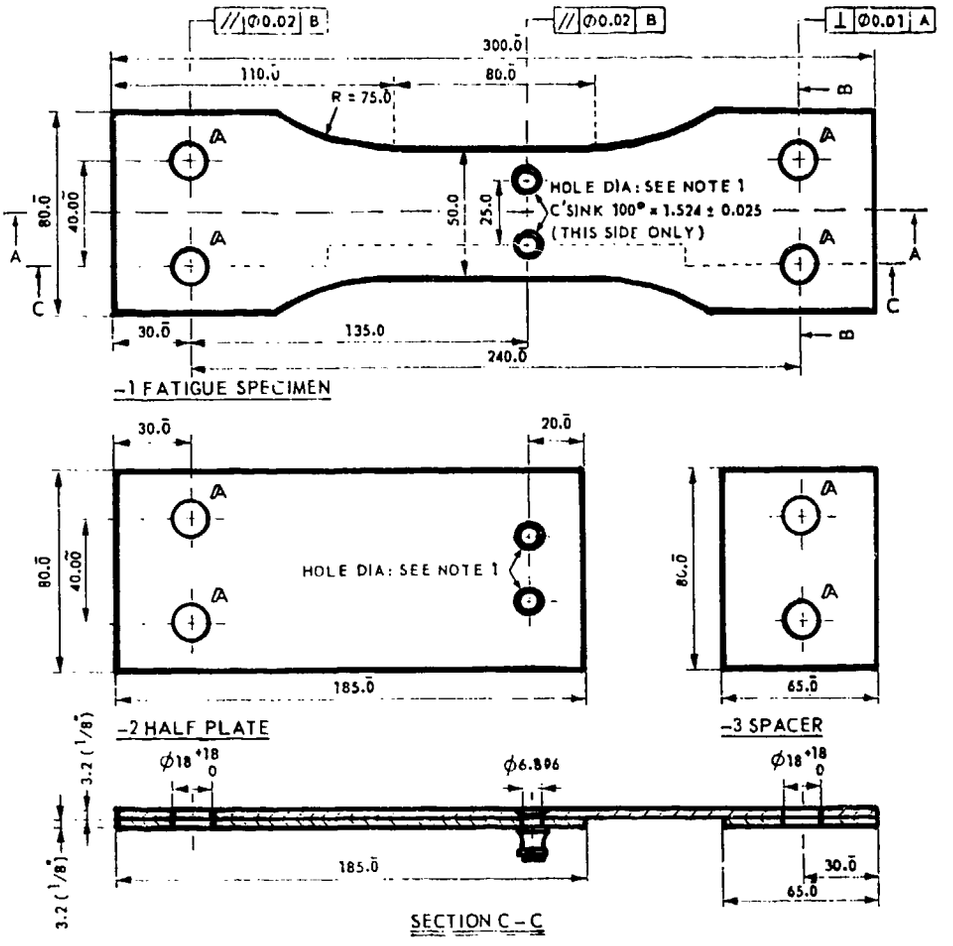
//|Φ0.02| B
//|Φ0.02| B
⊥|Φ0.01| A
300.0
110.0
80.0
R = 75.0
HOLE DIA: SEE NOTE 1
C'SINK 100° x 1.524 ± 0.025
(THIS SIDE ONLY)
80.0
40.00
50.0
25.0
30.0
135.0
240.0
-1 FATIGUE SPECIMEN
30.0
20.0
HOLE DIA: SEE NOTE 1
185.0
-2 HALF PLATE
65.0
-3 SPACER
3.2 (1/8")
φ18 +18 0
φ6.896
SECTION C-C

FIGURE 1

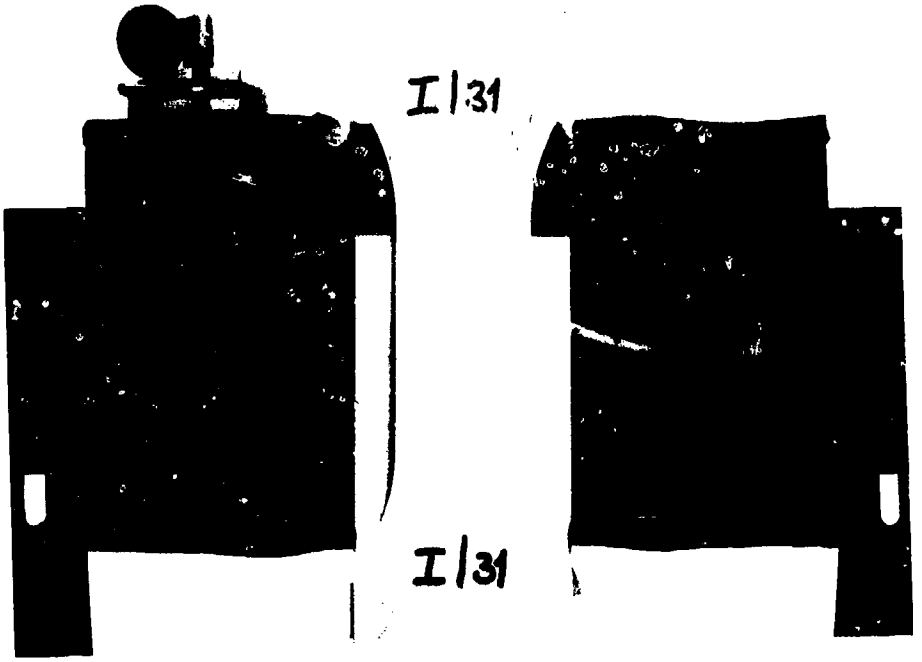

FIGURE 2

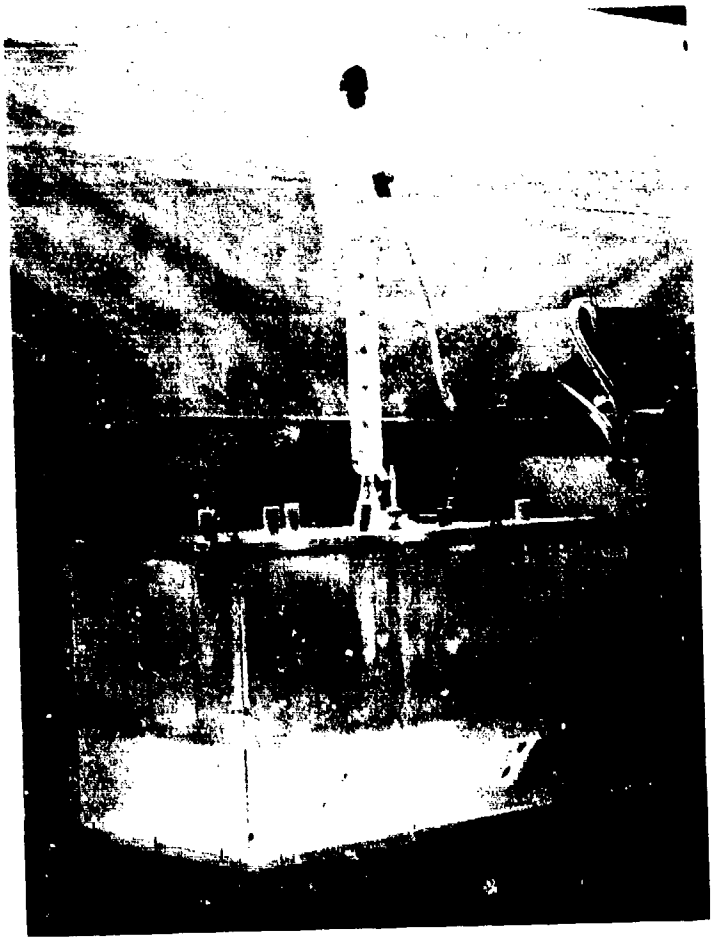

FIGURE 3

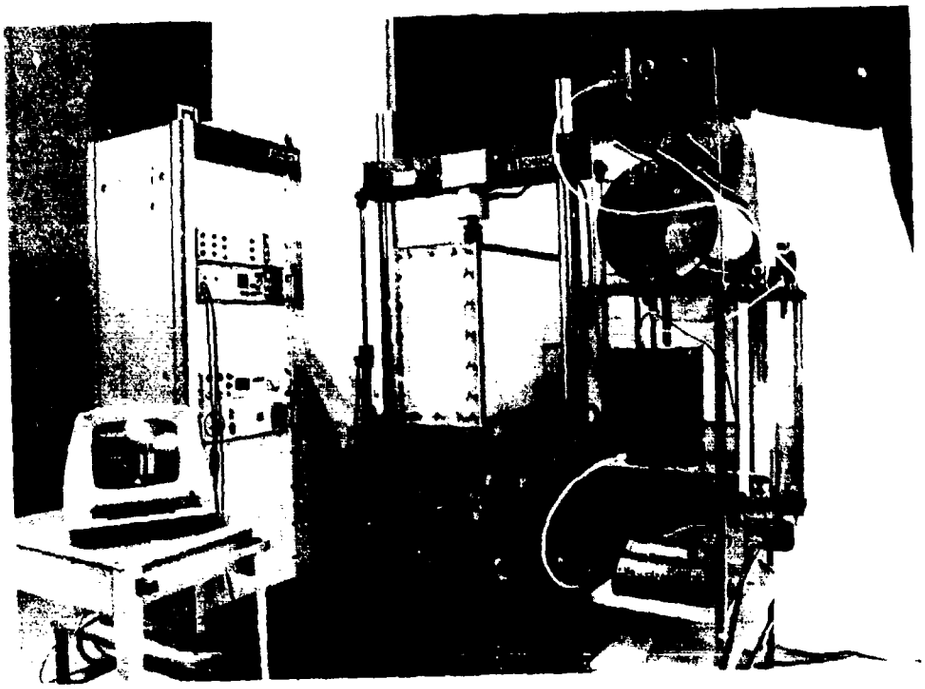

FIGURE 4

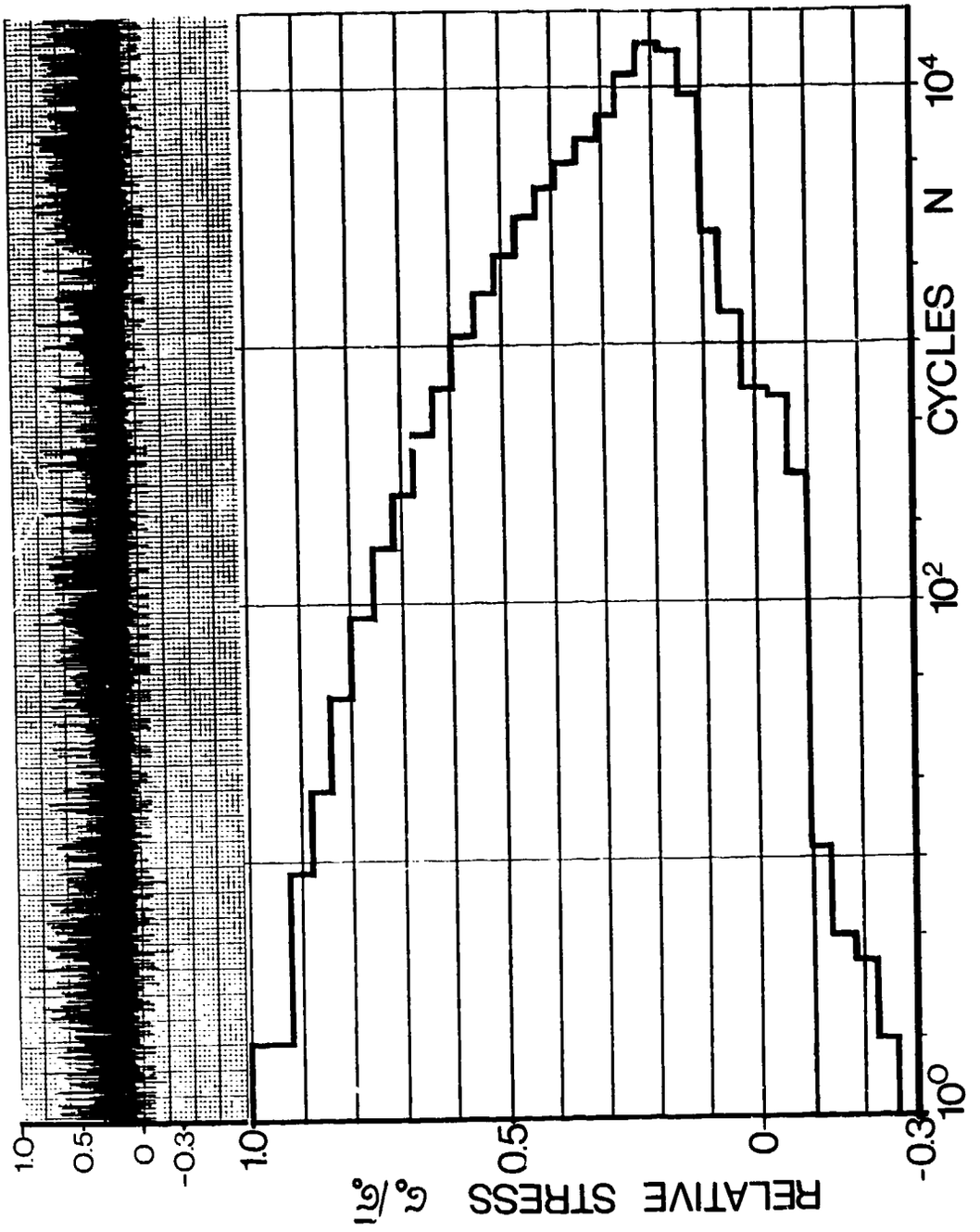

FIGURE 5: Stress Sequence and Stress Spectrum of FALSTAFF

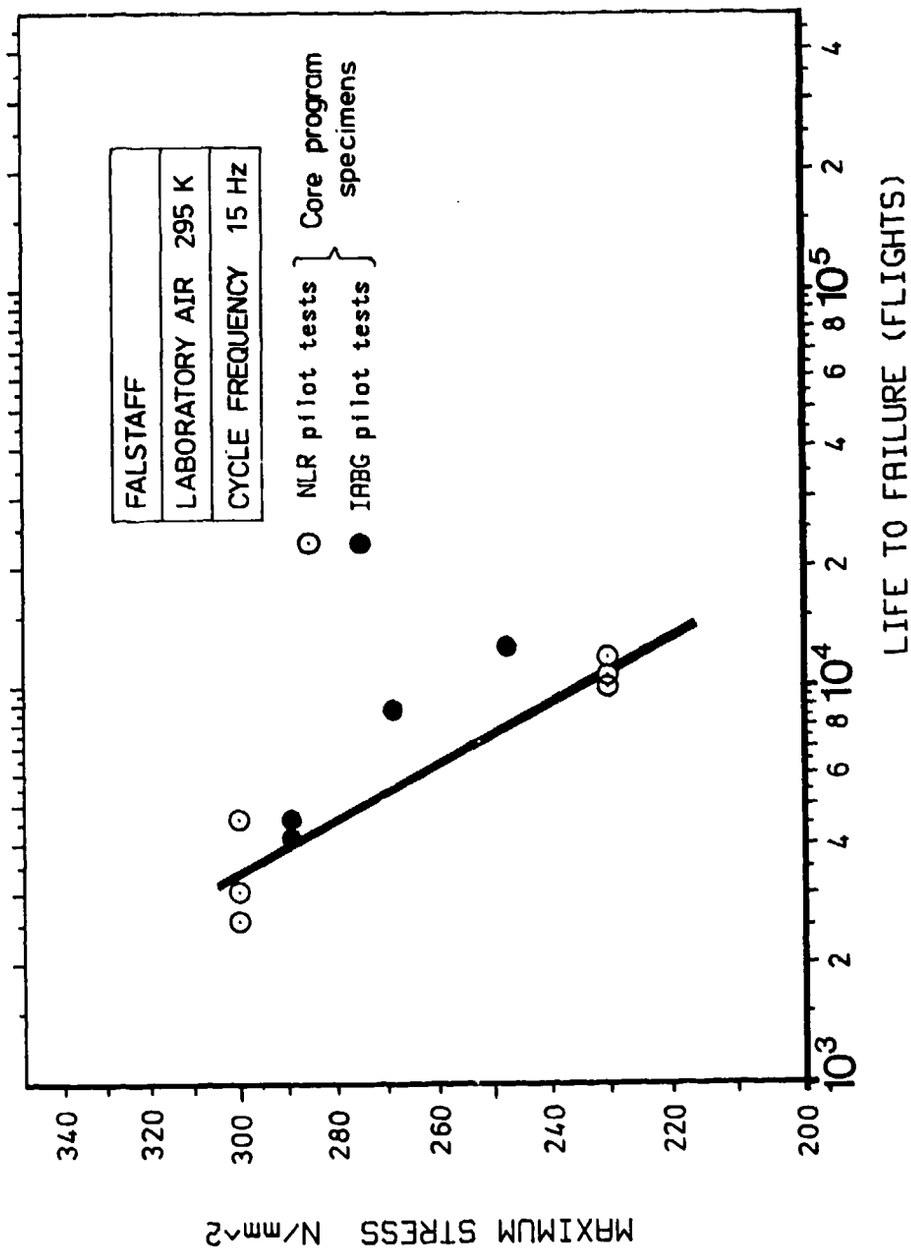
FALSTAFF
LABORATORY AIR 295 K
CYCLE FREQUENCY 15 Hz
NLR pilot tests
IABG pilot tests
Core program specimens
MAXIMUM STRESS N/mm^2
LIFE TO FAILURE (FLIGHTS)
340
320
300
280
260
240
220
200
10^3
2
4
6
8
10^4
2
4
6
8
10^5
2
4

FIGURE 6

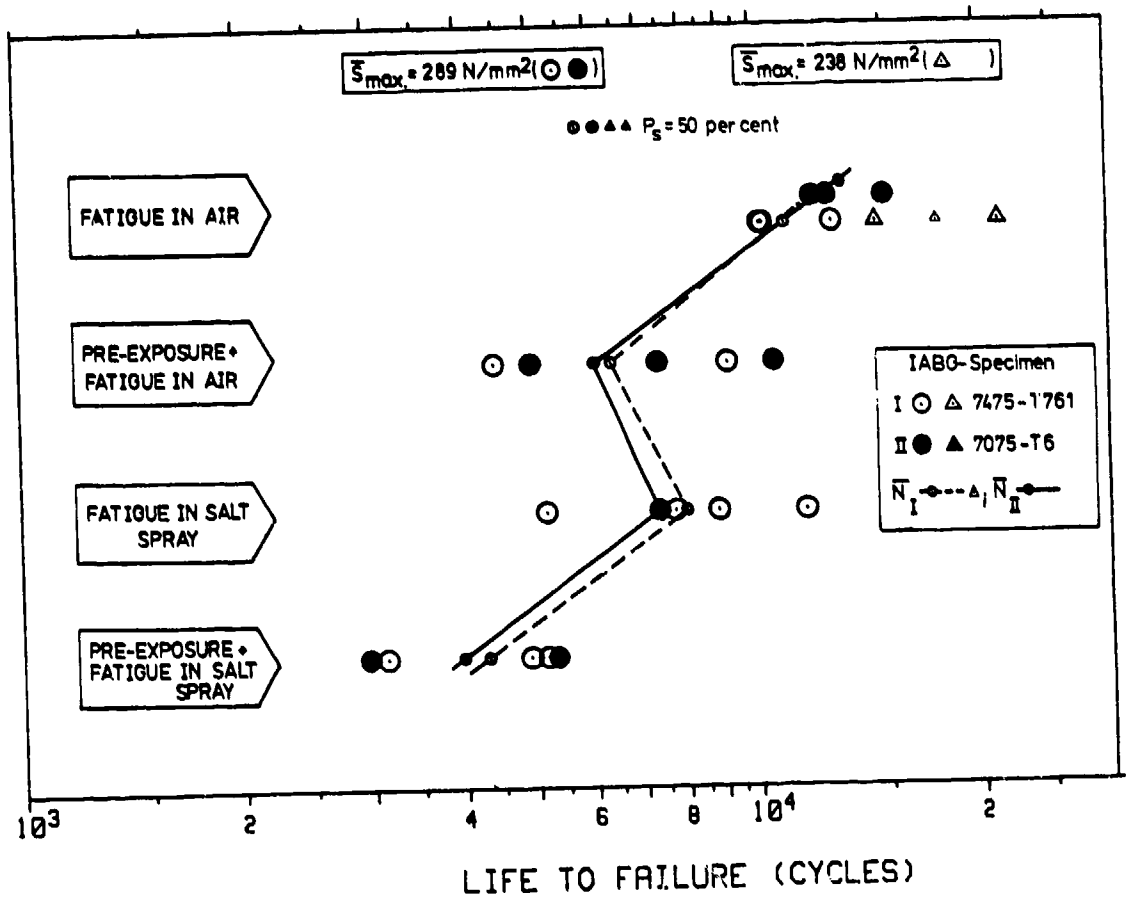

FIGURE 7

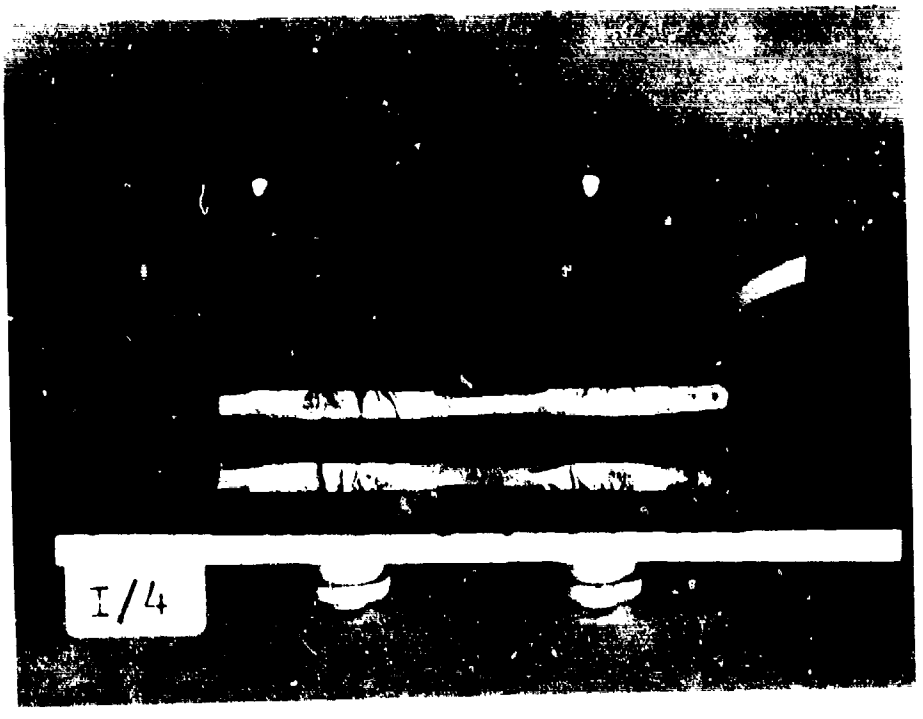

FIGURE 8

REPORT DOCUMENTATION PAGE			
1. Recipient's Reference	2. Originator's Reference AGARD-CP-316	3. Further Reference ISBN 92-835-1402-5	4. Security Classification of Document UNCLASSIFIED

5. Originator	Advisory Group for Aerospace Research and Development North Atlantic Treaty Organization 7 Rue Ancelle, 92200 Neuilly sur Seine, France
6. Title	CORROSION FATIGUE
7. Presented at	the 52nd Meeting of the AGARD Structures and Materials Panel held in Çeşme, Turkey, on 5–10 April 1981

8. Author(s)/Editor(s) Various	9. Date October 1981
10. Author's/Editor's Address Various	11. Pages 94

12. Distribution Statement	This document is distributed in accordance with AGARD policies and regulations, which are outlined on the Outside Back Cover of all AGARD publications.

13. Keywords/Descriptors

Corrosion fatigue
Fatigue tests
Corrosion prevention
Structures

14. Abstract

The objectives and scope of the AGARD Corrosion Fatigue Cooperative Testing Programme were described and plans developed for a supplemental programme of considerably wider scope. In addition, six papers were presented, stimulating thought on the fundamentals of corrosion fatigue and on its combat for real structures.

AGARD Conference Proceedings No.316
Advisory Group for Aerospace Research and Development, NATO
CORROSION FATIGUE
Published October 1981
94 Pages

The objectives and scope of the AGARD Corrosion Fatigue Cooperative Testing Programme were described and plans developed for a supplemental programme of considerably wider scope. In addition, six papers were presented, stimulating thought on the fundamentals of corrosion fatigue and on its combat for real structures.

Papers presented at the 52nd Meeting of the AGARD Structures and Materials Panel held in Çeşme, Turkey, on 5–10 April 1981.

ISBN 92-835-1402-5

AGARD-CP-316

Corrosion fatigue
Fatigue tests
Corrosion prevention
Structures

AGARD Conference Proceedings No.316
Advisory Group for Aerospace Research and Development, NATO
CORROSION FATIGUE
Published October 1981
94 Pages

The objectives and scope of the AGARD Corrosion Fatigue Cooperative Testing Programme were described and plans developed for a supplemental programme of considerably wider scope. In addition, six papers were presented, stimulating thought on the fundamentals of corrosion fatigue and on its combat for real structures.

Papers presented at the 52nd Meeting of the AGARD Structures and Materials Panel held in Çeşme, Turkey, on 5–10 April 1981.

ISBN 92-835-1402-5

AGARD-CP-316

Corrosion fatigue
Fatigue tests
Corrosion prevention
Structures

AGARD Conference Proceedings No.316
Advisory Group for Aerospace Research and Development, NATO
CORROSION FATIGUE
Published October 1981
94 Pages

The objectives and scope of the AGARD Corrosion Fatigue Cooperative Testing Programme were described and plans developed for a supplemental programme of considerably wider scope. In addition, six papers were presented, stimulating thought on the fundamentals of corrosion fatigue and on its combat for real structures.

Papers presented at the 52nd Meeting of the AGARD Structures and Materials Panel held in Çeşme, Turkey, on 5–10 April 1981.

ISBN 92-835-1402-5

AGARD-CP-316

Corrosion fatigue
Fatigue tests
Corrosion prevention
Structures

B128
4

AGARD
NATO OTAN
7 RUE ANCELLE · 92200 NEUILLY-SUR-SEINE
FRANCE
Telephone 745.08.10 · Telex 610176

DISTRIBUTION OF UNCLASSIFIED AGARD PUBLICATIONS

AGARD does NOT hold stocks of AGARD publications at the above address for general distribution. Initial distribution of AGARD publications is made to AGARD Member Nations through the following National Distribution Centres. Further copies are sometimes available from these Centres, but if not may be purchased in Microfiche or Photocopy form from the Purchase Agencies listed below.

NATIONAL DISTRIBUTION CENTRES

BELGIUM
Coordonnateur AGARD - VSL
Etat-Major de la Force Aérienne
Quartier Reine Elisabeth
Rue d'Evere, 1140 Bruxelles

CANADA
Defence Science Information Services
Department of National Defence
Ottawa, Ontario K1A 0K2

DENMARK
Danish Defence Research Board
Østerbrogades Kaserne
Copenhagen Ø

FRANCE
O.N.E.R.A. (Direction)
29 Avenue de la Division Leclerc
92320 Châtillon sous Bagneux

GERMANY
Fachinformationszentrum Energie,
Physik, Mathematik GmbH
Kernforschungszentrum
D-7514 Eggenstein-Leopoldshafen 2

GREECE
Hellenic Air Force General Staff
Research and Development Directorate
Holargos, Athens

ICELAND
Director of Aviation
c/o Flugrad
Reykjavik

ITALY
Aeronautica Militare
Ufficio del Delegato Nazionale all'AGARD
3, Piazzale Adenauer
Roma/EUR

LUXEMBOURG
See Belgium

NETHERLANDS
Netherlands Delegation to AGARD
National Aerospace Laboratory, NLR
P.O. Box 126
2600 A.C. Delft

NORWAY
Norwegian Defence Research Establishment
Main Library
P.O. Box 25
N-2007 Kjeller

PORTUGAL
Direcção do Serviço de Material
da Força Aerea
Rua da Escola Politécnica 42
Lisboa
Attn: AGARD National Delegate

TURKEY
Department of Research and Development (ARGE)
Ministry of National Defence, Ankara

UNITED KINGDOM
Defence Research Information Centre
Station Square House
St. Mary Cray
Orpington, Kent BR5 3RE

UNITED STATES
National Aeronautics and Space Administration (NASA)
Langley Field, Virginia 23365
Attn: Report Distribution and Storage Unit

THE UNITED STATES NATIONAL DISTRIBUTION CENTRE (NASA) DOES NOT HOLD STOCKS OF AGARD PUBLICATIONS, AND APPLICATIONS FOR COPIES SHOULD BE MADE DIRECT TO THE NATIONAL TECHNICAL INFORMATION SERVICE (NTIS) AT THE ADDRESS BELOW.

PURCHASE AGENCIES

Microfiche or Photocopy
National Technical
Information Service (NTIS)
5285 Port Royal Road
Springfield
Virginia 22161, USA

Microfiche
Space Documentation Service
European Space Agency
10, rue Mário Nikis
75015 Paris, France

Microfiche
Technology Reports
Centre (DTI)
Station Square House
St. Mary Cray
Orpington, Kent BR5 3RF
England

Requests for microfiche or photocopies of AGARD documents should include the AGARD serial number, title, author or editor, and publication date. Requests to NTIS should include the NASA accession report number. Full bibliographical references and abstracts of AGARD publications are given in the following journals:

Scientific and Technical Aerospace Reports (STAR)
published by NASA Scientific and Technical
Information Facility
Post Office Box 8757
Baltimore/Washington International Airport
Maryland 21240, USA

Government Reports Announcements (GRA)
published by the National Technical
Information Services, Springfield
Virginia 22161, USA

Printed by Technical Editing and Reproduction Ltd
Harford House, 7–9 Charlotte St, London W1P 1HD

ISBN 92-835-1402-5